

CERN-PH-EP-2012-148

Submitted to: Physical Review D

Underlying event characteristics and their dependence on jet size of charged-particle jet events in pp collisions at $\sqrt{s} = 7$ TeV with the ATLAS detector

The ATLAS Collaboration

Abstract

Distributions sensitive to the underlying event are studied in events containing one or more charged-particle jets produced in pp collisions at $\sqrt{s} = 7$ TeV with the ATLAS detector at the Large Hadron Collider (LHC). These measurements reflect $800\mu\text{b}^{-1}$ of data taken during 2010. Jets are reconstructed using the anti- k_t algorithm with radius parameter R varying between 0.2 and 1.0. Distributions of the charged-particle multiplicity, the scalar sum of the transverse momentum of charged particles, and the average charged-particle p_T are measured as functions of p_T^{jet} in regions transverse to and opposite the leading jet for $4 \text{ GeV} < p_T^{\text{jet}} < 100 \text{ GeV}$. In addition, the R -dependence of the mean values of these observables is studied. In the transverse region, both the multiplicity and the scalar sum of the transverse momentum at fixed p_T^{jet} vary significantly with R , while the average charged-particle transverse momentum has a minimal dependence on R . Predictions from several Monte Carlo tunes have been compared to the data; the predictions from PYTHIA 6, based on tunes that have been determined using LHC data, show reasonable agreement with the data, including the dependence on R . Comparisons with other generators indicate that additional tuning of soft-QCD parameters is necessary for these generators. The measurements presented here provide a testing ground for further development of the Monte Carlo models.

Underlying event characteristics and their dependence on jet size of charged-particle jet events in pp collisions at $\sqrt{s} = 7$ TeV with the ATLAS detector

The ATLAS Collaboration
(Dated: March 9, 2013)

Distributions sensitive to the underlying event are studied in events containing one or more charged-particle jets produced in pp collisions at $\sqrt{s} = 7$ TeV with the ATLAS detector at the Large Hadron Collider (LHC). These measurements reflect $800\mu\text{b}^{-1}$ of data taken during 2010. Jets are reconstructed using the anti- k_t algorithm with radius parameter R varying between 0.2 and 1.0. Distributions of the charged-particle multiplicity, the scalar sum of the transverse momentum of charged particles, and the average charged-particle p_T are measured as functions of p_T^{jet} in regions transverse to and opposite the leading jet for $4 \text{ GeV} < p_T^{\text{jet}} < 100 \text{ GeV}$. In addition, the R -dependence of the mean values of these observables is studied. In the transverse region, both the multiplicity and the scalar sum of the transverse momentum at fixed p_T^{jet} vary significantly with R , while the average charged-particle transverse momentum has a minimal dependence on R . Predictions from several Monte Carlo tunes have been compared to the data; the predictions from PYTHIA 6, based on tunes that have been determined using LHC data, show reasonable agreement with the data, including the dependence on R . Comparisons with other generators indicate that additional tuning of soft-QCD parameters is necessary for these generators. The measurements presented here provide a testing ground for further development of the Monte Carlo models.

PACS numbers: 13.85.Hd,13.87.-a

I. INTRODUCTION AND OVERVIEW

Quantum Chromodynamics (QCD) [1, 2] predicts the cross sections for the production of objects with large transverse momentum (p_T) [3] in hadronic collisions. Such calculations are performed by factorizing the interaction into a hard scattering process that can be calculated perturbatively and a set of soft processes that must be described phenomenologically. The high- p_T jet production cross section is calculated [4] by convolving the matrix elements for the scattering of two initial-state partons (quarks and gluons), with the corresponding parton distribution functions (PDF), to produce a partonic final state. To predict the momentum spectrum of the final particles, additional effects must be considered. The outgoing partons fragment into jets of hadrons. The beam remnants also hadronize and the spectator partons in the proton can also interact, leading to multiple parton interactions (MPI). QCD radiation from the initial- and final-state partons occurs, leading to additional jets and to an increase in the ambient energy. These effects vary with the momentum transfer of the hard parton scattering. Some of these processes take place at an energy scale where the QCD coupling constant is large and perturbation theory cannot be used. They must therefore be described using QCD-motivated phenomenological models, implemented in Monte Carlo (MC) event generators. In general, these models contain a number of free parameters with values that must be obtained by fitting to experimental data.

For a single proton-proton (pp) collision, the Underlying Event (UE) is defined to be any hadronic activity not associated with the jets or leptons produced in the hard scattering process. In practice, because color fields connect all the strongly interacting partons in the proton-

proton event, no unambiguous assignment of particles to the hard scattering partons or UE is possible. Instead, distributions that are sensitive to UE modeling are constructed from the tracks that are far from the direction of the products of the hard scatter. This direction is approximated by the direction of the highest- p_T (leading) object in the event.

Measurements of observables sensitive to the UE characteristics in $p\bar{p}$ collisions were performed at the Tevatron by CDF using jet events at center-of-mass energies $\sqrt{s} = 630 \text{ GeV}$ and $\sqrt{s} = 1.8 \text{ TeV}$ [5], and using Drell-Yan and jet events at $\sqrt{s} = 1.96 \text{ TeV}$ [6]. Underlying event observables have been measured in pp collisions with $\sqrt{s} = 900 \text{ GeV}$ and $\sqrt{s} = 7 \text{ TeV}$ from the distribution of charged particles in the region transverse to leading charged particles and leading charged-particle jets by CMS [7, 8] and in the regions transverse to and away from leading charged particles by ATLAS [9] and ALICE [10]. A complementary analysis by ATLAS studied UE properties using both neutral and charged particles [11].

This paper extends previous studies of the UE by measuring the charged-particle multiplicity and transverse-momentum density in the transverse and away regions with respect to leading charged-particle jets reconstructed using the anti- k_t [12] algorithm and varying the radius parameter, R , of that algorithm between 0.2 and 1.0. We can regard the leading charged particle as a charged-particle jet with $R \approx 0$. As long as R remains below a characteristic value determined by the momentum transfer (q^2) of the hard scatter, the p_T of charged-particle jets formed with larger R are better indicators of the hard scatter energy. Such charged-particle jets are reconstructed with high efficiency at low jet transverse momentum, p_T^{jet} , and can therefore be used to study the behavior of the UE in the transition region between

soft QCD interactions and hard partonic scattering. At larger p_T^{jet} , charged-particle jets provide a complement to calorimeter-based measurements, with results that are independent of calorimeter calibrations, selections and uncertainties. Variations in the mean values of these UE observables with R provide additional information on the interplay between the perturbative and non-perturbative components of QCD-inspired MC models.

This paper is organized as follows. The ATLAS detector is described briefly in Section II. The QCD Monte Carlo models used in this analysis are discussed in Section III. The variables sensitive to UE activity are defined in Section IV. The event and object selections are presented in Section V. Section VI contains a description of the analysis. In Section VII, the treatment of systematic uncertainties is discussed. Fully corrected data distributions are presented in Section VIII and the results are compared to the predictions of several Monte Carlo generators. Section IX discusses the dependence of the UE observables on R . Conclusions are provided in Section X.

II. THE ATLAS DETECTOR

The ATLAS detector is described in detail in Ref. [13]. The subsystems relevant for this analysis are the inner detector (ID) and the trigger system.

The ID is used to measure the trajectories and momenta of charged particles. It consists of three detectors: a pixel detector, a silicon strip tracker (SCT) and a transition radiation straw-tube tracker (TRT). These detectors are located inside a solenoid that provides a 2 T axial magnetic field, and have full coverage in the azimuthal angle ϕ over the pseudorapidity range $|\eta| < 2.5$. The ID barrel (end-cap) typically has 3 (2×3) pixel layers, 4 (2×9) layers of double-sided silicon strip modules, and 73 (2×160) layers of TRT straw tubes. A track traversing the barrel typically has 11 silicon hits (3 pixel clusters, and 8 strip clusters), and more than 30 straw-tube hits. Typical position resolutions are 10, 17 and 130 μm for the r - ϕ coordinate of the pixel detector, SCT, and TRT respectively. The resolution of the second measured coordinate is 115 μm for the pixel detector and 580 μm for the SCT.

The ATLAS trigger consists of three levels of event selection: Level-1 (L1), Level-2 (L2), and Event Filter. The trigger relevant for this analysis is the single-arm L1 minimum bias trigger [14], which uses information from the Beam Pickup Timing devices (BPTX) and the Minimum Bias Trigger Scintillators (MBTS). The BPTX stations are composed of electrostatic button pickup detectors attached to the beam pipe at ± 175 m from the center of the ATLAS detector. The coincidence of the BPTX signal between the two sides of the detector is used to determine when bunches collide in the center of the detector. The MBTS consists of 32 scintillation counters located at pseudorapidities $2.09 < |\eta| < 3.84$. The trigger requires a single hit above threshold in the MBTS together with

a BPTX coincidence.

III. MONTE CARLO SAMPLES

MC event samples are used to compute detector acceptance and reconstruction efficiencies, determine background contributions, unfold the measurements for detector effects, and estimate systematic uncertainties on the final results. The samples used here are the same as those used in Ref. [15]. The baseline Monte Carlo event generator used to determine acceptance and efficiencies is PYTHIA 6.4.21 [16] with the ATLAS tune AMBT1, which uses the MRST2007LO* PDF [17]. This tune was derived using the measured properties of minimum bias events [18]. Generated events are simulated using the ATLAS detector simulation [19], which is based on the Geant4 toolkit [20]. The simulated events are processed using the same software as the data. Several other simulated samples are used to assess systematic uncertainties on the detector response: PYTHIA 6 using the Perugia 2010 tune [16] (CTEQ5L PDF [21]), PYTHIA 6 with the ATLAS MC09 tune [22] (MRST2007LO* PDF) and PYTHIA 8.145 with tune 4C [23] (CTEQ6L1 PDF).

In the past year, significant work has been done to improve agreement between the MC generators and LHC data by tuning the parameters of the phenomenological models used to describe soft QCD processes [24, 25]. UE data, after applying corrections for detector effects, are compared to recent tunes of several MC event generators. Samples with high statistics were produced using the PYTHIA 6.4.21, PYTHIA 8.145, and Herwig++ 2.5.1 [26] generators. Several different PYTHIA 6 samples were generated with different UE tunes. AUET2B [27] is an ATLAS tune that uses the p_T -ordered parton shower, interleaved initial-state radiation (ISR) and MPI which has been tuned to UE data from CDF and ATLAS. This employs the MRST2007LO** [17] PDF. The CMS tune Z1 [25] is very similar, but is fitted to CMS UE data, and uses CTEQ5L PDF. The Perugia 2011 tune [28] uses similar settings, with the UE parameters constrained by minimum bias and UE data from CDF and ATLAS. Perugia 2011 NOCR is a tune of the p_T -ordered model which does not employ color reconnection. The PYTHIA 8 generator includes many new features over PYTHIA 6, such as fully interleaved p_T -ordered MPI+ISR+FSR evolution, and a different model of hard diffraction. The default author tune 4C [29] with CTEQ6L1 PDF [30] is used. The recently released Herwig++ 2.5.1 version with tune UE7-2 used here has angle-ordered parton showers, employs MRST2007LO* PDF and has an improved model of color reconnection.

IV. DEFINITION OF VARIABLES

After reconstructing jets from charged tracks in the event, p_T^{jet} refers to the transverse momentum (p_T) of the

jet with the highest p_T . The variation of the UE properties with p_T^{jet} is measured in this analysis. In addition, the dependence of these properties on R is studied.

Particles are defined to be in the *transverse* region if their azimuthal angle differs from that of the leading jet ($|\Delta\phi| \equiv |\phi^{\text{particle}} - \phi^{\text{jet}}|$) by between $\pi/3$ and $2\pi/3$ radians, as shown in Figure 1. This region is most sensitive to the UE. Particles with $|\Delta\phi| > 2\pi/3$ are defined to be in the *away* region. This region is likely to contain the fragmentation products of the sub-leading parton produced in the hard scattering.

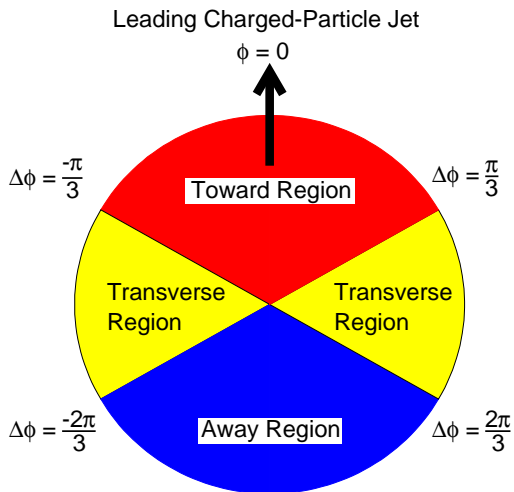


FIG. 1. Definition of the transverse and away regions with respect to the leading jet.

Three observables sensitive to UE activity are studied in the transverse and away regions:

- N_{ch} : the number of tracks in the region
- Σp_T : the scalar sum of the transverse momentum of the tracks in the region
- \bar{p}_T : the average p_T of the tracks in the region ($\bar{p}_T \equiv \Sigma p_T / N_{\text{ch}}$)

V. EVENT SELECTION AND RECONSTRUCTION

The events used in this analysis were collected with the ATLAS detector at a center-of-mass energy $\sqrt{s} = 7$ TeV during early 2010. The data sample, event selection and reconstruction are identical to those used to measure the cross section and fragmentation functions of jets reconstructed from tracks [15]. Events are required to have passed the L1 minimum bias trigger which was highly

prescaled. The sample represents an integrated luminosity of $800 \mu\text{b}^{-1}$ after the trigger prescale. The average number of collisions per bunch crossing, μ , varied throughout the data-taking period, but never exceeded a value of $\mu = 0.14$. Over half the data were taken with $\mu \lesssim 0.01$. Thus, effects due to the presence of more than one collision in the same bunch crossing (“pile-up”) are minimal. Primary vertex reconstruction [31] is performed using tracks with $p_T > 0.4$ GeV and $|\eta| < 2.5$. A minimum of two tracks is required to form a vertex. To further reduce the contributions of pile-up, events are rejected if more than one primary vertex is reconstructed.

Tracks used in the reconstruction of jets and UE observables are required to have $p_T > 0.5$ GeV, $|\eta| < 2.5$, transverse impact parameter with respect to the primary vertex $|d_0| < 1.5$ mm and longitudinal impact parameter with respect to the primary vertex $|z_0 \sin \theta| < 1.5$ mm. Only tracks with at least one pixel hit and six SCT hits are considered. To minimize the contribution of particles produced by secondary interactions in the ID, tracks are required to have a hit in the innermost pixel layer if the extrapolated track passes through an active portion of that layer.

For each event, jet collections are constructed, corresponding to the output obtained when the anti- k_t algorithm is applied to the tracks for five separate values of R : 0.2, 0.4, 0.6, 0.8 and 1.0. For each jet collection, the leading jet is defined to be the jet with the largest p_T^{jet} satisfying the requirements $p_T^{\text{jet}} > 4$ GeV and $|\eta^{\text{jet}}| < 1.5$. This maximum $|\eta^{\text{jet}}|$ cut ensures that all tracks associated with jets in the fiducial region are within the fully-efficient tracking volume.

VI. ANALYSIS PROCEDURE

The analysis is performed in parallel on each of the five jet collections using the following procedure. First, the leading jet is selected and events are rejected if there is no jet that satisfies the requirements described in the previous section. Next, the $\Delta\phi$ of each track with respect to the leading jet is calculated and the tracks in the transverse and away regions are identified. In addition to satisfying the selection criteria discussed in Section V, tracks used for the UE measurements are required to pass the same pseudorapidity cut as the jets, $|\eta| < 1.5$. This requirement minimizes the contamination in the UE calculation, from constituent tracks of a leading jet with $|\eta^{\text{jet}}| > 1.5$.

The selected tracks are used to calculate the three event observables N_{ch} , Σp_T and \bar{p}_T , denoted generically as \mathcal{O} , in the transverse and away regions. The final results presented here are the distributions and mean values of these observables for specific ranges (bins) of p_T^{jet} . To allow comparisons with MC generators, the data distributions are corrected for detector acceptance, reconstruction efficiency, and for bin migration due to track and jet momentum-resolution effects. The corrections

used in this unfolding procedure are obtained by matching the jets reconstructed in simulated MC samples with those obtained when the anti- k_t algorithm is applied to the primary charged particles produced by the generator. Primary charged particles are defined as charged particles with a mean lifetime $\tau > 0.3 \times 10^{-10}$ s, which are produced in the primary collision or from subsequent decays of particles with a shorter lifetime. Thus, the charged decay products of K_S^0 and Λ particles are not included. A reconstructed jet is considered to be matched to a particle-level jet if their centers are separated by $\sqrt{(\Delta\eta)^2 + (\Delta\phi)^2} < R/2$.

Jets below the minimum p_T^{jet} cut or outside the maximum $|\eta^{\text{jet}}|$ cut are used in the procedure that corrects for the effects of resolution smearing. Thus, looser requirements of $p_T^{\text{jet}} \geq 1$ GeV and $|\eta^{\text{jet}}| \leq 2.5$ are imposed during the reconstruction. In addition, since corrections for migration of jets into the fiducial volume require knowledge of the population outside that volume, the transverse momentum of the leading jet outside the fiducial volume (p_T^{ext}) is also determined in each reconstructed jet collection for each event and, in MC samples, for each collection of particle-level charged-particle jets.

The events satisfying these requirements are corrected back to the primary charged-particle spectra satisfying the event-level requirement of at least one anti- k_t jet with $p_T^{\text{jet}} \geq 4$ GeV and $|\eta^{\text{jet}}| < 1.5$ reconstructed from charged primary particles with $p_T > 0.5$ GeV and $|\eta| < 2.5$. Data distributions are unfolded using an iterative method [32] based on Bayes' theorem, implemented in the RooUnfold [33] software package. The procedure requires three inputs: a measured input distribution (stored as a multi-dimensional histogram), a response matrix (obtained from simulated data) that provides a mapping between reconstructed objects and those obtained directly from the event generator, and an initial choice for the prior probability distribution, or *prior* for short. Each observable \mathcal{O} is stored in a three-dimensional histogram (one histogram for each observable and separate histograms for the transverse and away regions) where the binning variables are p_T^{jet} , \mathcal{O} and p_T^{ext} . To accommodate the decreasing statistics in the data with p_T^{jet} and the variation of the p_T^{jet} and p_T^{track} resolution with transverse momentum, these histograms have variable bin width. The response matrix is stored as a six-dimensional histogram that specifies the probability that observed values of p_T^{jet} , p_T^{ext} and \mathcal{O} are measured for given true values of p_T^{jet} , p_T^{ext} and \mathcal{O} . This response matrix is not unitary because in mapping from generator to reconstruction some events and jets are lost due to inefficiencies and some are gained due to misreconstruction or migration of true objects from outside the fiducial acceptance into the reconstructed observables.

Unfolding the experimental distribution to obtain the corrected distribution is done as follows. The response matrix, measured data and initial prior are used as inputs to the unfolding algorithm to produce an updated

distribution, the *posterior*. This posterior is used as the input prior for another iteration of the algorithm, and this process is repeated. The inputs to each iteration of the unfolding algorithm are the baseline response matrix, measured data and the posterior of the previous iteration. The optimal number of iterations is determined from MC studies. In this analysis, a total of four iterations are performed for each measured distribution. The initial prior is taken to be the prediction of the baseline Monte Carlo generator. Systematic uncertainties associated with this choice and with the modeling of the response matrix are discussed in Section VII.

Once the corrected distributions have been obtained in bins of p_T^{jet} , the mean value of \mathcal{O} for each p_T^{jet} bin is determined from these distributions. Some care must be taken to avoid bias when the mean is calculated since the output of the unfolding procedure is a histogram and the distribution of the population varies across the bin. For Σp_T and N_{ch} , the cumulative distribution function of the unfolded distribution is calculated and fit to a cubic spline and the mean is determined from the results of the spline fit. This step reduces the bias between the binned and unbinned calculation of the mean from a few percent to less than 0.5%. The \bar{p}_T distributions have sufficiently fine binning that the bias is below 0.5% without this step.

VII. SYSTEMATIC UNCERTAINTIES

A summary of the systematic uncertainties and how they affect the measurements is presented in Table I. The following sources of systematic uncertainty have been considered:

1. The track reconstruction efficiency and momentum reconstruction uncertainty.
2. Potential bias arising from the unfolding procedure.
3. Misidentification of the leading jet due to cases where the leading reconstructed jet does not correspond to the true leading jet.
4. The uncertainty in the response matrix, which is derived using a particular MC sample and thus depends on the details of the event generator.
5. Uncertainty in the calculation of the means from the distributions of observables due to discretization effects arising from the finite bin-width of the unfolded distributions.

Uncertainties on the tracking efficiency are η -dependent and vary between 2% (for $|\eta^{\text{track}}| \leq 1.3$) and 7% (for $2.3 < |\eta^{\text{track}}| \leq 2.5$) [34]. The dominant source of this uncertainty comes from possible inaccuracies in the description of the detector material in the simulation. The effect of this uncertainty on the measured observables is assessed by randomly removing from the data a fraction of the tracks consistent with the uncertainty on

TABLE I. The systematic uncertainties associated with measurement of the mean values of Σp_T , N_{ch} and \bar{p}_T .

| Relative Systematic Uncertainties | | | | | | |
|-----------------------------------|-------------------|---------------------|-----------------|------------------|---------------------|-----------------|
| Source | TRANSVERSE region | | | AWAY region | | |
| | Σp_T (%) | N_{ch} (%) | \bar{p}_T (%) | Σp_T (%) | N_{ch} (%) | \bar{p}_T (%) |
| Tracking Reconstruction | 2.1–2.5 | 2.0–2.3 | 0.2–0.3 | 2.1–2.6 | 2.0–2.3 | 0.1–0.2 |
| Unfolding Procedure | 1.5–6.0 | 1.5–4.0 | 1.0–4.0 | 1.5–5.0 | 1.5–4.0 | 1.0–4.0 |
| Leading Jet Misidentification | ≤ 1.0 | ≤ 1.0 | ≤ 0.5 | ≤ 1.0 | ≤ 1.0 | ≤ 0.5 |
| Response Matrix | 0.5–2.1 | 0.5–1.6 | 0.5–1.6 | 0.5–2.2 | 0.5–1.6 | 0.5–1.2 |
| Discretization Effects | ≤ 0.5 | ≤ 0.5 | ≤ 0.5 | ≤ 0.5 | ≤ 0.5 | ≤ 0.5 |
| Total | 2.7–6.6 | 2.6–4.7 | 1.3–4.1 | 2.7–5.7 | 2.6–4.7 | 1.3–4.1 |

the tracking efficiency and recalculating the observable. The resulting uncertainty is then assumed to be symmetric. Uncertainties on the track momentum resolution are parameterized as an additional η -dependent broadening of the resolution in track curvature with values that vary from 0.4 TeV^{-1} to 0.9 TeV^{-1} [35]. Systematic uncertainties on the tracking performance lead to relative uncertainties on the mean values of Σp_T and N_{ch} that vary with R from 2.1% ($R = 0.2$) to 2.6% ($R = 1.0$). Uncertainties on \bar{p}_T are below the percent level for all values of R and p_T^{jet} .

The performance of the unfolding procedure is studied by unfolding the distributions measured in simulated MC control samples and comparing them to the known generator-level distributions. These closure tests have been performed using all the simulated samples described in Section III. In each case, before the test is performed, the input MC sample is reweighted so that the truth distributions of p_T^{jet} and of the observable \mathcal{O} reproduce the unfolded distributions in the data. The resulting deviations on the mean value of \mathcal{O} are lowest (1%–1.5%) at low p_T^{jet} and increase to 4%–6% at large p_T^{jet} for all three observables.

At least three effects can result in differences between the leading reconstructed jet and the true leading jet. One possibility is that a jet with $p_T^{\text{jet}} < 4 \text{ GeV}$ or with $|\eta^{\text{jet}}| > 1.5$ is reconstructed to be inside the acceptance (“feed-in” jets). Another effect is that due to differences in the distributions of true and reconstructed particles the anti- k_t algorithm, when applied to the reconstructed data, produces jets that do not match any jets obtained when the algorithm is applied to true particles (“accidental jets”). A third possibility is that a non-leading jet is identified as a leading jet due to resolution smearing and inefficiencies in the track reconstruction. The unfolding procedure intrinsically corrects for migration into the fiducial region. Residual uncertainties on the contribution from misidentification of the leading jet have been assessed by reweighting the simulation to reproduce the observed distributions of the subleading p_T^{jet} and the azimuthal angle between the leading and subleading jet,

and applying the unfolding procedure to the reweighted sample. Changes in the resulting output from the unfolding differ from the default by $< 1\%$. Studies with simulated data indicate that the rate for accidental jets is below 0.1% for all values of R and p_T^{jet} . Therefore, the systematic uncertainty due to accidental jets is judged to be negligible. The systematic uncertainty on the fraction of non-leading jets that are misidentified as the leading jet due to uncertainties in the tracking efficiency is already included in the tracking systematic uncertainty described above.

Systematic uncertainties due to discretization effects (finite bin size) have been studied using simulated data by comparing the mean calculated from the binned data to the mean calculated from unbinned data. The differences are below 0.5% for all observables and all values of R .

The sensitivity to the number of iterations used for unfolding is determined by comparing the baseline results to those obtained when the number of iterations is varied. Changes in the unfolded results are below 0.5% for all the observables.

The response matrix is derived using a particular MC sample; therefore, it depends on the details of the event generator and tune. The sensitivity of the result to differences between the baseline MC sample and the data have been studied by comparing the baseline results to those obtained when the data are unfolded using an alternative response matrix constructed after the MC sample has been reweighted to reproduce the raw p_T^{jet} and UE observables. Relative differences between the baseline measurements and those obtained with the reweighted response matrix are below 0.25% for all three observables. The effects of statistical uncertainties in the response matrix are evaluated using the bootstrap method [36] to create 50 statistically independent samples of the reweighted MC simulation and repeating the unfolding procedure on the data for each sample. The RMS (relative to the baseline) of the resulting ensemble of unfolded results is less than 0.1%.

When comparing the mean values of UE observables for different values of R , the correlations among the systematic uncertainties must be properly treated. Uncertainties due to track reconstruction efficiency and due to discretization effects are fully correlated among the measurements and thus do not contribute to the systematic uncertainty on the ratio of the mean responses measured for different R . Uncertainties due to unfolding are partially correlated. The systematic uncertainties on the ratios of UE observables for different values of R are determined from the deviations from the baseline ratios, of the ratios obtained from MC samples where the input spectra are varied concurrently for all jet collections. The uncertainties on the ratios are typically below 1.5% except for the highest bin in p_T^{jet} , where the uncertainty on the ratio of $R = 0.2$ to $R = 0.6$ rises to 6% for Σp_T in the transverse region.

The same events are used to reconstruct all the jet collections; therefore, the statistical uncertainties are also correlated among the measurements. The statistical uncertainties on the ratio of the observables measured with one value of R to those measured with a different R are obtained by applying a bootstrap method to the data.

VIII. MEASUREMENTS OF UE DISTRIBUTIONS

The dependence on p_T^{jet} of the mean values of the unfolded Σp_T , N_{ch} and \bar{p}_T distributions is shown in Figures 2, 3 and 4, respectively. The dependence is shown for all five values of R for the transverse region. To facilitate comparisons with previous measurements, these mean values are reported as densities per unit $\eta\phi$. Therefore, the mean values of Σp_T and N_{ch} are divided by $2\pi = \Delta\phi \times \Delta\eta$, where $\Delta\phi = 2\pi/3$ ($\pi/3 \leq |\Delta\phi| \leq 2\pi/3$) and $\Delta\eta = 3$ ($-1.5 \leq \eta \leq 1.5$ contributes $\Delta\eta = 3$). The qualitative behavior of the distributions is the same for all five R values. The mean values of Σp_T rise rapidly with p_T^{jet} for low p_T^{jet} and continue to rise slowly for high p_T^{jet} . The mean values of \bar{p}_T exhibit qualitatively similar behavior as those of Σp_T . The mean value of N_{ch} rises rapidly with p_T^{jet} for low p_T^{jet} and approaches a plateau for high p_T^{jet} . The systematic differences in the measurements as R is varied are discussed in Section IX.

The unfolded data are compared to several MC generators and tunes. In general, the level of agreement between the data and MC samples is reasonable, with differences below 20% for all observables and all p_T^{jet} bins. The PYTHIA 6 Z1 sample reproduces the mean values of Σp_T within uncertainties for all p_T^{jet} bins. This MC sample tends to slightly overestimate N_{ch} for $p_T^{\text{jet}} \gtrsim 15$ GeV, and this manifests itself as a slight underestimation of \bar{p}_T in the same p_T^{jet} range. The PYTHIA 6 AUET2B sample tends to slightly underestimate Σp_T for $p_T^{\text{jet}} \lesssim 20$ GeV, and overestimate Σp_T at higher p_T^{jet} . PYTHIA 6 AUET2B reproduces N_{ch} for $p_T^{\text{jet}} \lesssim 15$ GeV, and overestimates

N_{ch} for $p_T^{\text{jet}} \gtrsim 15$ GeV. This MC sample slightly underestimates the mean values of \bar{p}_T in all p_T^{jet} bins. PYTHIA 6 Perugia2011 exhibits reasonable agreement with the data Σp_T distributions, having tendencies to underestimate the data at low p_T^{jet} and overestimate it for $p_T^{\text{jet}} \gtrsim 15$ GeV. This MC sample tends to overestimate N_{ch} and slightly underestimate \bar{p}_T . The other tunes show somewhat worse agreement for all distributions. PYTHIA 8 tune 4C underestimates all three observables, although the agreement is better for \bar{p}_T . Herwig++ tune UE7-2 underestimates the Σp_T and N_{ch} . The PYTHIA 6 Perugia 2011 NOCR tune is disfavored by the \bar{p}_T data.

Figures 5 through 7 show the unfolded distributions $(1/N_{\text{ev}})dN_{\text{ev}}/d\Sigma p_T$, $(1/N_{\text{ev}})dN_{\text{ev}}/dN_{\text{ch}}$ and $(1/N_{\text{ev}})dN_{\text{ev}}/d\bar{p}_T$ in the transverse region for three representative values of R and for low (5–6 GeV) and high (31–50 GeV) bins of p_T^{jet} . Here N_{ev} is the number of events in the sample with $p_T^{\text{jet}} > 4$ GeV and $|\eta^{\text{jet}}| < 1.5$. The PYTHIA 6 Z1 tune shows differences with respect to the data of less than 20%–30% for most distributions and p_T^{jet} bins. The PYTHIA 6 AUET2B shows discrepancies of up to a factor of two for the Σp_T and N_{ch} distributions at large values of p_T^{jet} . For $p_T^{\text{jet}} \approx 5$ GeV, the Perugia 2011 tune undershoots the data for $R = 0.2$ by 30%–75% for $N_{\text{ch}} \gtrsim 20$ and by 20%–80% for $\Sigma p_T \gtrsim 20$ GeV. The differences are smaller for $p_T^{\text{jet}} \approx 30$ GeV and for large R values Herwig++ shows an excess of events at low Σp_T and low N_{ch} for small p_T^{jet} ; at high p_T^{jet} it does a reasonable job of predicting the shape of the distributions but underestimates the normalization of Σp_T and N_{ch} distributions by about 50%.

The measured distributions in the away region, together with MC comparisons, are shown in Appendix A. The Σp_T , N_{ch} and \bar{p}_T all continue to rise with p_T^{jet} , as expected. This behavior indicates the presence of a second jet recoiling against the leading jet.

IX. DEPENDENCE OF THE UE ON R

The distributions of the UE observables change with the value of R used in the jet reconstruction. The variations are summarized in Figure 8, which compares the results obtained for the observables in the transverse region for $R = 0.2, 0.6$ and 1.0 . For low p_T^{jet} , the mean values of the Σp_T and N_{ch} densities are largest for the smallest value of R , while they are largest for the highest value of R at high p_T^{jet} . In contrast, the mean value of \bar{p}_T in the transverse region shows little variation with R .

As noted in Section I, the phenomenological description of jet production and the UE is complex. This is especially true in the low p_T^{jet} region where the distinction between the hard scattering process and the soft physics associated with the beam remnants is an artifact of the model used to parameterize this physics. Nevertheless, several general features of jet production are useful for interpreting the observed R dependence of the UE ob-

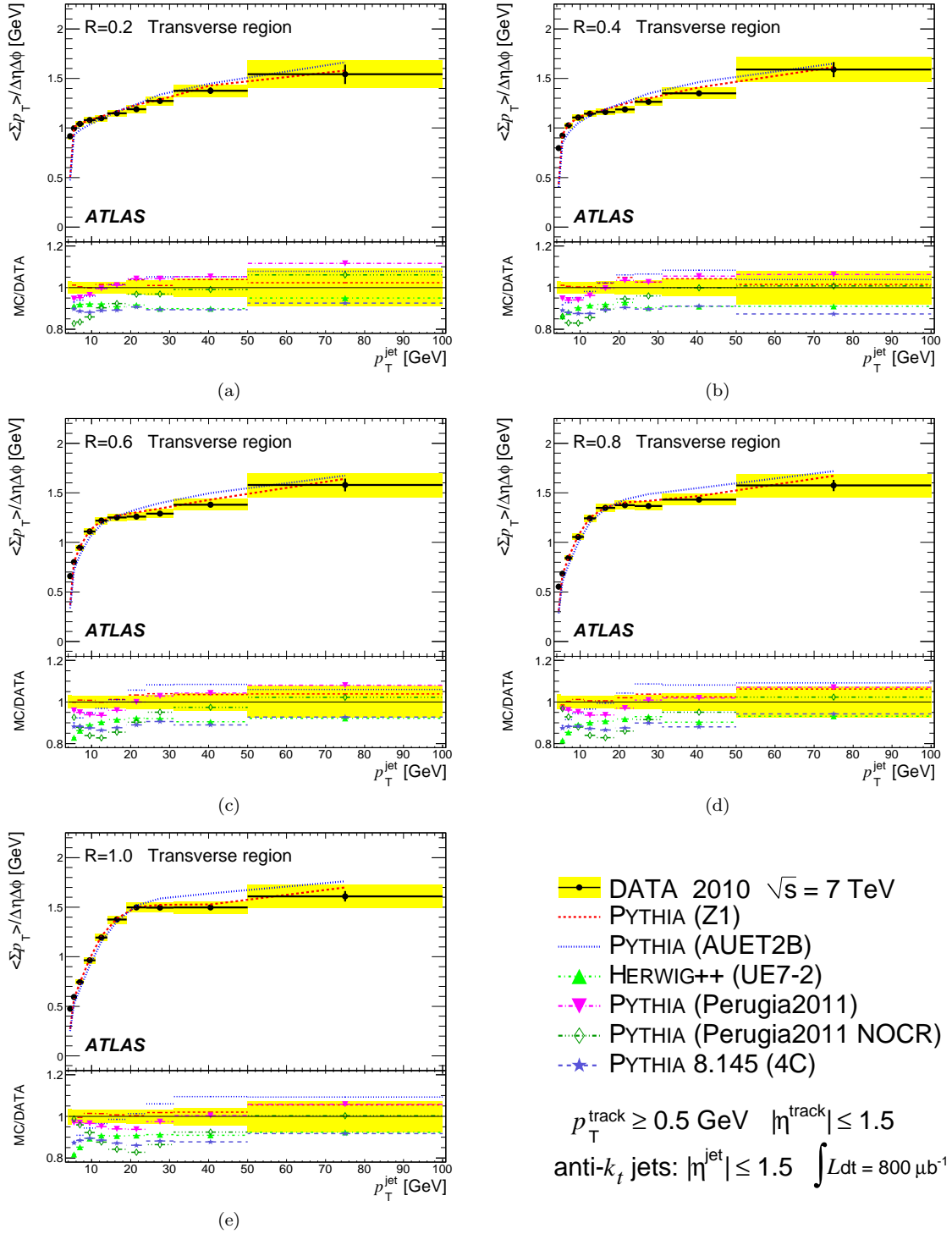


FIG. 2. The mean value, per unit $\eta - \phi$, of Σp_T in the transverse region, as a function of p_T^{jet} for (a) $R = 0.2$, (b) $R = 0.4$, (c) $R = 0.6$, (d) $R = 0.8$ and (e) $R = 1.0$. The shaded band shows the combined statistical and systematic uncertainty on the data. The data are compared to the predictions obtained with PYTHIA 6 using the AUET2B and Z1 tunes. The bottom insert shows the ratio of MC predictions to data for several recent MC tunes.

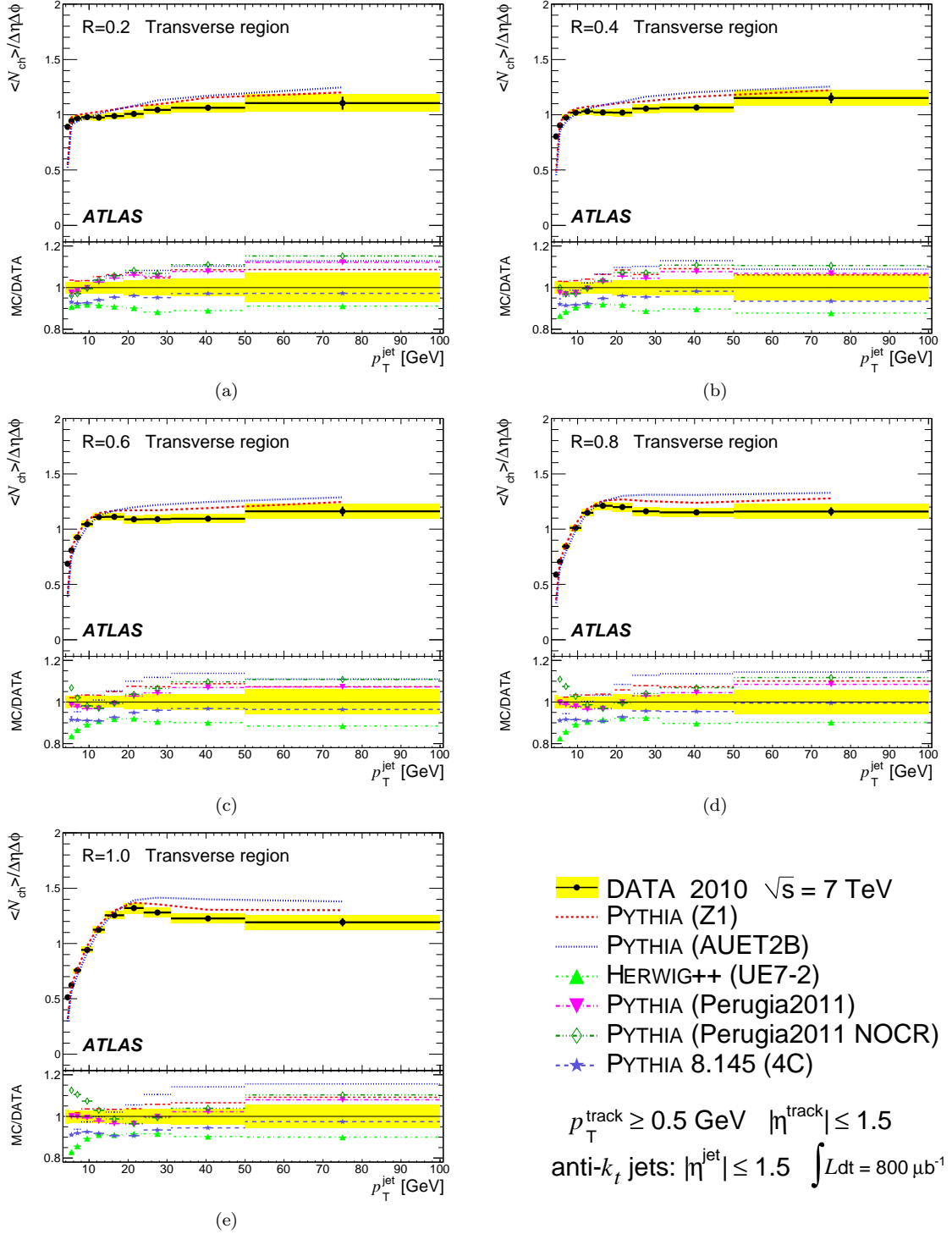


FIG. 3. The mean value, per unit $\eta - \phi$, of N_{ch} in the transverse region, as a function of $p_{\text{T}}^{\text{jet}}$ for (a) $R = 0.2$, (b) $R = 0.4$, (c) $R = 0.6$, (d) $R = 0.8$ and (e) $R = 1.0$. The shaded band shows the combined statistical and systematic uncertainty on the data. The data are compared to the predictions obtained with PYTHIA 6 using the AUET2B and Z1 tunes. The bottom insert shows the ratio of MC predictions to data for several recent MC tunes.

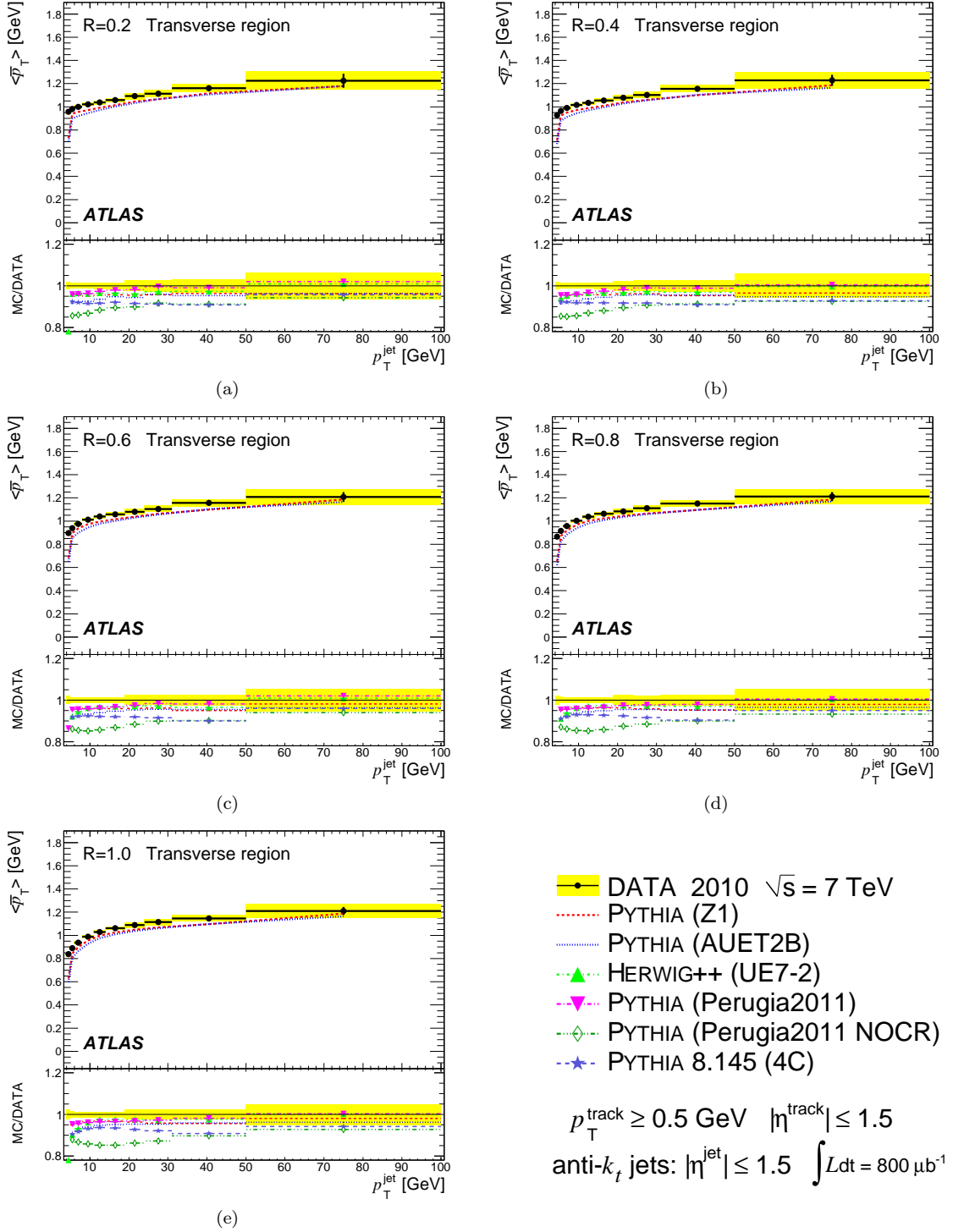


FIG. 4. The mean value of \bar{p}_T in the transverse region, as a function of p_T^{jet} for (a) $R = 0.2$, (b) $R = 0.4$, (c) $R = 0.6$, (d) $R = 0.8$ and (e) $R = 1.0$. The shaded band shows the combined statistical and systematic uncertainty on the data. The data are compared to the predictions obtained with PYTHIA 6 using the AUET2B and Z1 tunes. The bottom insert shows the ratio of MC predictions to data for several recent MC tunes.

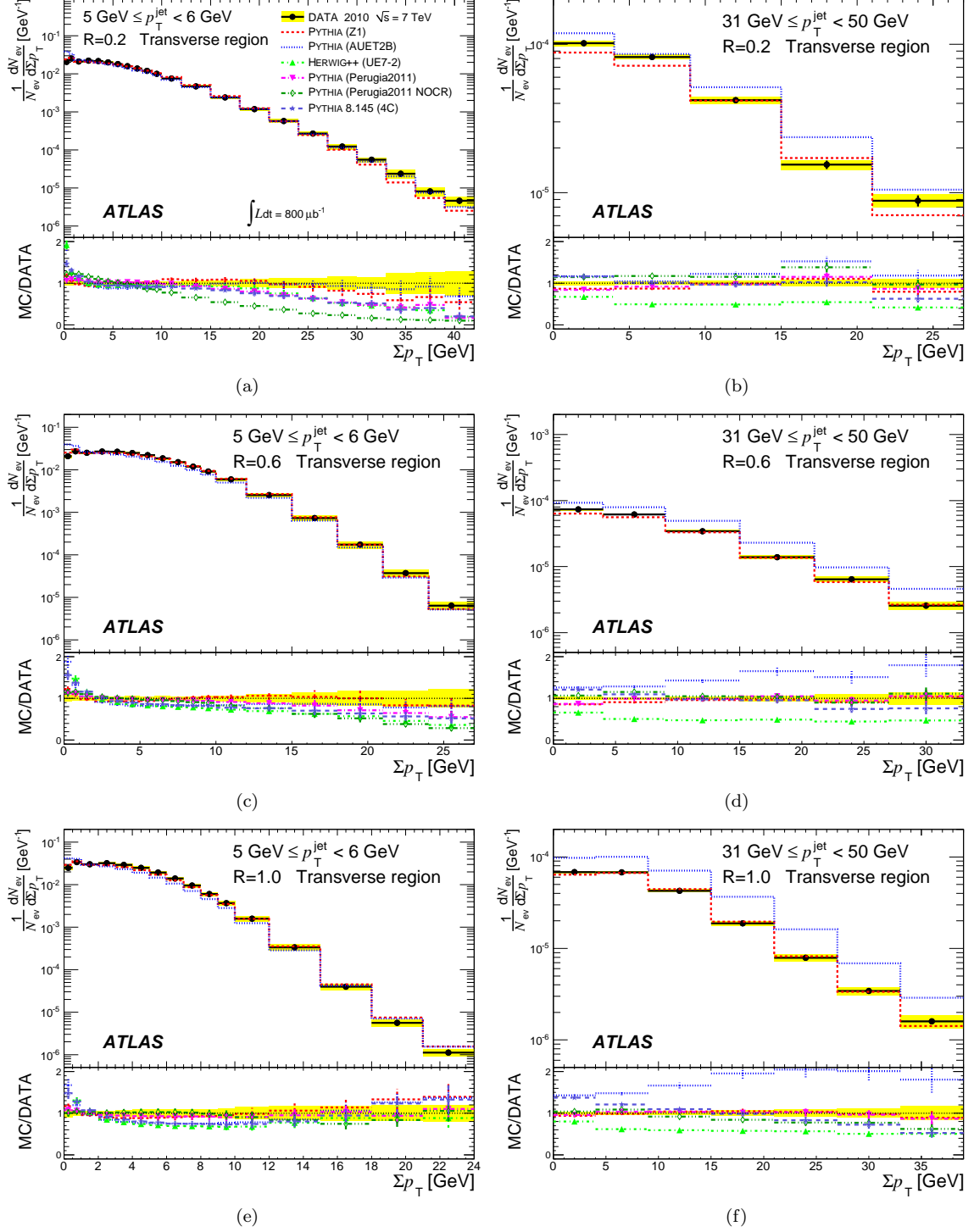


FIG. 5. Distributions of Σp_T in the transverse region for (a) $R = 0.2$ and $5 \text{ GeV} \leq p_T^{\text{jet}} < 6 \text{ GeV}$, (b) $R = 0.2$ and $31 \text{ GeV} \leq p_T^{\text{jet}} < 50 \text{ GeV}$, (c) $R = 0.6$ and $5 \text{ GeV} \leq p_T^{\text{jet}} < 6 \text{ GeV}$, (d) $R = 0.6$ and $31 \text{ GeV} \leq p_T^{\text{jet}} < 50 \text{ GeV}$ (e) $R = 1.0$ and $5 \text{ GeV} \leq p_T^{\text{jet}} < 6 \text{ GeV}$ and (f) $R = 1.0$ and $31 \text{ GeV} \leq p_T^{\text{jet}} < 50 \text{ GeV}$. The shaded band shows the combined statistical and systematic uncertainty on the data. The histograms show the predictions of several MC models with the same legend as in Fig. (a) and also Figs. [2, 3, 4].

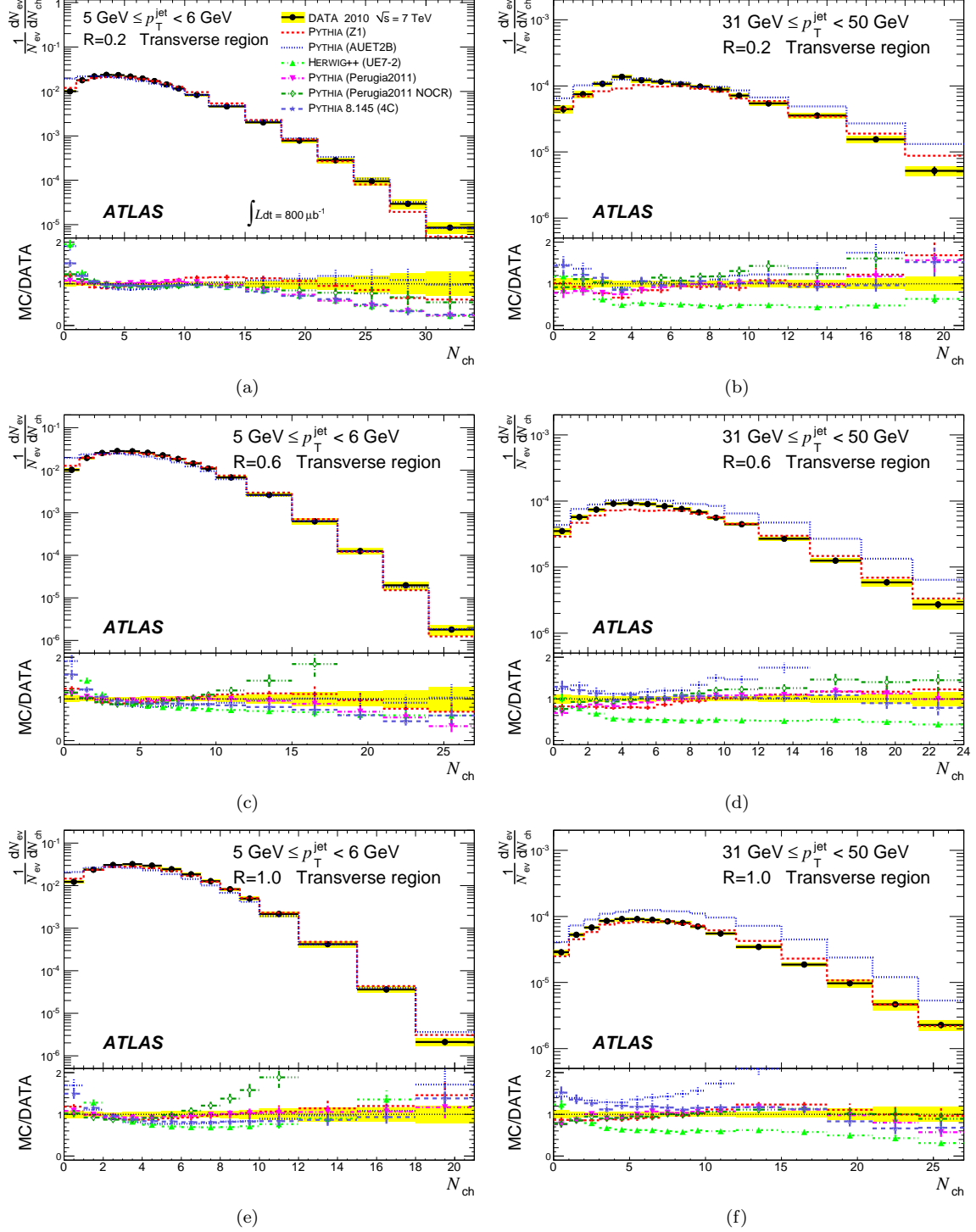


FIG. 6. Distributions of N_{ch} in the transverse region for (a) $R = 0.2$ and $5 \text{ GeV} \leq p_T^{\text{jet}} < 6 \text{ GeV}$, (b) $R = 0.2$ and $31 \text{ GeV} \leq p_T^{\text{jet}} < 50 \text{ GeV}$, (c) $R = 0.6$ and $5 \text{ GeV} \leq p_T^{\text{jet}} < 6 \text{ GeV}$, (d) $R = 0.6$ and $31 \text{ GeV} \leq p_T^{\text{jet}} < 50 \text{ GeV}$ (e) $R = 1.0$ and $5 \text{ GeV} \leq p_T^{\text{jet}} < 6 \text{ GeV}$ and (f) $R = 1.0$ and $31 \text{ GeV} \leq p_T^{\text{jet}} < 50 \text{ GeV}$. The shaded band shows the combined statistical and systematic uncertainty on the data. The histograms show the predictions of several MC models with the same legend as in Fig. (a) and also Figs. [2, 3, 4].

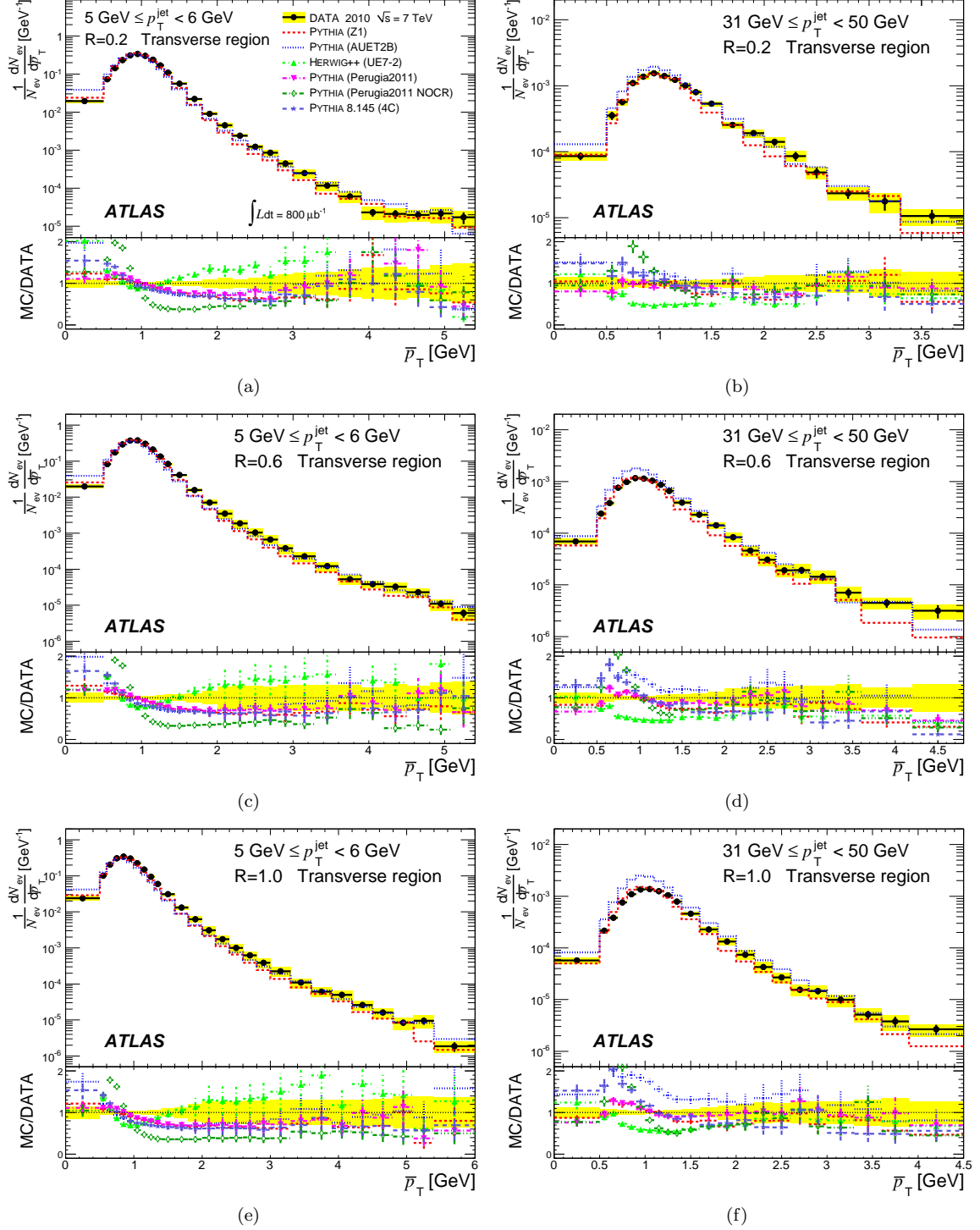


FIG. 7. Distributions of \bar{p}_T in the transverse region for (a) $R = 0.2$ and $5 \text{ GeV} \leq p_T^{\text{jet}} < 6 \text{ GeV}$, (b) $R = 0.2$ and $31 \text{ GeV} \leq p_T^{\text{jet}} < 50 \text{ GeV}$, (c) $R = 0.6$ and $5 \text{ GeV} \leq p_T^{\text{jet}} < 6 \text{ GeV}$, (d) $R = 0.6$ and $31 \text{ GeV} \leq p_T^{\text{jet}} < 50 \text{ GeV}$ (e) $R = 1.0$ and $5 \text{ GeV} \leq p_T^{\text{jet}} < 6 \text{ GeV}$ and (f) $R = 1.0$ and $31 \text{ GeV} \leq p_T^{\text{jet}} < 50 \text{ GeV}$. The shaded band shows the combined statistical and systematic uncertainty on the data. The histograms show the predictions of several MC models with the same legend as in Fig. (a) and also Figs. [2, 3, 4].

servables. For example, the inclusive jet cross section depends on R . Also, leading jets obtained with different R parameters will not in general have the same reconstructed centroid position, resulting in differences in the definitions of the transverse and away regions. Furthermore, the amount of transverse momentum collected in a jet increases with the value of R used for the reconstruction.

Measurements of the inclusive cross section for jets reconstructed from tracks show that this cross section increases significantly as the radius parameter R is increased [15]. Both the Z1 and AUET2B tunes of PYTHIA 6 do a remarkably good job of reproducing the measurements therein. The number of jets reconstructed in the data depends strongly on the value of R used in the anti- k_t algorithm. For the events passing the trigger and primary vertex requirements described in Section V, the fraction of events with at least one reconstructed jet with $p_T^{\text{jet}} > 4$ GeV and $|\eta| < 1.5$ varies from 4.4% to 19.8% as R is increased from 0.2 to 1.0. These additional jets reconstructed for large R largely populate the region of low p_T^{jet} . The results shown in Figure 8 indicate that including these jets reduces the average hadronic activity for $p_T^{\text{jet}} \lesssim 10$ GeV, i.e. the additional $R=1.0$ jets are found in events with less hadronic activity.

The difference in azimuthal angle between the leading jet reconstructed with $R = 0.2$ and the leading jet reconstructed with $R = 1.0$ has been studied as a function of p_T^{jet} . These studies demonstrate that event re-orientation effects due to changes in the reconstructed position of the leading jet for different values of R are small. For $p_T^{\text{jet}} \simeq 4$ GeV, 7% of events are reoriented by $\pi/3 \leq |\Delta\phi| \leq 2\pi/3$. For $p_T^{\text{jet}} \gtrsim 15$ GeV the effect is much smaller; less than 1% of events are reoriented.

For cases where jets reconstructed with different R parameters are matched, the p_T of the jet reconstructed with larger R will exceed that of the jet reconstructed with smaller R , leading to migration of events to bins with higher p_T^{jet} . Many physical processes influence the amount of migration as the radius parameter increases. These effects include the collection of additional fragmentation particles, the inclusion of additional hadrons produced via soft gluon radiation from the final-state parton, and the sweeping of particles from the UE into the jet cone. Attempts to compensate for the observed R -dependence by correcting p_T^{jet} using the average UE energy deposited within the jet cone were unsuccessful. This might be due to the fact that there is a correlation between the amount of p_T migration and the level of UE activity in the event because UE activity exhibits long-range correlations in η - ϕ . Events with higher UE activity will exhibit larger p_T migration as R is increased. Thus, the ability of the MC generators to model the variation of the UE with R depends not only on how well the generator reproduces the mean UE response, but also on how well it models the fluctuations in the UE and how correlated these fluctuations are spatially.

X. CONCLUSION

Observables sensitive to UE activity in events containing one or more charged-particle jets produced in pp collisions at $\sqrt{s} = 7$ TeV have been measured. The properties of the UE activity have been studied both in the transverse and away regions. The jets are reconstructed with the anti- k_t algorithm, with a radius parameter R varying between 0.2 and 1.0. Measurements of the evolution of the UE activity with R are also presented. Predictions from several MC tunes have been compared to the data. The predictions from PYTHIA 6 based on tunes that have been determined using LHC data, namely Z1, AUET2B and Perugia 2011, show reasonable agreement with the data, not only for the mean event activity but also for fluctuations in UE activity within events. Other tunes, such as Perugia 2011 NOCR, are disfavored by the data. The comparison of the predictions from PYTHIA 8.145 tune 4C and the Herwig++ 2.5.1 UE7-2 tune to the data indicates that additional tuning of UE parameters is necessary in these cases. The measurements presented here provide a testing ground for further development of the Monte Carlo models.

ACKNOWLEDGMENTS

We thank CERN for the very successful operation of the LHC, as well as the support staff from our institutions without whom ATLAS could not be operated efficiently.

We acknowledge the support of ANPCyT, Argentina; YerPhI, Armenia; ARC, Australia; BMWF, Austria; ANAS, Azerbaijan; SSTC, Belarus; CNPq and FAPESP, Brazil; NSERC, NRC and CFI, Canada; CERN; CONICYT, Chile; CAS, MOST and NSFC, China; COLCIENCIAS, Colombia; MSMT CR, MPO CR and VSC CR, Czech Republic; DNRF, DNSRC and Lundbeck Foundation, Denmark; EPLANET and ERC, European Union; IN2P3-CNRS, CEA-DSM/IRFU, France; GNAS, Georgia; BMBF, DFG, HGF, MPG and AvH Foundation, Germany; GSRT, Greece; ISF, MINERVA, GIF, DIP and Benoziyo Center, Israel; INFN, Italy; MEXT and JSPS, Japan; CNRST, Morocco; FOM and NWO, Netherlands; RCN, Norway; MNiSW, Poland; GRICES and FCT, Portugal; MERYS (MECTS), Romania; MES of Russia and ROSATOM, Russian Federation; JINR; MSTD, Serbia; MSSR, Slovakia; ARRS and MVZT, Slovenia; DST/NRF, South Africa; MICINN, Spain; SRC and Wallenberg Foundation, Sweden; SER, SNSF and Cantons of Bern and Geneva, Switzerland; NSC, Taiwan; TAEK, Turkey; STFC, the Royal Society and Leverhulme Trust, United Kingdom; DOE and NSF, United States of America.

The crucial computing support from all WLCG partners is acknowledged gratefully, in particular from CERN and the ATLAS Tier-1 facilities at TRIUMF (Canada), NDGF (Denmark, Norway, Sweden), CC-IN2P3 (France), KIT/GridKA (Germany), INFN-CNAF

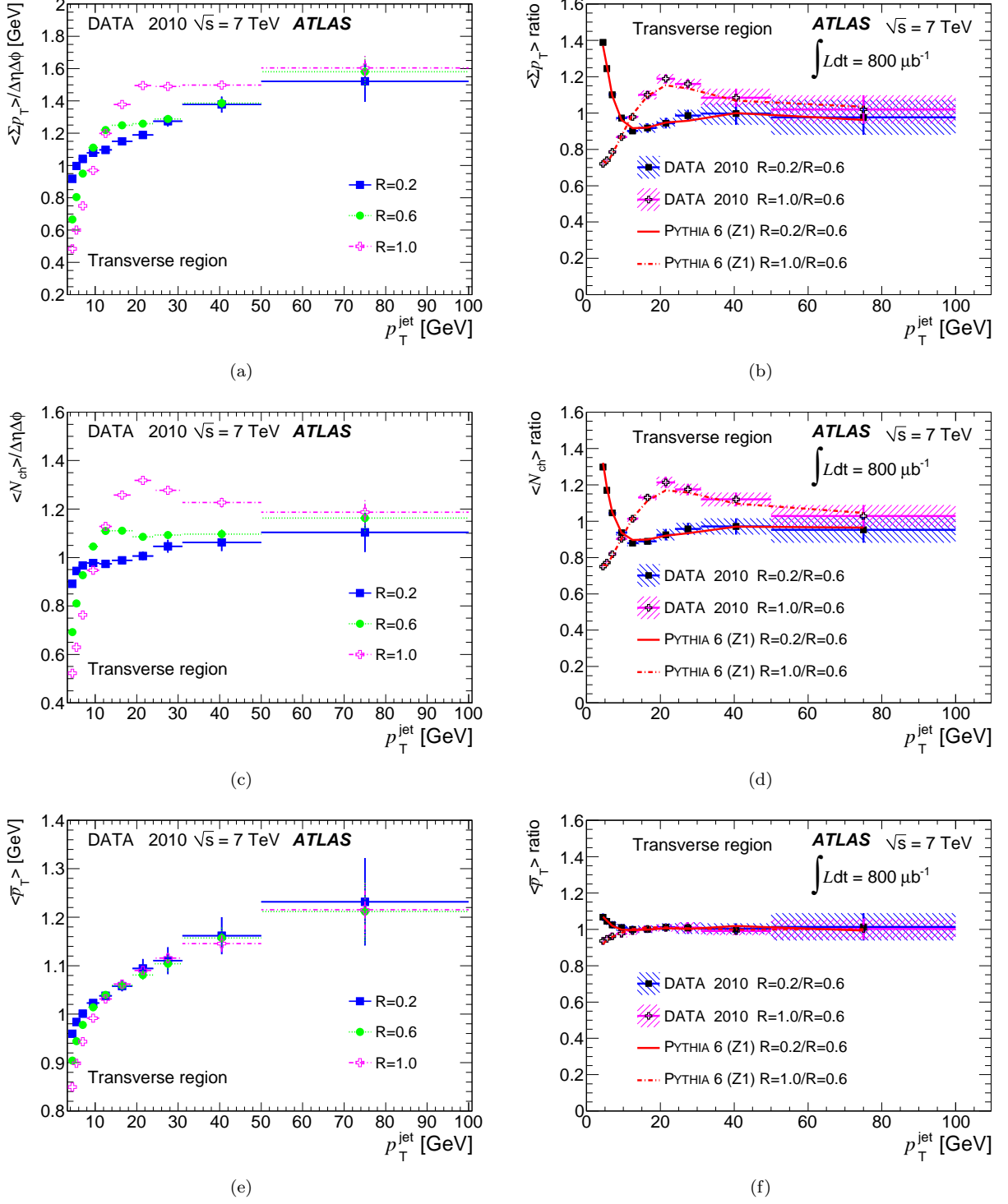


FIG. 8. The mean value of (a) Σp_T (per unit $\eta - \phi$), (c) N_{ch} (per unit $\eta - \phi$) and (e) \bar{p}_T in the transverse region as a function of p_T^{jet} for $R = 0.2$, $R = 0.6$ and $R = 1.0$; because the systematic uncertainties are correlated among the different R values, only statistical uncertainties are shown. And the ratio of the mean value of (b) Σp_T , (d) N_{ch} and (f) \bar{p}_T in the transverse region measured for $R = 0.2$ and $R = 1.0$ to that measured for $R = 0.6$. The shaded bands show the total uncertainty. The lines show the predictions of PYTHIA 6 with the Z1 tune; predictions for AUET2B show comparable agreement.

(Italy), NL-T1 (Netherlands), PIC (Spain), ASGC (Tai-

wan), RAL (UK) and BNL (USA) and in the Tier-2 facilities worldwide.

-
- [1] D. J. Gross and F. Wilczek, Phys. Rev. Lett. **30**, 1343 (1973).
- [2] H. D. Politzer, Phys. Rev. Lett. **30**, 1346 (1973).
- [3] ATLAS uses a right-handed coordinate system with its origin at the nominal interaction point (IP) in the center of the detector and the z -axis along the beam pipe. The x -axis points from the IP to the center of the LHC ring, and the y axis points upward. Cylindrical coordinates (r, ϕ) are used in the transverse plane, ϕ being the azimuthal angle around the beam pipe. The pseudorapidity is defined in terms of the polar angle θ as $\eta = -\ln \tan(\theta/2)$. The transverse momentum p_T is defined as $p_T \equiv \sqrt{E^2 - m^2} \sin(\theta)$, where E is the total energy and m is the mass.
- [4] R.K. Ellis, W.J. Stirling and B.R. Webber, *QCD and Collider Physics* (Cambridge University Press, 1996).
- [5] CDF Collaboration, Phys.Rev. **D70**, 072002 (2004).
- [6] CDF Collaboration, Phys.Rev. **D82**, 034001 (2010).
- [7] CMS Collaboration, Eur. Phys. J. **C70**, 555 (2010).
- [8] CMS Collaboration, JHEP **1109**, 109 (2011).
- [9] ATLAS Collaboration, Phys. Rev. D **83**, 112001 (2011).
- [10] ALICE Collaboration, CERN-PH-EP-2011-204, arXiv:1112.2082v2 [hep-ex] (2011).
- [11] ATLAS Collaboration, Eur. Phys. J. **C71**, 1636 (2011).
- [12] M. Cacciari, G. P. Salam, and G. Soyez, JHEP **04**, 063 (2008).
- [13] ATLAS Collaboration, JINST **3**, S08003 (2008).
- [14] ATLAS Collaboration, ATLAS-CONF-2010-068, <http://cdsweb.cern.ch/record/1299573> (2010).
- [15] ATLAS Collaboration, Phys. Rev. D **84** (2011).
- [16] T. Sjöstrand, S. Mrenna, and P. Z. Skands, JHEP **05**, 026 (2006).
- [17] A. Sherstnev and R. Thorne, Eur. Phys. J. **C55**, 553 (2008).
- [18] ATLAS Collaboration, New J. Phys. **13**, 053033 (2011).
- [19] ATLAS Collaboration, Eur. Phys. J. **C70**, 823 (2010).
- [20] S. Agostinelli *et al.* (The GEANT4 Collaboration), Nucl. Instrum. Meth. **A506**, 250 (2003).
- [21] J. Pumplin *et al.*, JHEP **07**, 012 (2002).
- [22] ATLAS Collaboration, ATL-PHYS-PUB-2010-002, <http://cdsweb.cern.ch/record/1247375> (2010).
- [23] T. Sjöstrand, S. Mrenna, and P. Z. Skands, Comput. Phys. Commun. **178**, 852 (2008).
- [24] ATLAS Collaboration, ATL-PHYS-PUB-2011-014, <http://cdsweb.cern.ch/record/1400677> (2011).
- [25] Rick Field, “Early LHC Underlying Event Data - Findings and Surprises,” (2010), arXiv:1010.3558v1.
- [26] S. Gieseke, D. Grellscheid, K. Hamilton, A. Papaefstathiou, S. Platzer, *et al.*, “Herwig++ 2.5 Release Note,” arXiv.1102.1672 (2011).
- [27] ATLAS Collaboration, ATLAS-CONF-2011-009, <http://cdsweb.cern.ch/record/1363300> (2011).
- [28] P. Z. Skands, Phys. Rev. **D82**, 074018 (2010).
- [29] R. Corke and T. Sjöstrand, JHEP **03**, 032 (2011).
- [30] J. Pumplin *et al.*, JHEP **02**, 032 (2006).
- [31] ATLAS Collaboration, ATLAS-CONF-2010-069, <http://cdsweb.cern.ch/record/1281344> (2010).
- [32] G. D’Agostini, Nucl. Instrum. Meth. **A362**, 487 (1995).
- [33] T. Adye, <http://hepunix.rl.ac.uk/~adye/software/unfold/RooUnf> (2007).
- [34] ATLAS Collaboration, New J.Phys. **13**, 053033 (2011).
- [35] ATLAS Collaboration, ATLAS-COM-CONF-2011-046, <http://cdsweb.cern.ch/record/1338575> (2011).
- [36] B. Efron, Annals of Statistics **7**, 1 (1979).

Appendix A: UE Distributions in the Away Region

The dependence on p_T^{jet} of the mean value of Σp_T , N_{ch} and \bar{p}_T for all five values of R is shown in Figures 9 through 11 for the away region. The Σp_T , N_{ch} and \bar{p}_T values all continue to rise with p_T^{jet} . The away region is expected to have smaller Σp_T than the towards region. This is mainly because the leading jet by definition has the highest summed transverse momentum and the distribution of the fraction of the momentum carried by charged particles is broad. For $p_T^{\text{jet}} \gtrsim 10$ GeV, the mean Σp_T contained in charged particles in the away region is typically between 60% (large p_T^{jet} and large R) and 100% (small p_T^{jet} and small R) of the leading jet p_T . Herwig++ overestimates \bar{p}_T for $p_T^{\text{jet}} \gtrsim 10$ GeV. PYTHIA 6 Perugia 2011 (without color reconnection) underestimates \bar{p}_T for $p_T^{\text{jet}} \lesssim 40$ GeV.

Figures 12 through 14 show the unfolded distributions $(1/N_{\text{ev}})dN_{\text{ev}}/d\Sigma p_T$, $(1/N_{\text{ev}})dN_{\text{ev}}/dN_{\text{ch}}$ and $(1/N_{\text{ev}})dN_{\text{ev}}/d\bar{p}_T$ in the away region for three representative values of R and for low (5–6 GeV) and high (31–50 GeV) bins of p_T^{jet} . Here N_{ev} is the number of events in the sample with $p_T^{\text{jet}} > 4$ GeV and $|\eta^{\text{jet}}| < 1.5$. Most of the MC models reproduce the shapes of the distributions reasonably, with PYTHIA 6 Z1 and Perugia 2011 providing the best agreement. PYTHIA 6 AUET2B predicts values of Σp_T and N_{ch} that are higher than the data at large p_T^{jet} .

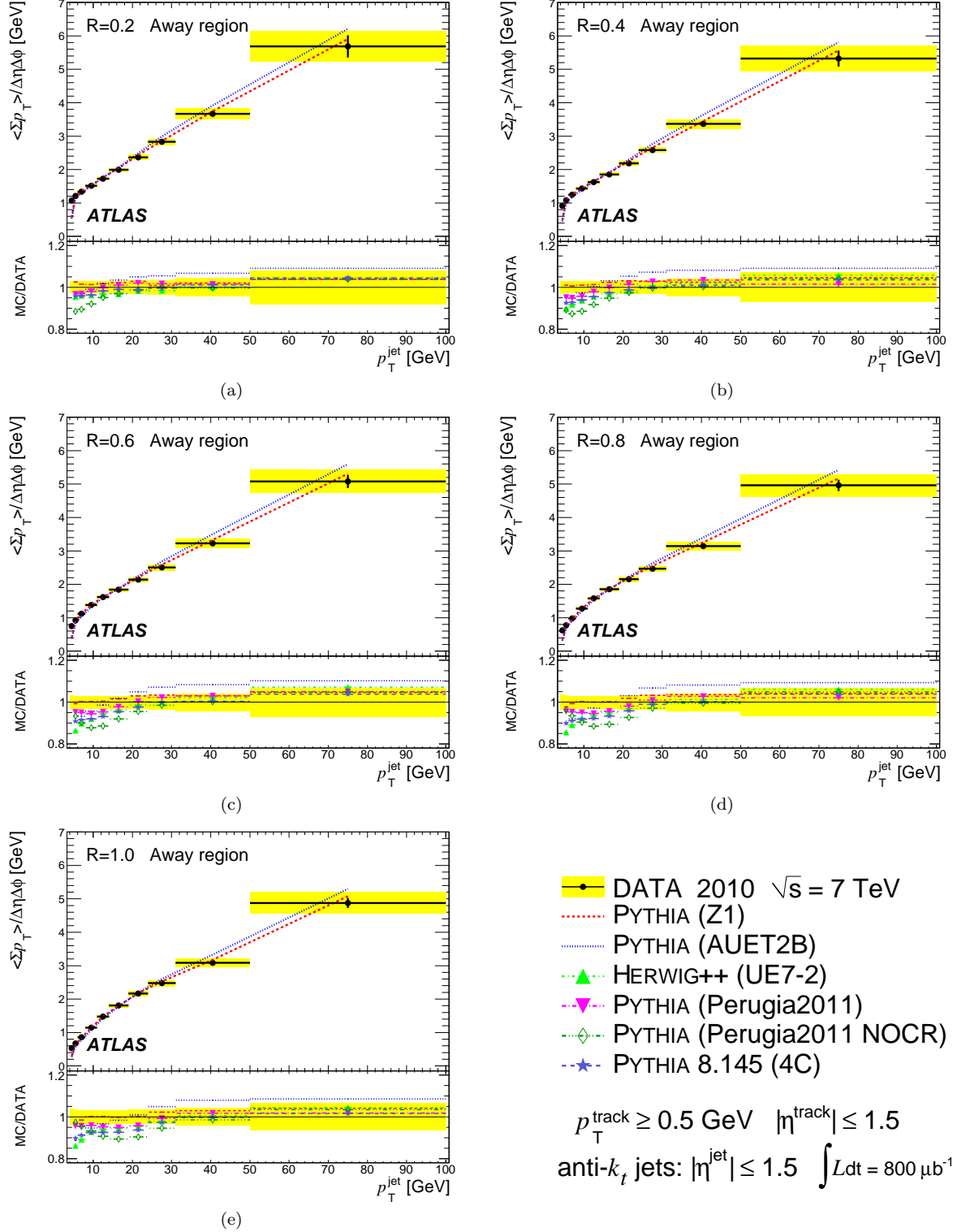


FIG. 9. The mean value, per unit $\eta - \phi$, of Σp_T in the away region, as a function of p_T^{jet} (a) for $R = 0.2$, (b) for $R = 0.4$, (c) for $R = 0.6$, (d) for $R = 0.8$ and (e) for $R = 1.0$. The shaded band shows the combined statistical and systematic uncertainty on the data. The data are compared to the predictions obtained with PYTHIA 6 using the AUET2B and Z1 tunes. The bottom insert shows the ratio of MC predictions to data for several recent MC tunes.

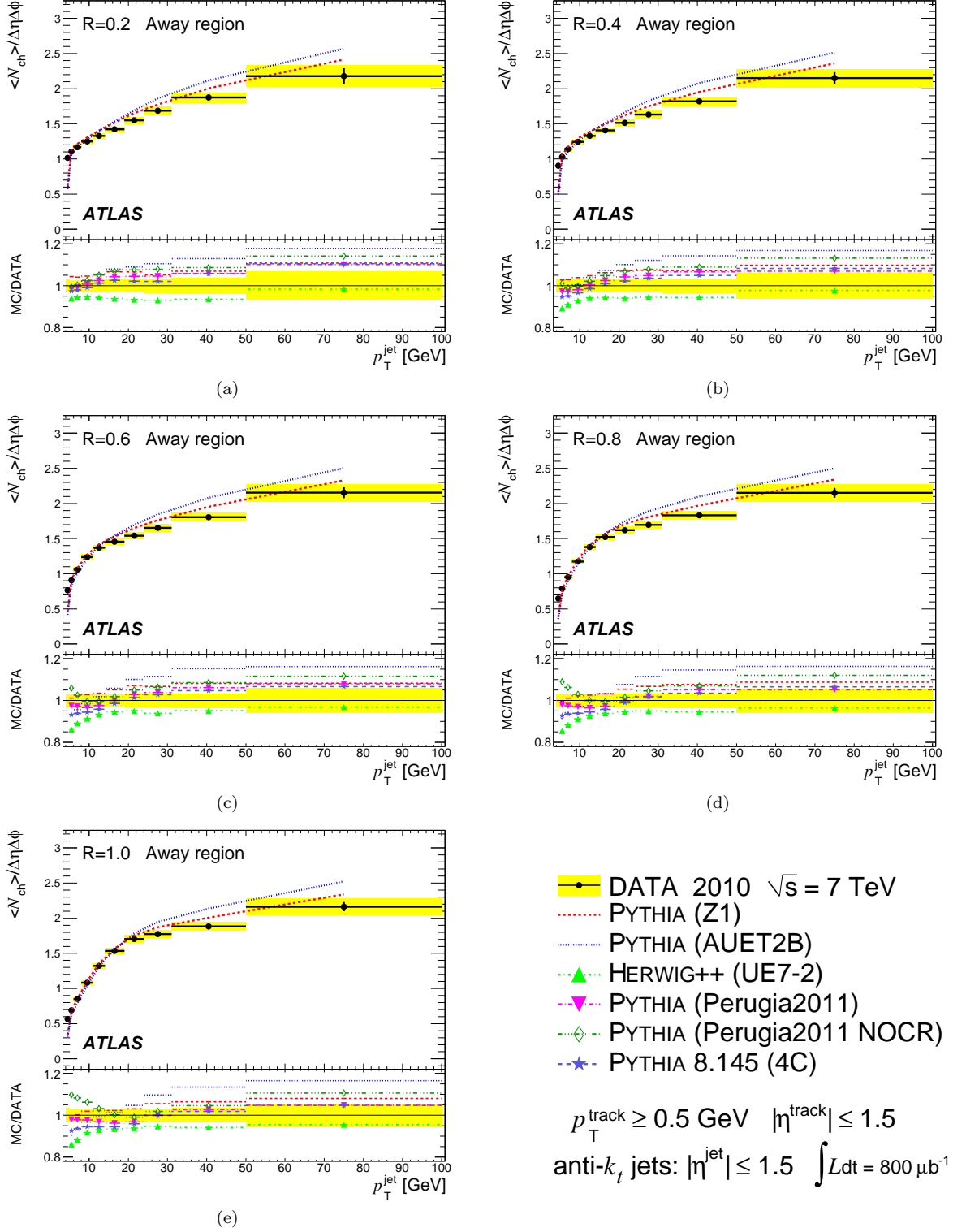


FIG. 10. The mean value, per unit $\eta - \phi$, of N_{ch} in the away region, as a function of $p_{\text{T}}^{\text{jet}}$ (a) for $R = 0.2$, (b) for $R = 0.4$, (c) for $R = 0.6$, (d) for $R = 0.8$ and (e) for $R = 1.0$. The shaded band shows the combined statistical and systematic uncertainty on the data. The data are compared to the predictions obtained with PYTHIA 6 using the AUET2B and Z1 tunes. The bottom insert shows the ratio of MC predictions to data for several recent MC tunes.

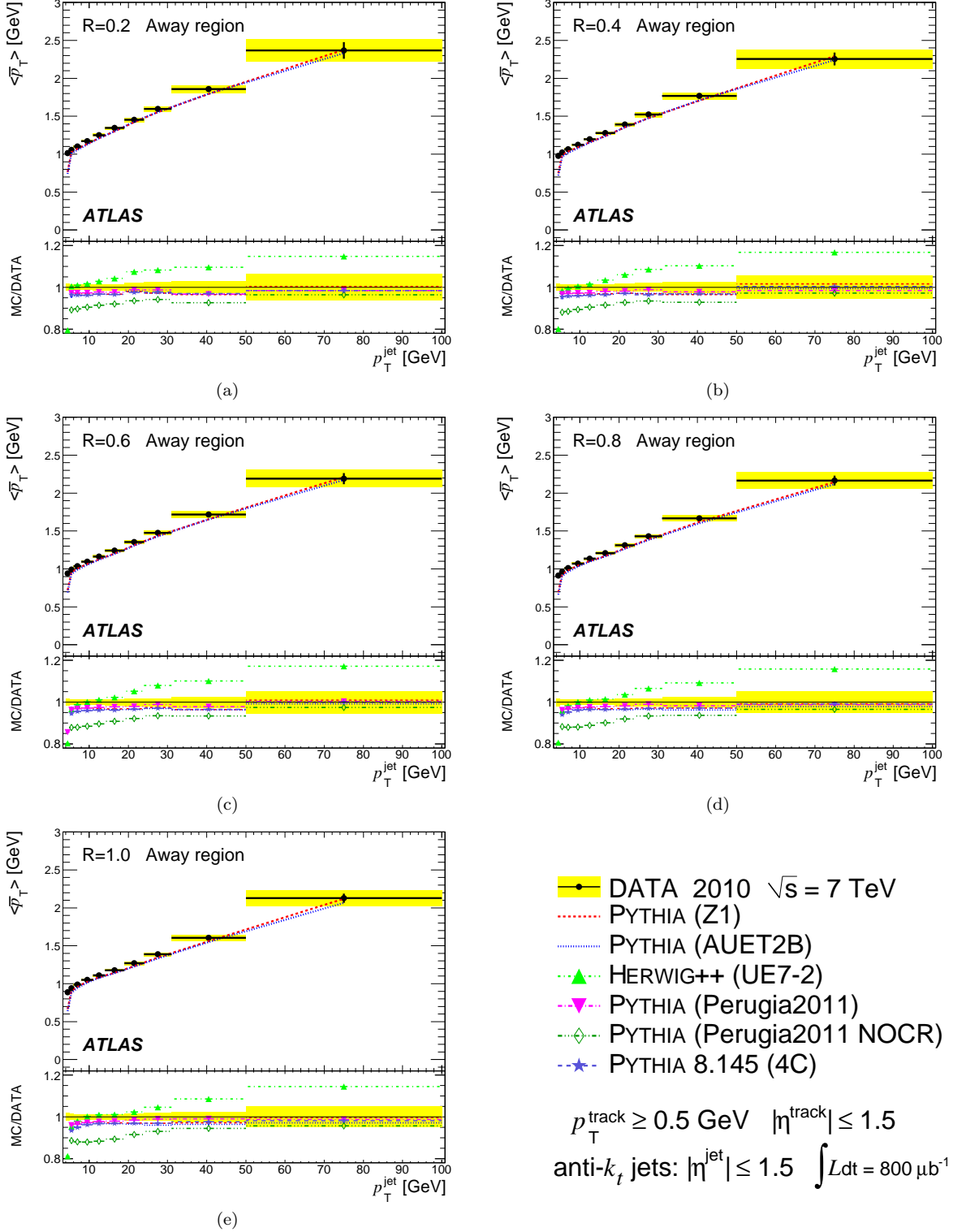


FIG. 11. The mean value of \bar{p}_T in the away region, as a function of p_T^{jet} (a) for $R = 0.2$, (b) for $R = 0.4$, (c) for $R = 0.6$, (d) for $R = 0.8$ and (e) for $R = 1.0$. The shaded band shows the combined statistical and systematic uncertainty on the data. The data are compared to the predictions obtained with PYTHIA 6 using the AUET2B and Z1 tunes. The bottom insert shows the ratio of MC predictions to data for several recent MC tunes.

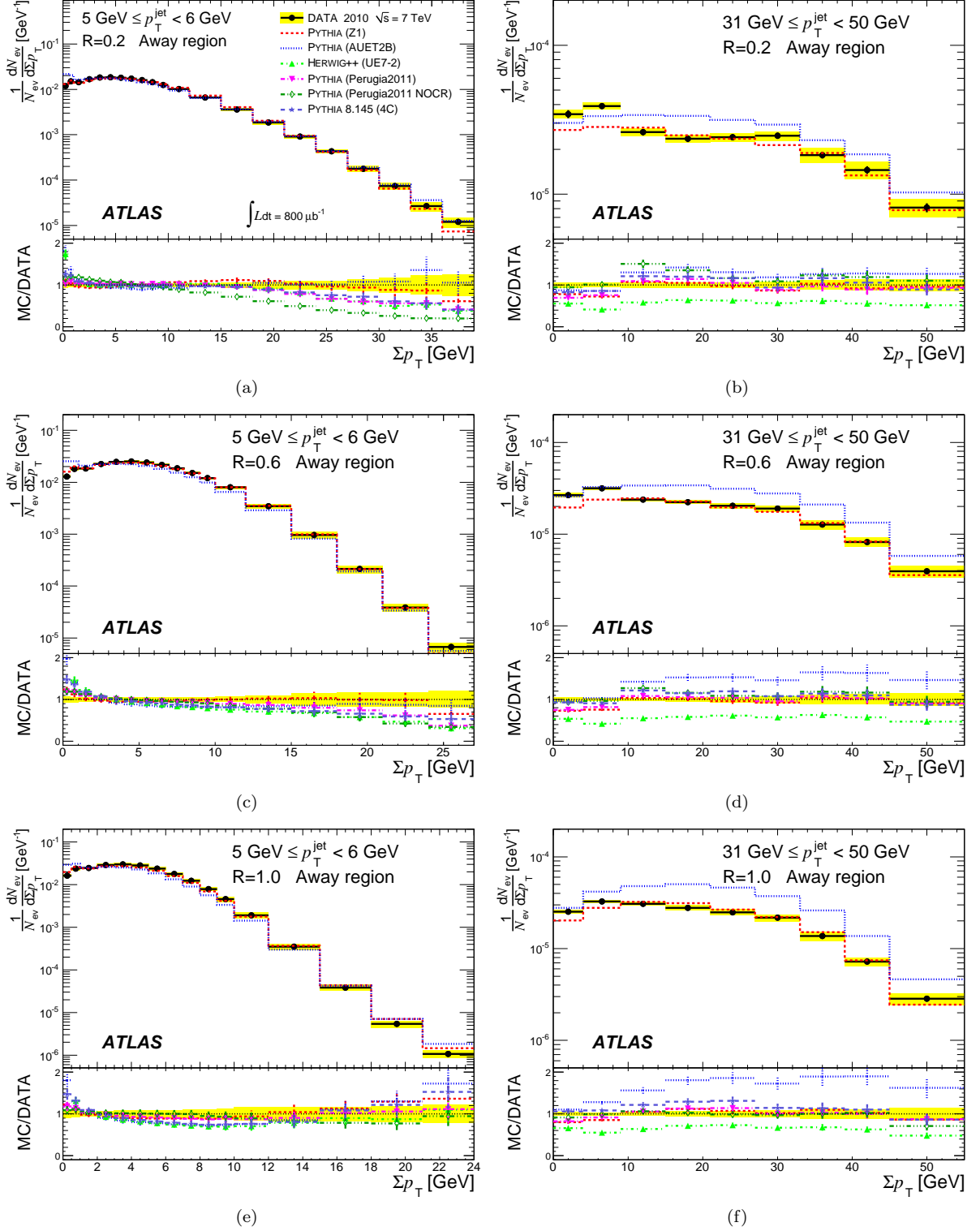


FIG. 12. Distributions of Σp_T in the away region for (a) $R = 0.2$ and $5 \text{ GeV} \leq p_T^{\text{jet}} < 6 \text{ GeV}$, (b) $R = 0.2$ and $31 \text{ GeV} \leq p_T^{\text{jet}} < 50 \text{ GeV}$, (c) $R = 0.6$ and $5 \text{ GeV} \leq p_T^{\text{jet}} < 6 \text{ GeV}$, (d) $R = 0.6$ and $31 \text{ GeV} \leq p_T^{\text{jet}} < 50 \text{ GeV}$ (e) $R = 1.0$ and $5 \text{ GeV} \leq p_T^{\text{jet}} < 6 \text{ GeV}$ and (f) $R = 1.0$ and $31 \text{ GeV} \leq p_T^{\text{jet}} < 50 \text{ GeV}$. The shaded band shows the combined statistical and systematic uncertainty on the data. The histograms show the predictions of several MC models. The bottom insert shows the ratio of the MC predictions to the data.

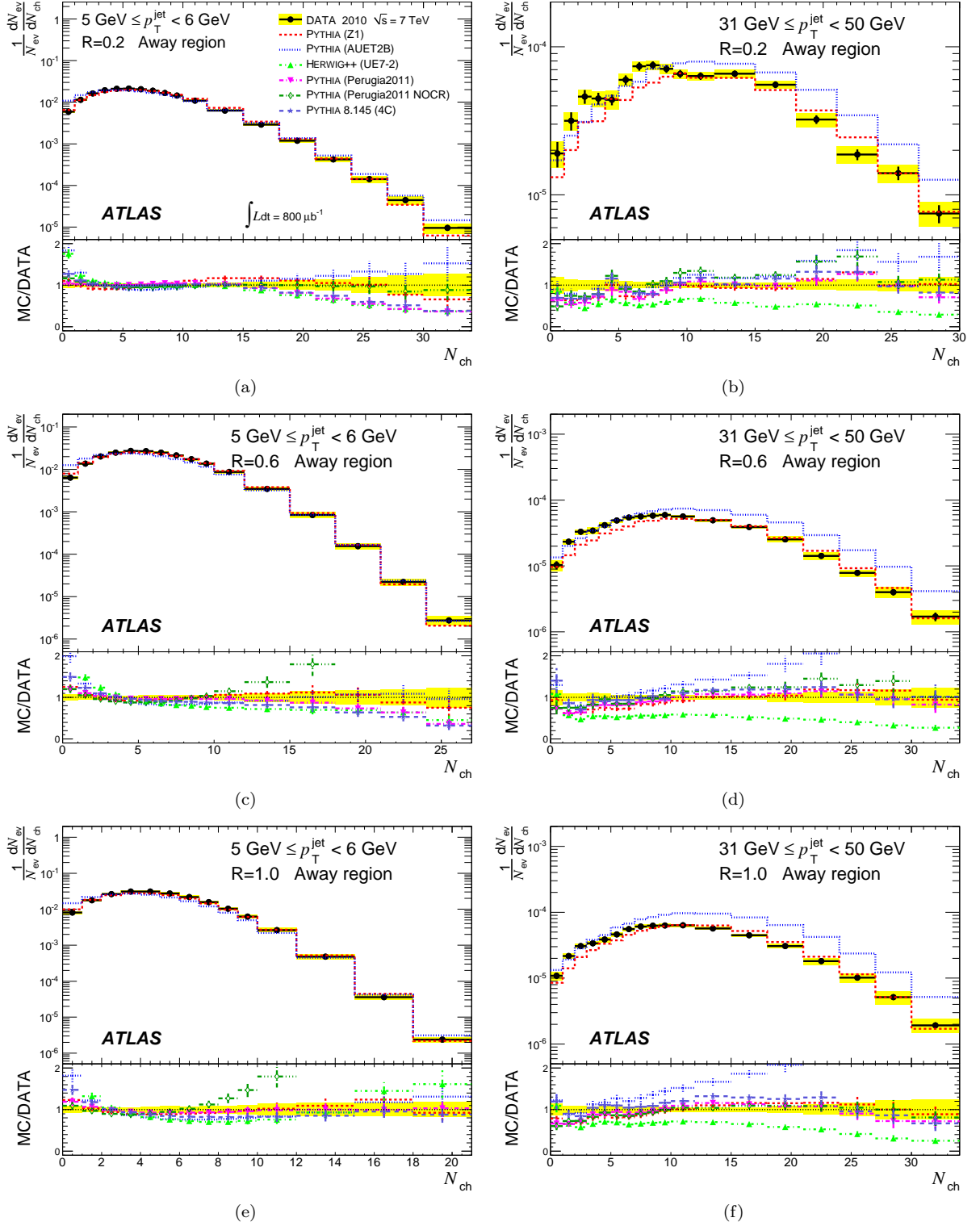


FIG. 13. Distributions of N_{ch} in the away region for (a) $R = 0.2$ and $5 \text{ GeV} \leq p_T^{jet} < 6 \text{ GeV}$, (b) $R = 0.2$ and $31 \text{ GeV} \leq p_T^{jet} < 50 \text{ GeV}$, (c) $R = 0.6$ and $5 \text{ GeV} \leq p_T^{jet} < 6 \text{ GeV}$, (d) $R = 0.6$ and $31 \text{ GeV} \leq p_T^{jet} < 50 \text{ GeV}$ (e) $R = 1.0$ and $5 \text{ GeV} \leq p_T^{jet} < 6 \text{ GeV}$ and (f) $R = 1.0$ and $31 \text{ GeV} \leq p_T^{jet} < 50 \text{ GeV}$. The shaded band shows the combined statistical and systematic uncertainty on the data. The histograms show the predictions of several MC models. The bottom insert shows the ratio of the MC predictions to the data.

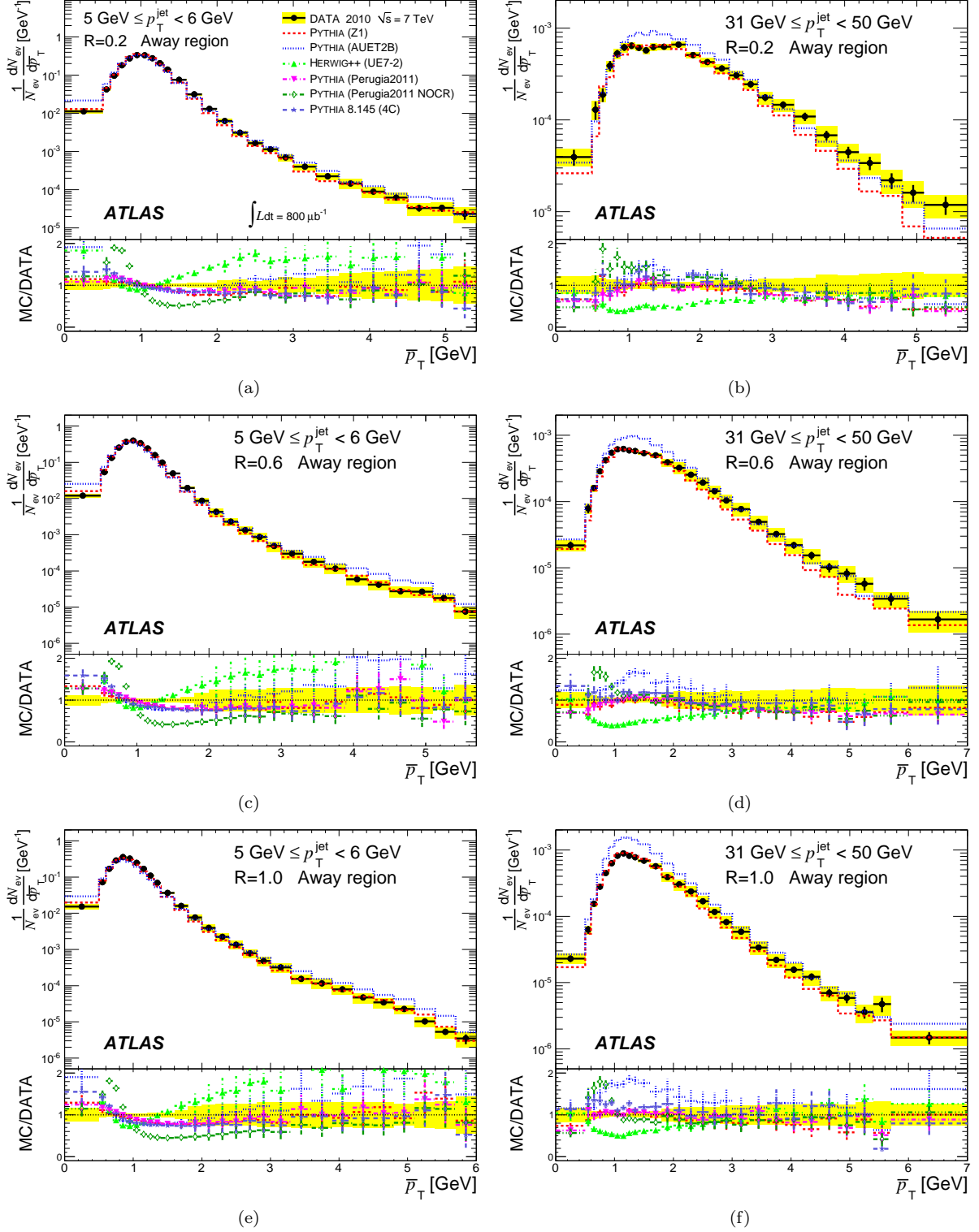


FIG. 14. Distributions of \bar{p}_T in the away region for (a) $R = 0.2$ and $5 \text{ GeV} \leq p_T^{\text{jet}} < 6 \text{ GeV}$, (b) $R = 0.2$ and $31 \text{ GeV} \leq p_T^{\text{jet}} < 50 \text{ GeV}$, (c) $R = 0.6$ and $5 \text{ GeV} \leq p_T^{\text{jet}} < 6 \text{ GeV}$, (d) $R = 0.6$ and $31 \text{ GeV} \leq p_T^{\text{jet}} < 50 \text{ GeV}$ (e) $R = 1.0$ and $5 \text{ GeV} \leq p_T^{\text{jet}} < 6 \text{ GeV}$ and (f) $R = 1.0$ and $31 \text{ GeV} \leq p_T^{\text{jet}} < 50 \text{ GeV}$. The shaded band shows the combined statistical and systematic uncertainty on the data. The histograms show the predictions of several MC models. The bottom insert shows the ratio of the MC predictions to the data.

The ATLAS Collaboration

G. Aad⁴⁸, B. Abbott¹¹¹, J. Abdallah¹¹, S. Abdel Khalek¹¹⁵, A.A. Abdelalim⁴⁹, O. Abdinov¹⁰, B. Abi¹¹², M. Abolins⁸⁸, O.S. AbouZeid¹⁵⁸, H. Abramowicz¹⁵³, H. Abreu¹³⁶, E. Acerbi^{89a,89b}, B.S. Acharya^{164a,164b}, L. Adamczyk³⁷, D.L. Adams²⁴, T.N. Addy⁵⁶, J. Adelman¹⁷⁶, S. Adomeit⁹⁸, P. Adragna⁷⁵, T. Adye¹²⁹, S. Aefsky²², J.A. Aguilar-Saavedra^{124b,a}, M. Aharrouche⁸¹, S.P. Ahlen²¹, F. Ahles⁴⁸, A. Ahmad¹⁴⁸, M. Ahsan⁴⁰, G. Aielli^{133a,133b}, T. Akdogan^{18a}, T.P.A. Åkesson⁷⁹, G. Akimoto¹⁵⁵, A.V. Akimov⁹⁴, A. Akiyama⁶⁶, M.S. Alam¹, M.A. Alam⁷⁶, J. Albert¹⁶⁹, S. Albrand⁵⁵, M. Aleksa²⁹, I.N. Aleksandrov⁶⁴, F. Alessandria^{89a}, C. Alexa^{25a}, G. Alexander¹⁵³, G. Alexandre⁴⁹, T. Alexopoulos⁹, M. Alhroob^{164a,164c}, M. Aliev¹⁵, G. Alimonti^{102a,102b}, J. Alison¹²⁰, B.M.M. Allbrooke¹⁷, P.P. Allport⁷³, S.E. Allwood-Spiers⁵³, J. Almond⁸², A. Aloisio^{102a,102b}, R. Alon¹⁷², A. Alonso⁷⁹, B. Alvarez Gonzalez⁸⁸, M.G. Alviggi^{102a,102b}, K. Amako⁶⁵, C. Amelung²², V.V. Ammosov^{128,*}, A. Amorim^{124a,b}, N. Amram¹⁵³, C. Anastopoulos²⁹, L.S. Ancu¹⁶, N. Andari¹¹⁵, T. Andeen³⁴, C.F. Anders^{58b}, G. Anders^{58a}, K.J. Anderson³⁰, A. Andreazza^{89a,89b}, V. Andrei^{58a}, X.S. Anduaga⁷⁰, P. Anger⁴³, A. Angerami³⁴, F. Anghinolfi²⁹, A. Anisenkov¹⁰⁷, N. Anjos^{124a}, A. Annovi⁴⁷, A. Antonaki⁸, M. Antonelli⁴⁷, A. Antonov⁹⁶, J. Antos^{144b}, F. Anulli^{132a}, S. Aoun⁸³, L. Aperio Bella⁴, R. Apolle^{118,c}, G. Arabidze⁸⁸, I. Aracena¹⁴³, Y. Arai⁶⁵, A.T.H. Arce⁴⁴, S. Arfaoui¹⁴⁸, J-F. Arguin¹⁴, E. Arik^{18a,*}, M. Arik^{18a}, A.J. Armbruster⁸⁷, O. Arnaez⁸¹, V. Arnal⁸⁰, C. Arnault¹¹⁵, A. Artamonov⁹⁵, G. Artoni^{132a,132b}, D. Arutinov²⁰, S. Asai¹⁵⁵, R. Asfandiyarov¹⁷³, S. Ask²⁷, B. Åsman^{146a,146b}, L. Asquith⁵, K. Assamagan²⁴, A. Astbury¹⁶⁹, B. Aubert⁴, E. Auge¹¹⁵, K. Augsten¹²⁷, M. Aurousseau^{145a}, G. Avolio¹⁶³, R. Avramidou⁹, D. Axen¹⁶⁸, G. Azuelos^{93,d}, Y. Azuma¹⁵⁵, M.A. Baak²⁹, G. Baccaglioni^{89a}, C. Bacci^{134a,134b}, A.M. Bach¹⁴, H. Bachacou¹³⁶, K. Bachas²⁹, M. Backes⁴⁹, M. Backhaus²⁰, E. Badescu^{25a}, P. Bagnaia^{132a,132b}, S. Bahinipati², Y. Bai^{32a}, D.C. Bailey¹⁵⁸, T. Bain¹⁵⁸, J.T. Baines¹²⁹, O.K. Baker¹⁷⁶, M.D. Baker²⁴, S. Baker⁷⁷, E. Banas³⁸, P. Banerjee⁹³, Sw. Banerjee¹⁷³, D. Banfi²⁹, A. Bangert¹⁵⁰, V. Bansal¹⁶⁹, H.S. Bansil¹⁷, L. Barak¹⁷², S.P. Baranov⁹⁴, A. Barbaro Galtieri¹⁴, T. Barber⁴⁸, E.L. Barberio⁸⁶, D. Barberis^{50a,50b}, M. Barbero²⁰, D.Y. Bardin⁶⁴, T. Barillari⁹⁹, M. Barisonzi¹⁷⁵, T. Barklow¹⁴³, N. Barlow²⁷, B.M. Barnett¹²⁹, R.M. Barnett¹⁴, A. Baroncelli^{134a}, G. Barone⁴⁹, A.J. Barr¹¹⁸, F. Barreiro⁸⁰, J. Barreiro Guimarães da Costa⁵⁷, P. Barrillon¹¹⁵, R. Bartoldus¹⁴³, A.E. Barton⁷¹, V. Bartsch¹⁴⁹, R.L. Bates⁵³, L. Batkova^{144a}, J.R. Batley²⁷, A. Battaglia¹⁶, M. Battistin²⁹, F. Bauer¹³⁶, H.S. Bawa^{143,e}, S. Beale⁹⁸, T. Beau⁷⁸, P.H. Beauchemin¹⁶¹, R. Becherle^{50a}, P. Bechtel²⁰, H.P. Beck¹⁶, A.K. Becker¹⁷⁵, S. Becker⁹⁸, M. Beckingham¹³⁸, K.H. Becks¹⁷⁵, A.J. Beddall^{18c}, A. Beddall^{18c}, S. Bedikian¹⁷⁶, V.A. Bednyakov⁶⁴, C.P. Bee⁸³, M. Begel²⁴, S. Behar Harpaz¹⁵², M. Beimforde⁹⁹, C. Belanger-Champagne⁸⁵, P.J. Bell⁴⁹, W.H. Bell⁴⁹, G. Bella¹⁵³, L. Bellagamba^{19a}, F. Bellina²⁹, M. Bellomo²⁹, A. Belloni⁵⁷, O. Beloborodova^{107,f}, K. Belotskiy⁹⁶, O. Beltramello²⁹, O. Benary¹⁵³, D. Bencheikroun^{135a}, K. Bendtz^{146a,146b}, N. Benekos¹⁶⁵, Y. Benhammou¹⁵³, E. Benhar Nocchi⁴⁹, J.A. Benitez Garcia^{159b}, D.P. Benjamin⁴⁴, M. Benoit¹¹⁵, J.R. Bensinger²², K. Benslama¹³⁰, S. Bentvelsen¹⁰⁵, D. Berge²⁹, E. Bergeas Kuutmann⁴¹, N. Berger⁴, F. Berghaus¹⁶⁹, E. Berglund¹⁰⁵, J. Beringer¹⁴, P. Bernat⁷⁷, R. Bernhard⁴⁸, C. Bernius²⁴, T. Berry⁷⁶, C. Bertella⁸³, A. Bertin^{19a,19b}, F. Bertolucci^{122a,122b}, M.I. Besana^{89a,89b}, G.J. Besjes¹⁰⁴, N. Besson¹³⁶, S. Bethke⁹⁹, W. Bhimji⁴⁵, R.M. Bianchi²⁹, M. Bianco^{72a,72b}, O. Biebel⁹⁸, S.P. Bieniek⁷⁷, K. Bierwagen⁵⁴, J. Biesiada¹⁴, M. Biglietti^{134a}, H. Bilokon⁴⁷, M. Bindi^{19a,19b}, S. Binet¹¹⁵, A. Bingul^{18c}, C. Bini^{132a,132b}, C. Biscarat¹⁷⁸, U. Bitenc⁴⁸, K.M. Black²¹, R.E. Blair⁵, J.-B. Blanchard¹³⁶, G. Blanchot²⁹, T. Blazek^{144a}, C. Blocker²², J. Blocki³⁸, A. Blondel⁴⁹, W. Blum⁸¹, U. Blumenschein⁵⁴, G.J. Bobbink¹⁰⁵, V.B. Bobrovnikov¹⁰⁷, S.S. Bocchetta⁷⁹, A. Bocci⁴⁴, C.R. Boddy¹¹⁸, M. Boehler⁴¹, J. Boek¹⁷⁵, N. Boelaert³⁵, J.A. Bogaerts²⁹, A. Bogdanchikov¹⁰⁷, A. Bogouch^{90,*}, C. Bohm^{146a}, J. Bohm¹²⁵, V. Boisvert⁷⁶, T. Bold³⁷, V. Boldea^{25a}, N.M. Bolnet¹³⁶, M. Bomben⁷⁸, M. Bona⁷⁵, M. Bondioli¹⁶³, M. Boonekamp¹³⁶, C.N. Booth¹³⁹, S. Bordini⁷⁸, C. Borer¹⁶, A. Borisov¹²⁸, G. Borissov⁷¹, I. Borjanovic^{12a}, M. Borri⁸², S. Borroni⁸⁷, V. Bortolotto^{134a,134b}, K. Bos¹⁰⁵, D. Boscherini^{19a}, M. Bosman¹¹, H. Boterenbrood¹⁰⁵, D. Botterill¹²⁹, J. Bouchami⁹³, J. Boudreau¹²³, E.V. Bouhova-Thacker⁷¹, D. Boumediene³³, C. Bourdarios¹¹⁵, N. Bousson⁸³, A. Boveia³⁰, J. Boyd²⁹, I.R. Boyko⁶⁴, N.I. Bozhko¹²⁸, I. Bozovic-Jelisavcic^{12b}, J. Bracinik¹⁷, P. Branchini^{134a}, A. Brandt⁷, G. Brandt¹¹⁸, O. Brandt⁵⁴, U. Bratzler¹⁵⁶, B. Brau⁸⁴, J.E. Brau¹¹⁴, H.M. Braun^{175,*}, B. Brelief¹⁵⁸, J. Bremer²⁹, K. Brendlinger¹²⁰, R. Brenner¹⁶⁶, S. Bressler¹⁷², D. Britton⁵³, F.M. Brochu²⁷, I. Brock²⁰, R. Brock⁸⁸, E. Brodet¹⁵³, F. Broggi^{89a}, C. Bromberg⁸⁸, J. Bronner⁹⁹, G. Brooijmans³⁴, W.K. Brooks^{31b}, G. Brown⁸², H. Brown⁷, P.A. Bruckman de Renstrom³⁸, D. Bruncko^{144b}, R. Brunelie⁴⁸, S. Brunet⁶⁰, A. Bruni^{19a}, G. Bruni^{19a}, M. Bruschi^{19a}, T. Buanes¹³, Q. Buat⁵⁵, F. Bucci⁴⁹, J. Buchanan¹¹⁸, P. Buchholz¹⁴¹, R.M. Buckingham¹¹⁸, A.G. Buckley⁴⁵, S.I. Buda^{25a}, I.A. Budagov⁶⁴, B. Budick¹⁰⁸, V. Büscher⁸¹, L. Bugge¹¹⁷, O. Bulekov⁹⁶, A.C. Bundock⁷³, M. Bunse⁴², T. Buran¹¹⁷, H. Burkhardt²⁹, S. Burdin⁷³, T. Burgess¹³, S. Burke¹²⁹, E. Busato³³, P. Bussey⁵³, C.P. Buszello¹⁶⁶, B. Butler¹⁴³, J.M. Butler²¹, C.M. Buttar⁵³, J.M. Butterworth⁷⁷, W. Buttinger²⁷, S. Cabrera Urbán¹⁶⁷, D. Caforio^{19a,19b}, O. Cakir^{3a}, P. Calafiura¹⁴, G. Calderini⁷⁸, P. Calfayan⁹⁸, R. Calkins¹⁰⁶, L.P. Caloba^{23a}, R. Caloi^{132a,132b}, D. Calvet³³, S. Calvet³³, R. Camacho Toro³³, P. Camarri^{133a,133b}, D. Cameron¹¹⁷, L.M. Caminada¹⁴, S. Campana²⁹, M. Campanelli⁷⁷, V. Canale^{102a,102b}, F. Canelli^{30,g}, A. Canepa^{159a}, J. Cantero⁸⁰, R. Cantrill⁷⁶, L. Capasso^{102a,102b}, M.D.M. Capeans Garrido²⁹, I. Caprini^{25a}, M. Caprini^{25a}, D. Capriotti⁹⁹,

M. Capua^{36a,36b}, R. Caputo⁸¹, R. Cardarelli^{133a}, T. Carli²⁹, G. Carlino^{102a}, L. Carminati^{89a,89b}, B. Caron⁸⁵,
 S. Caron¹⁰⁴, E. Carquin^{31b}, G.D. Carrillo Montoya¹⁷³, A.A. Carter⁷⁵, J.R. Carter²⁷, J. Carvalho^{124a,h},
 D. Casadei¹⁰⁸, M.P. Casado¹¹, M. Cascella^{122a,122b}, C. Caso^{50a,50b,*}, A.M. Castaneda Hernandez^{173,i},
 E. Castaneda-Miranda¹⁷³, V. Castillo Gimenez¹⁶⁷, N.F. Castro^{124a}, G. Cataldi^{72a}, P. Catastini⁵⁷, A. Catinaccio²⁹,
 J.R. Catmore²⁹, A. Cattai²⁹, G. Cattani^{133a,133b}, S. Caughron⁸⁸, P. Cavalleri⁷⁸, D. Cavalli^{89a}, M. Cavalli-Sforza¹¹,
 V. Cavasinni^{122a,122b}, F. Ceradini^{134a,134b}, A.S. Cerqueira^{23b}, A. Cerri²⁹, L. Cerrito⁷⁵, F. Cerutti⁴⁷, S.A. Cetin^{18b},
 A. Chafaq^{135a}, D. Chakraborty¹⁰⁶, I. Chalupkova¹²⁶, K. Chan², B. Chapleau⁸⁵, J.D. Chapman²⁷, J.W. Chapman⁸⁷,
 E. Chareyre⁷⁸, D.G. Charlton¹⁷, V. Chavda⁸², C.A. Chavez Barajas²⁹, S. Cheatham⁸⁵, S. Chekanov⁵,
 S.V. Chekulaev^{159a}, G.A. Chelkov⁶⁴, M.A. Chelstowska¹⁰⁴, C. Chen⁶³, H. Chen²⁴, S. Chen^{32c}, X. Chen¹⁷³,
 A. Cheplakov⁶⁴, R. Cherkaoui El Moursli^{135e}, V. Chernyatin²⁴, E. Cheu⁶, S.L. Cheung¹⁵⁸, L. Chevalier¹³⁶,
 G. Chiefari^{102a,102b}, L. Chikovani^{51a,*}, J.T. Childers²⁹, A. Chilingarov⁷¹, G. Chiodini^{72a}, A.S. Chisholm¹⁷,
 R.T. Chislett⁷⁷, M.V. Chizhov⁶⁴, G. Choudalakis³⁰, S. Chouridou¹³⁷, I.A. Christidi⁷⁷, A. Christov⁴⁸,
 D. Chromek-Burckhart²⁹, M.L. Chu¹⁵¹, J. Chudoba¹²⁵, G. Ciapetti^{132a,132b}, A.K. Ciftci^{3a}, R. Ciftci^{3a}, D. Cinca³³,
 V. Cindro⁷⁴, C. Ciocca^{19a,19b}, A. Ciocio¹⁴, M. Cirilli⁸⁷, M. Citterio^{89a}, M. Ciubancan^{25a}, A. Clark⁴⁹, P.J. Clark⁴⁵,
 W. Cleland¹²³, J.C. Clemens⁸³, B. Clement⁵⁵, C. Clement^{146a,146b}, Y. Coadou⁸³, M. Cobal^{164a,164c}, A. Cocco¹³⁸,
 J. Cochran⁶³, P. Coe¹¹⁸, J.G. Cogan¹⁴³, J. Coggeshall¹⁶⁵, E. Cogneras¹⁷⁸, J. Colas⁴, A.P. Colijn¹⁰⁵, N.J. Collins¹⁷,
 C. Collins-Tooth⁵³, J. Collot⁵⁵, T. Colombo^{119a,119b}, G. Colon⁸⁴, P. Conde Muño^{124a}, E. Coniavitis¹¹⁸,
 M.C. Conidi¹¹, S.M. Consonni^{89a,89b}, V. Consorti⁴⁸, S. Constantinescu^{25a}, C. Conta^{119a,119b}, G. Conti⁵⁷,
 F. Conventi^{102a,j}, M. Cooke¹⁴, B.D. Cooper⁷⁷, A.M. Cooper-Sarkar¹¹⁸, K. Copic¹⁴, T. Cornelissen¹⁷⁵,
 M. Corradi^{19a}, F. Corriveau^{85,k}, A. Cortes-Gonzalez¹⁶⁵, G. Cortiana⁹⁹, G. Costa^{89a}, M.J. Costa¹⁶⁷, D. Costanzo¹³⁹,
 T. Costin³⁰, D. Côté²⁹, L. Courneyea¹⁶⁹, G. Cowan⁷⁶, C. Cowden²⁷, B.E. Cox⁸², K. Cranmer¹⁰⁸,
 F. Crescioli^{122a,122b}, M. Cristinziani²⁰, G. Crosetti^{36a,36b}, R. Crupi^{72a,72b}, S. Crépe-Renaudin⁵⁵, C.-M. Cuciuc^{25a},
 C. Cuenca Almenar¹⁷⁶, T. Cuhadar Donszelmann¹³⁹, M. Curatolo⁴⁷, C.J. Curtis¹⁷, C. Cuthbert¹⁵⁰, P. Cwetanski⁶⁰,
 H. Czirr¹⁴¹, P. Czodrowski⁴³, Z. Czczula¹⁷⁶, S. D'Auria⁵³, M. D'Onofrio⁷³, A. D'Orazio^{132a,132b},
 M.J. Da Cunha Sargedas De Sousa^{124a}, C. Da Via⁸², W. Dabrowski³⁷, A. Dafinca¹¹⁸, T. Dai⁸⁷, C. Dallapiccola⁸⁴,
 M. Dam³⁵, M. Dameri^{50a,50b}, D.S. Damiani¹³⁷, H.O. Danielsson²⁹, V. Dao⁴⁹, G. Darbo^{50a}, G.L. Darlea^{25b},
 W. Davey²⁰, T. Davidek¹²⁶, N. Davidson⁸⁶, R. Davidson⁷¹, E. Davies^{118,c}, M. Davies⁹³, A.R. Davison⁷⁷,
 Y. Davygora^{58a}, E. Dawe¹⁴², I. Dawson¹³⁹, R.K. Daya-Ishmukhametova²², K. De⁷, R. de Asmundis^{102a},
 S. De Castro^{19a,19b}, S. De Cecco⁷⁸, J. de Graat⁹⁸, N. De Groot¹⁰⁴, P. de Jong¹⁰⁵, C. De La Taille¹¹⁵,
 H. De la Torre⁸⁰, F. De Lorenzi⁶³, L. de Mora⁷¹, L. De Nooij¹⁰⁵, D. De Pedis^{132a}, A. De Salvo^{132a},
 U. De Sanctis^{164a,164c}, A. De Santo¹⁴⁹, J.B. De Vivie De Regie¹¹⁵, G. De Zorzi^{132a,132b}, W.J. Dearnaley⁷¹,
 R. Debbé²⁴, C. Debenedetti⁴⁵, B. Dechenaux⁵⁵, D.V. Dedovich⁶⁴, J. Degenhardt¹²⁰, C. Del Papa^{164a,164c},
 J. Del Peso⁸⁰, T. Del Prete^{122a,122b}, T. Delemontex⁵⁵, M. Deliyergiyev⁷⁴, A. Dell'Acqua²⁹, L. Dell'Asta²¹,
 M. Della Pietra^{102a,j}, D. della Volpe^{102a,102b}, M. Delmastro⁴, P.A. Delsart⁵⁵, C. Deluca¹⁰⁵, S. Demers¹⁷⁶,
 M. Demichev⁶⁴, B. Demirköz^{11,l}, J. Deng¹⁶³, S.P. Denisov¹²⁸, D. Derendarz³⁸, J.E. Derkaoui^{135d}, F. Derue⁷⁸,
 P. Dervan⁷³, K. Desch²⁰, E. Devetak¹⁴⁸, P.O. Deviveiros¹⁰⁵, A. Dewhurst¹²⁹, B. DeWilde¹⁴⁸, S. Dhaliwal¹⁵⁸,
 R. Dhullipudi^{24,m}, A. Di Ciaccio^{133a,133b}, L. Di Ciaccio⁴, A. Di Girolamo²⁹, B. Di Girolamo²⁹, S. Di Luise^{134a,134b},
 A. Di Mattia¹⁷³, B. Di Micco²⁹, R. Di Nardo⁴⁷, A. Di Simone^{133a,133b}, R. Di Sipio^{19a,19b}, M.A. Diaz^{31a},
 E.B. Diehl⁸⁷, J. Dietrich⁴¹, T.A. Dietzsch^{58a}, S. Diglio⁸⁶, K. Dindar Yagci³⁹, J. Dingfelder²⁰, C. Dionisi^{132a,132b},
 P. Dita^{25a}, S. Dita^{25a}, F. Dittus²⁹, F. Djama⁸³, T. Djobava^{51b}, M.A.B. do Vale^{23c}, A. Do Valle Wemans^{124a,n},
 T.K.O. Doan⁴, M. Dobbs⁸⁵, R. Dobinson^{29,*}, D. Dobos²⁹, E. Dobson^{29,o}, J. Dodd³⁴, C. Dogliani⁴⁹, T. Doherty⁵³,
 Y. Doi^{65,*}, J. Dolejsi¹²⁶, I. Dolenc⁷⁴, Z. Dolezal¹²⁶, B.A. Dolgoshein^{96,*}, T. Dohmae¹⁵⁵, M. Donadelli^{23d},
 M. Donega¹²⁰, J. Donini³³, J. Dopke²⁹, A. Doria^{102a}, A. Dos Anjos¹⁷³, A. Dotti^{122a,122b}, M.T. Dova⁷⁰,
 A.D. Doxiadis¹⁰⁵, A.T. Doyle⁵³, M. Dris⁹, J. Dubbert⁹⁹, S. Dube¹⁴, E. Duchovni¹⁷², G. Duckeck⁹⁸, A. Dudarev²⁹,
 F. Dudziak⁶³, M. Dührssen²⁹, I.P. Duerdoth⁸², L. Duflot¹¹⁵, M.-A. Dufour⁸⁵, M. Dunford²⁹, H. Duran Yildiz^{3a},
 R. Duxfield¹³⁹, M. Dwuznik³⁷, F. Dydak²⁹, M. Düren⁵², J. Ebke⁹⁸, S. Eckweiler⁸¹, K. Edmonds⁸¹, C.A. Edwards⁷⁶,
 N.C. Edwards⁵³, W. Ehrenzfeld⁴¹, T. Eifert¹⁴³, G. Eigen¹³, K. Einsweiler¹⁴, E. Eisenhandler⁷⁵, T. Ekelof¹⁶⁶,
 M. El Kacimi^{135c}, M. Ellert¹⁶⁶, S. Elles⁴, F. Ellinghaus⁸¹, K. Ellis⁷⁵, N. Ellis²⁹, J. Elmsheuser⁹⁸, M. Elsing²⁹,
 D. Emelianov¹²⁹, R. Engelmann¹⁴⁸, A. Engl⁹⁸, B. Epp⁶¹, A. Eppig⁸⁷, J. Erdmann⁵⁴, A. Ereditato¹⁶,
 D. Eriksson^{146a}, J. Ernst¹, M. Ernst²⁴, J. Ernwein¹³⁶, D. Errede¹⁶⁵, S. Errede¹⁶⁵, E. Ertel⁸¹, M. Escalier¹¹⁵,
 C. Escobar¹²³, X. Espinal Curull¹¹, B. Esposito⁴⁷, F. Etienne⁸³, A.I. Etievre¹³⁶, E. Etzion¹⁵³, D. Evangelakou⁵⁴,
 H. Evans⁶⁰, L. Fabbri^{19a,19b}, C. Fabre²⁹, R.M. Fakhrutdinov¹²⁸, S. Falciano^{132a}, Y. Fang¹⁷³, M. Fanti^{89a,89b},
 A. Farbin⁷, A. Farilla^{134a}, J. Farley¹⁴⁸, T. Farooque¹⁵⁸, S. Farrell¹⁶³, S.M. Farrington¹¹⁸, P. Farthouat²⁹,
 P. Fassnacht²⁹, D. Fassouliotis⁸, B. Fatholahzadeh¹⁵⁸, A. Favareto^{89a,89b}, L. Fayard¹¹⁵, S. Fazio^{36a,36b},
 R. Febbraro³³, P. Federic^{144a}, O.L. Fedin¹²¹, W. Fedorko⁸⁸, M. Fehling-Kaschek⁴⁸, L. Felgioni⁸³, D. Fellmann⁵,
 C. Feng^{32d}, E.J. Feng³⁰, A.B. Fenyuk¹²⁸, J. Ferencei^{144b}, W. Fernando⁵, S. Ferrag⁵³, J. Ferrando⁵³, V. Ferrara⁴¹,
 A. Ferrari¹⁶⁶, P. Ferrari¹⁰⁵, R. Ferrari^{119a}, D.E. Ferreira de Lima⁵³, A. Ferrer¹⁶⁷, D. Ferrere⁴⁹, C. Ferretti⁸⁷,
 A. Ferretto Parodi^{50a,50b}, M. Fiascaris³⁰, F. Fiedler⁸¹, A. Filipčić⁷⁴, F. Filthaut¹⁰⁴, M. Fincke-Keeler¹⁶⁹,

M.C.N. Fiolhais^{124a,h}, L. Fiorini¹⁶⁷, A. Firan³⁹, G. Fischer⁴¹, M.J. Fisher¹⁰⁹, M. Flechl⁴⁸, I. Fleck¹⁴¹, J. Fleckner⁸¹, P. Fleischmann¹⁷⁴, S. Fleischmann¹⁷⁵, T. Flick¹⁷⁵, A. Floderus⁷⁹, L.R. Flores Castillo¹⁷³, M.J. Flowerdew⁹⁹, T. Fonseca Martin¹⁶, A. Formica¹³⁶, A. Forti⁸², D. Fortin^{159a}, D. Fournier¹¹⁵, H. Fox⁷¹, P. Francavilla¹¹, S. Franchino^{119a,119b}, D. Francis²⁹, T. Frank¹⁷², M. Franklin⁵⁷, S. Franz²⁹, M. Fraternali^{119a,119b}, S. Fratina¹²⁰, S.T. French²⁷, C. Friedrich⁴¹, F. Friedrich⁴³, R. Froeschl²⁹, D. Froidevaux²⁹, J.A. Frost²⁷, C. Fukunaga¹⁵⁶, E. Fullana Torregrosa²⁹, B.G. Fulson¹⁴³, J. Fuster¹⁶⁷, C. Gabaldon²⁹, O. Gabizon¹⁷², T. Gadfort²⁴, S. Gadomski⁴⁹, G. Gagliardi^{50a,50b}, P. Gagnon⁶⁰, C. Galea⁹⁸, E.J. Gallas¹¹⁸, V. Gallo¹⁶, B.J. Gallop¹²⁹, P. Gallus¹²⁵, K.K. Gan¹⁰⁹, Y.S. Gao^{143,e}, A. Gaponenko¹⁴, F. Garberon¹⁷⁶, M. Garcia-Sciveres¹⁴, C. García¹⁶⁷, J.E. García Navarro¹⁶⁷, R.W. Gardner³⁰, N. Garelli²⁹, H. Garitaonandia¹⁰⁵, V. Garonne²⁹, J. Garvey¹⁷, C. Gatti⁴⁷, G. Gaudio^{119a}, B. Gaur¹⁴¹, L. Gauthier¹³⁶, P. Gauzzi^{132a,132b}, I.L. Gavrilenko⁹⁴, C. Gay¹⁶⁸, G. Gaycken²⁰, E.N. Gazis⁹, P. Ge^{32d}, Z. Gecse¹⁶⁸, C.N.P. Gee¹²⁹, D.A.A. Geerts¹⁰⁵, Ch. Geich-Gimbel²⁰, K. Gellerstedt^{146a,146b}, C. Gemme^{50a}, A. Gemmell⁵³, M.H. Genest⁵⁵, S. Gentile^{132a,132b}, M. George⁵⁴, S. George⁷⁶, P. Gerlach¹⁷⁵, A. Gershon¹⁵³, C. Geweniger^{58a}, H. Ghazlane^{135b}, N. Ghodbane³³, B. Giacobbe^{19a}, S. Giagu^{132a,132b}, V. Giakoumopoulou⁸, V. Giangiobbe¹¹, F. Gianotti²⁹, B. Gibbard²⁴, A. Gibson¹⁵⁸, S.M. Gibson²⁹, D. Gillberg²⁸, A.R. Gillman¹²⁹, D.M. Gingrich^{2,d}, J. Ginzburg¹⁵³, N. Giokaris⁸, M.P. Giordani^{164c}, R. Giordano^{102a,102b}, F.M. Giorgi¹⁵, P. Giovannini⁹⁹, P.F. Giraud¹³⁶, D. Giugni^{89a}, M. Giunta⁹³, P. Giusti^{19a}, B.K. Gjelsten¹¹⁷, L.K. Gladilin⁹⁷, C. Glasman⁸⁰, J. Glatzer⁴⁸, A. Glazov⁴¹, K.W. Glitza¹⁷⁵, G.L. Glonti⁶⁴, J.R. Goddard⁷⁵, J. Godfrey¹⁴², J. Godlewski²⁹, M. Goebel⁴¹, T. Göpfert⁴³, C. Goeringer⁸¹, C. Gössling⁴², S. Goldfarb⁸⁷, T. Golling¹⁷⁶, A. Gomes^{124a,b}, L.S. Gomez Fajardo⁴¹, R. Gonçalo⁷⁶, J. Goncalves Pinto Firmino Da Costa⁴¹, L. Gonella²⁰, S. Gonzalez¹⁷³, S. González de la Hoz¹⁶⁷, G. Gonzalez Parra¹¹, M.L. Gonzalez Silva²⁶, S. Gonzalez-Sevilla⁴⁹, J.J. Goodson¹⁴⁸, L. Goossens²⁹, P.A. Gorbounov⁹⁵, H.A. Gordon²⁴, I. Gorelov¹⁰³, G. Gorfine¹⁷⁵, B. Gorini²⁹, E. Gorini^{72a,72b}, A. Gorišek⁷⁴, E. Gornicki³⁸, B. Gosdzik⁴¹, A.T. Goshaw⁵, M. Gosselink¹⁰⁵, M.I. Gostkin⁶⁴, I. Gough Eschrich¹⁶³, M. Goughri^{135a}, D. Goudami^{135c}, M.P. Goulette⁴⁹, A.G. Goussiou¹³⁸, C. Goy⁴, S. Gozpinar²², I. Grabowska-Bold³⁷, P. Grafström²⁹, K.-J. Grahn⁴¹, F. Gracagnolo^{72a}, S. Gracagnolo¹⁵, V. Grassi¹⁴⁸, V. Gratchev¹²¹, N. Grau³⁴, H.M. Gray²⁹, J.A. Gray¹⁴⁸, E. Graziani^{134a}, O.G. Grebenyuk¹²¹, T. Greenshaw⁷³, Z.D. Greenwood^{24,m}, K. Gregersen³⁵, I.M. Gregor⁴¹, P. Grenier¹⁴³, J. Griffiths¹³⁸, N. Grigalashvili⁶⁴, A.A. Grillo¹³⁷, S. Grinstein¹¹, Y.V. Grishkevich⁹⁷, J.-F. Grivaz¹¹⁵, E. Gross¹⁷², J. Grosse-Knetter⁵⁴, J. Groth-Jensen¹⁷², K. Grybel¹⁴¹, D. Guest¹⁷⁶, C. Guicheney³³, A. Guida^{72a,72b}, S. Guindon⁵⁴, U. Gul⁵³, H. Guler^{85,p}, J. Gunther¹²⁵, B. Guo¹⁵⁸, J. Guo³⁴, V.N. Gushchin¹²⁸, P. Gutierrez¹¹¹, N. Guttman¹⁵³, O. Gutzwiller¹⁷³, C. Guyot¹³⁶, C. Gwenlan¹¹⁸, C.B. Gwilliam⁷³, A. Haas¹⁴³, S. Haas²⁹, C. Haber¹⁴, H.K. Hadavand³⁹, D.R. Hadley¹⁷, P. Haefner⁹⁹, F. Hahn²⁹, S. Haider²⁹, Z. Hajduk³⁸, H. Hakobyan¹⁷⁷, D. Hall¹¹⁸, J. Haller⁵⁴, K. Hamacher¹⁷⁵, P. Hamal¹¹³, M. Hamer⁵⁴, A. Hamilton^{145b,q}, S. Hamilton¹⁶¹, L. Han^{32b}, K. Hanagaki¹¹⁶, K. Hanawa¹⁶⁰, M. Hance¹⁴, C. Handel⁸¹, P. Hanke^{58a}, J.R. Hansen³⁵, J.B. Hansen³⁵, J.D. Hansen³⁵, P.H. Hansen³⁵, P. Hansson¹⁴³, K. Hara¹⁶⁰, G.A. Hare¹³⁷, T. Harenberg¹⁷⁵, S. Harkusha⁹⁰, D. Harper⁸⁷, R.D. Harrington⁴⁵, O.M. Harris¹³⁸, K. Harrison¹⁷, J. Hartert⁴⁸, F. Hartjes¹⁰⁵, T. Haruyama⁶⁵, A. Harvey⁵⁶, S. Hasegawa¹⁰¹, Y. Hasegawa¹⁴⁰, S. Hassani¹³⁶, S. Haug¹⁶, M. Hauschild²⁹, R. Hauser⁸⁸, M. Havranek²⁰, C.M. Hawkes¹⁷, R.J. Hawkings²⁹, A.D. Hawkins⁷⁹, D. Hawkins¹⁶³, T. Hayakawa⁶⁶, T. Hayashi¹⁶⁰, D. Hayden⁷⁶, C.P. Hays¹¹⁸, H.S. Hayward⁷³, S.J. Haywood¹²⁹, M. He^{32d}, S.J. Head¹⁷, V. Hedberg⁷⁹, L. Heelan⁷, S. Heim⁸⁸, B. Heinemann¹⁴, S. Heisterkamp³⁵, L. Helary⁴, C. Heller⁹⁸, M. Heller²⁹, S. Hellman^{146a,146b}, D. Hellmich²⁰, C. Helsen¹¹, R.C.W. Henderson⁷¹, M. Henke^{58a}, A. Henrichs⁵⁴, A.M. Henriques Correia²⁹, S. Henrot-Versille¹¹⁵, F. Henry-Couannier⁸³, C. Hensel⁵⁴, T. Henß¹⁷⁵, C.M. Hernandez⁷, Y. Hernández Jiménez¹⁶⁷, R. Herrberg¹⁵, G. Herten⁴⁸, R. Hertenberger⁹⁸, L. Hervas²⁹, G.G. Hesketh⁷⁷, N.P. Hessey¹⁰⁵, E. Higón-Rodríguez¹⁶⁷, J.C. Hill²⁷, K.H. Hiller⁴¹, S. Hillert²⁰, S.J. Hillier¹⁷, I. Hinchliffe¹⁴, E. Hines¹²⁰, M. Hirose¹¹⁶, F. Hirsch⁴², D. Hirschbuehl¹⁷⁵, J. Hobbs¹⁴⁸, N. Hod¹⁵³, M.C. Hodgkinson¹³⁹, P. Hodgson¹³⁹, A. Hoecker²⁹, M.R. Hoferkamp¹⁰³, J. Hoffman³⁹, D. Hoffmann⁸³, M. Hohlfeld⁸¹, M. Holder¹⁴¹, S.O. Holmgren^{146a}, T. Holy¹²⁷, J.L. Holzbauer⁸⁸, T.M. Hong¹²⁰, L. Hooft van Huysduyнен¹⁰⁸, C. Horn¹⁴³, S. Horner⁴⁸, J.-Y. Hostachy⁵⁵, S. Hou¹⁵¹, A. Hoummada^{135a}, J. Howard¹¹⁸, J. Howarth⁸², I. Hristova¹⁵, J. Hrivnac¹¹⁵, I. Hruska¹²⁵, T. Hryn'ova⁴, P.J. Hsu⁸¹, S.-C. Hsu¹⁴, Z. Hubacek¹²⁷, F. Hubaut⁸³, F. Huegging²⁰, A. Huettmann⁴¹, T.B. Huffman¹¹⁸, E.W. Hughes³⁴, G. Hughes⁷¹, M. Huhtinen²⁹, M. Hurwitz¹⁴, U. Husemann⁴¹, N. Huseynov^{64,r}, J. Huston⁸⁸, J. Huth⁵⁷, G. Iacobucci⁴⁹, G. Iakovidis⁹, M. Ibbotson⁸², I. Ibragimov¹⁴¹, L. Iconomidou-Fayard¹¹⁵, J. Idarraga¹¹⁵, P. Iengo^{102a}, O. Igonkina¹⁰⁵, Y. Ikegami⁶⁵, M. Ikeno⁶⁵, D. Iliadis¹⁵⁴, N. Ilic¹⁵⁸, T. Ince²⁰, J. Inigo-Golfin²⁹, P. Ioannou⁸, M. Iodice^{134a}, K. Iordanidou⁸, V. Ippolito^{132a,132b}, A. Irles Quiles¹⁶⁷, C. Isaksson¹⁶⁶, A. Ishikawa⁶⁶, M. Ishino⁶⁷, R. Ishmukhametov³⁹, C. Issever¹¹⁸, S. Istin^{18a}, A.V. Ivashin¹²⁸, W. Iwanski³⁸, H. Iwasaki⁶⁵, J.M. Izen⁴⁰, V. Izzo^{102a}, B. Jackson¹²⁰, J.N. Jackson⁷³, P. Jackson¹⁴³, M.R. Jaekel²⁹, V. Jain⁶⁰, K. Jakobs⁴⁸, S. Jakobsen³⁵, T. Jakoubek¹²⁵, J. Jakubek¹²⁷, D.K. Jana¹¹¹, E. Jansen⁷⁷, H. Jansen²⁹, A. Jantsch⁹⁹, M. Janus⁴⁸, G. Jarlskog⁷⁹, L. Jeanty⁵⁷, I. Jen-La Plante³⁰, P. Jenni²⁹, A. Jeremie⁴, P. Jez³⁵, S. Jézéquel⁴, M.K. Jha^{19a}, H. Ji¹⁷³, W. Ji⁸¹, J. Jia¹⁴⁸, Y. Jiang^{32b}, M. Jimenez Belenguer⁴¹, S. Jin^{32a}, O. Jinnouchi¹⁵⁷, M.D. Joergensen³⁵, D. Joffe³⁹, L.G. Johansen¹³, M. Johansen^{146a,146b}, K.E. Johansson^{146a}, P. Johansson¹³⁹,

S. Johnert⁴¹, K.A. Johns⁶, K. Jon-And^{146a,146b}, G. Jones¹⁷⁰, R.W.L. Jones⁷¹, T.J. Jones⁷³, C. Joram²⁹, P.M. Jorge^{124a}, K.D. Joshi⁸², J. Jovicevic¹⁴⁷, T. Jovin^{12b}, X. Ju¹⁷³, C.A. Jung⁴², R.M. Jungst²⁹, V. Juranek¹²⁵, P. Jussel⁶¹, A. Juste Rozas¹¹, S. Kabana¹⁶, M. Kaci¹⁶⁷, A. Kaczmarek³⁸, P. Kadlecik³⁵, M. Kado¹¹⁵, H. Kagan¹⁰⁹, M. Kagan⁵⁷, E. Kajomovitz¹⁵², S. Kalinin¹⁷⁵, L.V. Kalinovskaya⁶⁴, S. Kama³⁹, N. Kanaya¹⁵⁵, M. Kaneda²⁹, S. Kaneti²⁷, T. Kanno¹⁵⁷, V.A. Kantserov⁹⁶, J. Kanzaki⁶⁵, B. Kaplan¹⁷⁶, A. Kapliy³⁰, J. Kaplon²⁹, D. Kar⁵³, M. Karagounis²⁰, K. Karakostas⁹, M. Karnevskiy⁴¹, V. Kartvelishvili⁷¹, A.N. Karyukhin¹²⁸, L. Kashif¹⁷³, G. Kasieczka^{58b}, R.D. Kass¹⁰⁹, A. Kastanas¹³, M. Kataoka⁴, Y. Kataoka¹⁵⁵, E. Katsoufis⁹, J. Katzy⁴¹, V. Kaushik⁶, K. Kawagoe⁶⁹, T. Kawamoto¹⁵⁵, G. Kawamura⁸¹, M.S. Kayl¹⁰⁵, V.A. Kazanin¹⁰⁷, M.Y. Kazarinov⁶⁴, R. Keeler¹⁶⁹, R. Kehoe³⁹, M. Keil⁵⁴, G.D. Kekelidze⁶⁴, J.S. Keller¹³⁸, J. Kennedy⁹⁸, M. Kenyon⁵³, O. Kepka¹²⁵, N. Kerschen²⁹, B.P. Kerševan⁷⁴, S. Kersten¹⁷⁵, K. Kessoku¹⁵⁵, J. Keung¹⁵⁸, F. Khalil-zada¹⁰, H. Khandanyan¹⁶⁵, A. Khanov¹¹², D. Kharchenko⁶⁴, A. Khodinov⁹⁶, A. Khomich^{58a}, T.J. Khoo²⁷, G. Khorauli²⁰, A. Khoroshilov¹⁷⁵, V. Khovanskiy⁹⁵, E. Khramov⁶⁴, J. Khubua^{51b}, H. Kim^{146a,146b}, M.S. Kim², S.H. Kim¹⁶⁰, N. Kimura¹⁷¹, O. Kind¹⁵, B.T. King⁷³, M. King⁶⁶, R.S.B. King¹¹⁸, J. Kirk¹²⁹, A.E. Kiryunin⁹⁹, T. Kishimoto⁶⁶, D. Kisielewska³⁷, T. Kittelmann¹²³, A.M. Kiver¹²⁸, E. Kladiva^{144b}, M. Klein⁷³, U. Klein⁷³, K. Kleinknecht⁸¹, M. Klemetti⁸⁵, A. Klier¹⁷², P. Klimek^{146a,146b}, A. Klimentov²⁴, R. Klingenberg⁴², J.A. Klinger⁸², E.B. Klinkby³⁵, T. Klioutchnikova²⁹, P.F. Klok¹⁰⁴, S. Klous¹⁰⁵, E.-E. Kluge^{58a}, T. Kluge⁷³, P. Kluit¹⁰⁵, S. Kluth⁹⁹, N.S. Knecht¹⁵⁸, E. Kneringer⁶¹, E.B.F.G. Knoop⁸³, A. Knue⁵⁴, B.R. Ko⁴⁴, T. Kobayashi¹⁵⁵, M. Kobel⁴³, M. Kocian¹⁴³, P. Kodys¹²⁶, K. Köneke²⁹, A.C. König¹⁰⁴, S. Koenig⁸¹, L. Köpke⁸¹, F. Koetsveld¹⁰⁴, P. Koevesarki²⁰, T. Koffas²⁸, E. Koffeman¹⁰⁵, L.A. Kogan¹¹⁸, S. Kohlmann¹⁷⁵, F. Kohn⁵⁴, Z. Kohout¹²⁷, T. Kohriki⁶⁵, T. Koi¹⁴³, G.M. Kolachev^{107,*}, H. Kolanoski¹⁵, V. Kolesnikov⁶⁴, I. Koletsou^{89a}, J. Koll⁸⁸, M. Kollefrath⁴⁸, A.A. Komar⁹⁴, Y. Komori¹⁵⁵, T. Kondo⁶⁵, T. Kono^{41,s}, A.I. Kononov⁴⁸, R. Konoplich^{108,t}, N. Konstantinidis⁷⁷, A. Kootz¹⁷⁵, S. Koperny³⁷, K. Korcyl³⁸, K. Kordas¹⁵⁴, A. Korn¹¹⁸, A. Korol¹⁰⁷, I. Korolkov¹¹, E.V. Korolkova¹³⁹, V.A. Korotkov¹²⁸, O. Kortner⁹⁹, S. Kortner⁹⁹, V.V. Kostyukhin²⁰, S. Kotov⁹⁹, V.M. Kotov⁶⁴, A. Kotwal⁴⁴, C. Kourkoumelis⁸, V. Kouskoura¹⁵⁴, A. Koutsman^{159a}, R. Kowalewski¹⁶⁹, T.Z. Kowalski³⁷, W. Kozanecki¹³⁶, A.S. Kozhin¹²⁸, V. Kral¹²⁷, V.A. Kramarenko⁹⁷, G. Kramberger⁷⁴, M.W. Krasny⁷⁸, A. Krasznahorkay¹⁰⁸, J. Kraus⁸⁸, J.K. Kraus²⁰, S. Kreiss¹⁰⁸, F. Krejci¹²⁷, J. Kretzschmar⁷³, N. Krieger⁵⁴, P. Krieger¹⁵⁸, K. Kroeninger⁵⁴, H. Kroha⁹⁹, J. Kroll¹²⁰, J. Kroseberg²⁰, J. Krstic^{12a}, U. Kruchonak⁶⁴, H. Krüger²⁰, T. Kruker¹⁶, N. Krumnack⁶³, Z.V. Krumshyteyn⁶⁴, A. Kruth²⁰, T. Kubota⁸⁶, S. Kuday^{3a}, S. Kuehn⁴⁸, A. Kugel^{58c}, T. Kuhl⁴¹, D. Kuhn⁶¹, V. Kukhtin⁶⁴, Y. Kulchitsky⁹⁰, S. Kuleshov^{31b}, C. Kummer⁹⁸, M. Kuna⁷⁸, J. Kunkle¹²⁰, A. Kupco¹²⁵, H. Kurashige⁶⁶, M. Kurata¹⁶⁰, Y.A. Kurochkin⁹⁰, V. Kus¹²⁵, E.S. Kuwertz¹⁴⁷, M. Kuze¹⁵⁷, J. Kvita¹⁴², R. Kwee¹⁵, A. La Rosa⁴⁹, L. La Rotonda^{36a,36b}, L. Labarga⁸⁰, J. Labbe⁴, S. Lablak^{135a}, C. Lacasta¹⁶⁷, F. Lacava^{132a,132b}, H. Lacker¹⁵, D. Lacour⁷⁸, V.R. Lacuesta¹⁶⁷, E. Ladygin⁶⁴, R. Lafaye⁴, B. Laforge⁷⁸, T. Lagouri⁸⁰, S. Lai⁴⁸, E. Laisne⁵⁵, M. Lamanna²⁹, L. Lambourne⁷⁷, C.L. Lampen⁶, W. Lampl⁶, E. Lancon¹³⁶, U. Landgraf⁴⁸, M.P.J. Landon⁷⁵, J.L. Lane⁸², C. Lange⁴¹, A.J. Lankford¹⁶³, F. Lanni²⁴, K. Lantzsich¹⁷⁵, S. Laplace⁷⁸, C. Lapoire²⁰, J.F. Laporte¹³⁶, T. Lari^{89a}, A. Lerner¹¹⁸, M. Lassnig²⁹, P. Laurelli⁴⁷, V. Lavorini^{36a,36b}, W. Lavrijsen¹⁴, P. Laycock⁷³, O. Le Dortz⁷⁸, E. Le Guirrec⁸³, C. Le Maner¹⁵⁸, E. Le Menedeu¹¹, T. LeCompte⁵, F. Ledroit-Guillon⁵⁵, H. Lee¹⁰⁵, J.S.H. Lee¹¹⁶, S.C. Lee¹⁵¹, L. Lee¹⁷⁶, M. Lefebvre¹⁶⁹, M. Legendre¹³⁶, B.C. LeGeyt¹²⁰, F. Legger⁹⁸, C. Leggett¹⁴, M. Lehmacher²⁰, G. Lehmann Miotto²⁹, X. Lei⁶, M.A.L. Leite^{23d}, R. Leitner¹²⁶, D. Lellouch¹⁷², B. Lemmer⁵⁴, V. Lendermann^{58a}, K.J.C. Leney^{145b}, T. Lenz¹⁰⁵, G. Lenzen¹⁷⁵, B. Lenzi²⁹, K. Leonhardt⁴³, S. Leontsinis⁹, F. Lepold^{58a}, C. Leroy⁹³, J.-R. Lessard¹⁶⁹, C.G. Lester²⁷, C.M. Lester¹²⁰, J. Levêque⁴, D. Levin⁸⁷, L.J. Levinson¹⁷², A. Lewis¹¹⁸, G.H. Lewis¹⁰⁸, A.M. Leyko²⁰, M. Leyton¹⁵, B. Li⁸³, H. Li^{173,u}, S. Li^{32b,v}, X. Li⁸⁷, Z. Liang^{118,w}, H. Liao³³, B. Liberti^{133a}, P. Lichard²⁹, M. Lichtnecker⁹⁸, K. Lie¹⁶⁵, W. Liebig¹³, C. Limbach²⁰, A. Limosani⁸⁶, M. Limper⁶², S.C. Lin^{151,x}, F. Linde¹⁰⁵, J.T. Linnemann⁸⁸, E. Lipeles¹²⁰, A. Lipniacka¹³, T.M. Liss¹⁶⁵, D. Lissauer²⁴, A. Lister⁴⁹, A.M. Litke¹³⁷, C. Liu²⁸, D. Liu¹⁵¹, H. Liu⁸⁷, J.B. Liu⁸⁷, M. Liu^{32b}, Y. Liu^{32b}, M. Livan^{119a,119b}, S.S.A. Livermore¹¹⁸, A. Lleres⁵⁵, J. Llorente Merino⁸⁰, S.L. Lloyd⁷⁵, E. Lobodzinska⁴¹, P. Loch⁶, W.S. Lockman¹³⁷, T. Lodenkoetter²⁰, F.K. Loebinger⁸², A. Loginov¹⁷⁶, C.W. Loh¹⁶⁸, T. Lohse¹⁵, K. Lohwasser⁴⁸, M. Lokajicek¹²⁵, V.P. Lombardo⁴, R.E. Long⁷¹, L. Lopes^{124a}, D. Lopez Mateos⁵⁷, J. Lorenz⁹⁸, N. Lorenzo Martinez¹¹⁵, M. Losada¹⁶², P. Loscutoff¹⁴, F. Lo Sterzo^{132a,132b}, M.J. Losty^{159a}, X. Lou⁴⁰, A. Lounis¹¹⁵, K.F. Loureiro¹⁶², J. Love²¹, P.A. Love⁷¹, A.J. Lowe^{143,e}, F. Lu^{32a}, H.J. Lubatti¹³⁸, C. Luci^{132a,132b}, A. Lucotte⁵⁵, A. Ludwig⁴³, D. Ludwig⁴¹, I. Ludwig⁴⁸, J. Ludwig⁴⁸, F. Luehring⁶⁰, G. Luijckx¹⁰⁵, W. Lukas⁶¹, D. Lumb⁴⁸, L. Luminari^{132a}, E. Lund¹¹⁷, B. Lund-Jensen¹⁴⁷, B. Lundberg⁷⁹, J. Lundberg^{146a,146b}, J. Lundquist³⁵, M. Lungwitz⁸¹, D. Lynn²⁴, E. Lytken⁷⁹, H. Ma²⁴, L.L. Ma¹⁷³, J.A. Macana Goia⁹³, G. Maccarrone⁴⁷, A. Macchiolo⁹⁹, B. Maček⁷⁴, J. Machado Miguens^{124a}, R. Mackeprang³⁵, R.J. Madaras¹⁴, W.F. Mader⁴³, R. Maenner^{58c}, T. Maeno²⁴, P. Mättig¹⁷⁵, S. Mättig⁴¹, L. Magnoni²⁹, E. Magradze⁵⁴, K. Mahboubi⁴⁸, S. Mahmoud⁷³, G. Mahout¹⁷, C. Maiani¹³⁶, C. Maidantchik^{23a}, A. Maio^{124a,b}, S. Majewski²⁴, Y. Makida⁶⁵, N. Makovec¹¹⁵, P. Mal¹³⁶, B. Malaescu²⁹, Pa. Malecki³⁸, P. Malecki³⁸, V.P. Maleev¹²¹, F. Malek⁵⁵, U. Mallik⁶², D. Malon⁵, C. Malone¹⁴³, S. Maltezos⁹, V. Malyshev¹⁰⁷, S. Malyukov²⁹, R. Mameghani⁹⁸, J. Mamuzic^{12b}, A. Manabe⁶⁵, L. Mandelli^{89a}, I. Mandić⁷⁴, R. Mandrysch¹⁵, J. Maneira^{124a}, P.S. Mangeard⁸⁸, L. Manhaes de Andrade Filho^{23a}, A. Mann⁵⁴, P.M. Manning¹³⁷, A. Manousakis-Katsikakis⁸,

B. Mansoulie¹³⁶, A. Mapelli²⁹, L. Mapelli²⁹, L. March⁸⁰, J.F. Marchand²⁸, F. Marchese^{133a,133b}, G. Marchiori⁷⁸, M. Marcisovsky¹²⁵, C.P. Marino¹⁶⁹, F. Marroquim^{23a}, Z. Marshall²⁹, F.K. Martens¹⁵⁸, S. Marti-Garcia¹⁶⁷, B. Martin²⁹, B. Martin⁸⁸, J.P. Martin⁹³, T.A. Martin¹⁷, V.J. Martin⁴⁵, B. Martin dit Latour⁴⁹, S. Martin-Haugh¹⁴⁹, M. Martinez¹¹, V. Martinez Outschoorn⁵⁷, A.C. Martyniuk¹⁶⁹, M. Marx⁸², F. Marzano^{132a}, A. Marzin¹¹¹, L. Masetti⁸¹, T. Mashimo¹⁵⁵, R. Mashinistov⁹⁴, J. Masik⁸², A.L. Maslennikov¹⁰⁷, I. Massa^{19a,19b}, G. Massaro¹⁰⁵, N. Massol⁴, A. Mastroberardino^{36a,36b}, T. Masubuchi¹⁵⁵, P. Matricon¹¹⁵, H. Matsunaga¹⁵⁵, T. Matsushita⁶⁶, C. Mattravers^{118,c}, J. Maurer⁸³, S.J. Maxfield⁷³, A. Mayne¹³⁹, R. Mazini¹⁵¹, M. Mazur²⁰, L. Mazzaferro^{133a,133b}, M. Mazzanti^{89a}, S.P. Mc Kee⁸⁷, A. McCarn¹⁶⁵, R.L. McCarthy¹⁴⁸, T.G. McCarthy²⁸, N.A. McCubbin¹²⁹, K.W. McFarlane⁵⁶, J.A. Mcfayden¹³⁹, H. McGlone⁵³, G. Mchedlidze^{51b}, T. Mclaughlan¹⁷, S.J. McMahon¹²⁹, R.A. McPherson^{169,k}, A. Meade⁸⁴, J. Mechnich¹⁰⁵, M. Mechtel¹⁷⁵, M. Medinnis⁴¹, R. Meera-Lebbai¹¹¹, T. Meguro¹¹⁶, R. Mehdiyev⁹³, S. Mehlhase³⁵, A. Mehta⁷³, K. Meier^{58a}, B. Meirose⁷⁹, C. Melachrinou³⁰, B.R. Mellado Garcia¹⁷³, F. Meloni^{89a,89b}, L. Mendoza Navas¹⁶², Z. Meng^{151,u}, A. Mengarelli^{19a,19b}, S. Menke⁹⁹, E. Meoni¹¹, K.M. Mercurio⁵⁷, P. Mermod⁴⁹, L. Merola^{102a,102b}, C. Meroni^{89a}, F.S. Merritt³⁰, H. Merritt¹⁰⁹, A. Messina^{29,y}, J. Metcalfe¹⁰³, A.S. Mete¹⁶³, C. Meyer⁸¹, C. Meyer³⁰, J-P. Meyer¹³⁶, J. Meyer¹⁷⁴, J. Meyer⁵⁴, T.C. Meyer²⁹, W.T. Meyer⁶³, J. Miao^{32d}, S. Michal²⁹, L. Micu^{25a}, R.P. Middleton¹²⁹, S. Migas⁷³, L. Mijović⁴¹, G. Mikenberg¹⁷², M. Mikesstikova¹²⁵, M. Mikuz⁷⁴, D.W. Miller³⁰, R.J. Miller⁸⁸, W.J. Mills¹⁶⁸, C. Mills⁵⁷, A. Milov¹⁷², D.A. Milstead^{146a,146b}, D. Milstein¹⁷², A.A. Minaenko¹²⁸, M. Miñano Moya¹⁶⁷, I.A. Minashvili⁶⁴, A.I. Mincer¹⁰⁸, B. Mindur³⁷, M. Mineev⁶⁴, Y. Ming¹⁷³, L.M. Mir¹¹, G. Mirabelli^{132a}, J. Mitrevski¹³⁷, V.A. Mitsou¹⁶⁷, S. Mitsui⁶⁵, P.S. Miyagawa¹³⁹, K. Miyazaki⁶⁶, J.U. Mjörnmark⁷⁹, T. Moa^{146a,146b}, S. Moed⁵⁷, V. Moeller²⁷, K. Mönig⁴¹, N. Möser²⁰, S. Mohapatra¹⁴⁸, W. Mohr⁴⁸, R. Moles-Valls¹⁶⁷, J. Molina-Perez²⁹, J. Monk⁷⁷, E. Monnier⁸³, S. Montesano^{89a,89b}, F. Monticelli⁷⁰, S. Monzani^{19a,19b}, R.W. Moore², G.F. Moorhead⁸⁶, C. Mora Herrera⁴⁹, A. Moraes⁵³, N. Morange¹³⁶, J. Morel⁵⁴, G. Morello^{36a,36b}, D. Moreno⁸¹, M. Moreno Llacer¹⁶⁷, P. Moretini^{50a}, M. Morgenstern⁴³, M. Morii⁵⁷, J. Morin⁷⁵, A.K. Morley²⁹, G. Mornacchi²⁹, J.D. Morris⁷⁵, L. Morvaj¹⁰¹, H.G. Moser⁹⁹, M. Mosidze^{51b}, J. Moss¹⁰⁹, R. Mount¹⁴³, E. Mountricha^{9,z}, S.V. Mouraviev^{94,*}, E.J.W. Moyses⁸⁴, F. Mueller^{58a}, J. Mueller¹²³, K. Mueller²⁰, T.A. Müller⁹⁸, T. Mueller⁸¹, D. Muenstermann²⁹, Y. Munwes¹⁵³, W.J. Murray¹²⁹, I. Mussche¹⁰⁵, E. Musto^{102a,102b}, A.G. Myagkov¹²⁸, M. Myska¹²⁵, J. Nadal¹¹, K. Nagai¹⁶⁰, K. Nagano⁶⁵, A. Nagarkar¹⁰⁹, Y. Nagasaka⁵⁹, M. Nagel⁹⁹, A.M. Nairz²⁹, Y. Nakahama²⁹, K. Nakamura¹⁵⁵, T. Nakamura¹⁵⁵, I. Nakano¹¹⁰, G. Nanava²⁰, A. Napier¹⁶¹, R. Narayan^{58b}, M. Nash^{77,c}, T. Nattermann²⁰, T. Naumann⁴¹, G. Navarro¹⁶², H.A. Neal⁸⁷, P.Yu. Nechaeva⁹⁴, T.J. Neep⁸², A. Negri^{119a,119b}, G. Negri²⁹, S. Nektarijevic⁴⁹, A. Nelson¹⁶³, T.K. Nelson¹⁴³, S. Nemecek¹²⁵, P. Nemethy¹⁰⁸, A.A. Nepomuceno^{23a}, M. Nessi^{29,aa}, M.S. Neubauer¹⁶⁵, A. Neusiedl⁸¹, R.M. Neves¹⁰⁸, P. Nevski²⁴, P.R. Newman¹⁷, V. Nguyen Thi Hong¹³⁶, R.B. Nickerson¹¹⁸, R. Nicolaidou¹³⁶, B. Nicquevert²⁹, F. Niedercorn¹¹⁵, J. Nielsen¹³⁷, N. Nikiforou³⁴, A. Nikiforov¹⁵, V. Nikolaenko¹²⁸, I. Nikolic-Audit⁷⁸, K. Nikolics⁴⁹, K. Nikolopoulos²⁴, H. Nilsen⁴⁸, P. Nilsson⁷, Y. Ninomiya¹⁵⁵, A. Nisati^{132a}, T. Nishiyama⁶⁶, R. Nisius⁹⁹, L. Nodulman⁵, M. Nomachi¹¹⁶, I. Nomidis¹⁵⁴, M. Nordberg²⁹, P.R. Norton¹²⁹, J. Novakova¹²⁶, M. Nozaki⁶⁵, L. Nozka¹¹³, I.M. Nugent^{159a}, A.-E. Nuncio-Quiroz²⁰, G. Nunes Hanninger⁸⁶, T. Nunnemann⁹⁸, E. Nurse⁷⁷, B.J. O'Brien⁴⁵, S.W. O'Neale^{17,*}, D.C. O'Neil¹⁴², V. O'Shea⁵³, L.B. Oakes⁹⁸, F.G. Oakham^{28,d}, H. Oberlack⁹⁹, J. Ocariz⁷⁸, A. Ochi⁶⁶, S. Oda⁶⁹, S. Odaka⁶⁵, J. Odier⁸³, H. Ogren⁶⁰, A. Oh⁸², S.H. Oh⁴⁴, C.C. Ohm^{146a,146b}, T. Ohshima¹⁰¹, S. Okada⁶⁶, H. Okawa¹⁶³, Y. Okumura¹⁰¹, T. Okuyama¹⁵⁵, A. Olariu^{25a}, A.G. Olchevski⁶⁴, S.A. Olivares Pino^{31a}, M. Oliveira^{124a,h}, D. Oliveira Damazio²⁴, E. Oliver Garcia¹⁶⁷, D. Olivito¹²⁰, A. Olszewski³⁸, J. Olszowska³⁸, A. Onofre^{124a,ab}, P.U.E. Onyisi³⁰, C.J. Oram^{159a}, M.J. Oreglia³⁰, Y. Oren¹⁵³, D. Orestano^{134a,134b}, N. Orlando^{72a,72b}, I. Orlov¹⁰⁷, C. Oropeza Barrera⁵³, R.S. Orr¹⁵⁸, B. Osculati^{50a,50b}, R. Ospanov¹²⁰, C. Osuna¹¹, G. Otero y Garzon²⁶, J.P. Ottersbach¹⁰⁵, M. Ouchrif^{135d}, E.A. Ouellette¹⁶⁹, F. Ould-Saada¹¹⁷, A. Ouraou¹³⁶, Q. Ouyang^{32a}, A. Ovcharova¹⁴, M. Owen⁸², S. Owen¹³⁹, V.E. Ozcan^{18a}, N. Ozturk⁷, A. Pacheco Pages¹¹, C.P. Padilla Aranda¹¹, S. Pagan Griso¹⁴, E. Paganis¹³⁹, F. Paige²⁴, P. Pais⁸⁴, K. Pajchel¹¹⁷, G. Palacino^{159b}, C.P. Palestini²⁹, D. Pallin³³, A. Palma^{124a}, J.D. Palmer¹⁷, Y.B. Pan¹⁷³, E. Panagiotopoulou⁹, P. Pani¹⁰⁵, N. Panikashvili⁸⁷, S. Panitkin²⁴, D. Pantea^{25a}, A. Papadelis^{146a}, Th.D. Papadopoulos⁹, A. Paramonov⁵, D. Paredes Hernandez³³, W. Park^{24,ac}, M.A. Parker²⁷, F. Parodi^{50a,50b}, J.A. Parsons³⁴, U. Parzefall⁴⁸, S. Pashapour⁵⁴, E. Pasqualucci^{132a}, S. Passaggio^{50a}, A. Passeri^{134a}, F. Pastore^{134a,134b,*}, Fr. Pastore⁷⁰, G. Pásztor^{49,ad}, S. Patarraia¹⁷⁵, N. Patel¹⁵⁰, J.R. Pater⁸², S. Patricelli^{102a,102b}, T. Pauly²⁹, M. Pecsny^{144a}, M.I. Pedraza Morales¹⁷³, S.V. Peleganchuk¹⁰⁷, D. Pelikan¹⁶⁶, H. Peng^{32b}, B. Penning³⁰, A. Penson³⁴, J. Penwell⁶⁰, M. Perantoni^{23a}, K. Perez^{34,ae}, T. Perez Cavalcanti⁴¹, E. Perez Codina^{159a}, M.T. Pérez García-Estañ¹⁶⁷, V. Perez Reale³⁴, L. Perini^{89a,89b}, H. Pernegger²⁹, R. Perrino^{72a}, P. Perrodo⁴, S. Perseme^{3a}, V.D. Peshekhonov⁶⁴, K. Peters²⁹, B.A. Petersen²⁹, J. Petersen²⁹, T.C. Petersen³⁵, E. Petit⁴, A. Petridis¹⁵⁴, C. Petridou¹⁵⁴, E. Petrolo^{132a}, F. Petrucci^{134a,134b}, D. Petschull⁴¹, M. Petteni¹⁴², R. Pezoa^{31b}, A. Phan⁸⁶, P.W. Phillips¹²⁹, G. Piacquadio²⁹, A. Picazio⁴⁹, E. Piccaro⁷⁵, M. Piccinini^{19a,19b}, S.M. Picc⁴¹, R. Piegai²⁶, D.T. Pignotti¹⁰⁹, J.E. Pilcher³⁰, A.D. Pilkington⁸², J. Pina^{124a,b}, M. Pinamonti^{164a,164c}, A. Pinder¹¹⁸, J.L. Pinfeld², B. Pinto^{124a}, C. Pizio^{89a,89b}, M. Plamondon¹⁶⁹, M.-A. Pleier²⁴, E. Plotnikova⁶⁴, A. Poblaguev²⁴, S. Poddar^{58a}, F. Podlyski³³,

L. Poggioli¹¹⁵, T. Poghosyan²⁰, M. Pohl⁴⁹, F. Polci⁵⁵, G. Polesello^{119a}, A. Policicchio^{36a,36b}, A. Polini^{19a}, J. Poll⁷⁵, V. Polychronakos²⁴, D.M. Pomarede¹³⁶, D. Pomeroy²², K. Pommès²⁹, L. Pontecorvo^{132a}, B.G. Pope⁸⁸, G.A. Popeneciu^{25a}, D.S. Popovic^{12a}, A. Poppleton²⁹, X. Portell Bueso²⁹, G.E. Pospelov⁹⁹, S. Pospisil¹²⁷, I.N. Potrap⁹⁹, C.J. Potter¹⁴⁹, C.T. Potter¹¹⁴, G. Poulard²⁹, J. Poveda¹⁷³, V. Pozdnyakov⁶⁴, R. Prabhu⁷⁷, P. Pralavorio⁸³, A. Pranko¹⁴, S. Prasad²⁹, R. Pravahan²⁴, S. Prell⁶³, K. Pretzl¹⁶, D. Price⁶⁰, J. Price⁷³, L.E. Price⁵, D. Prieur¹²³, M. Primavera^{72a}, K. Prokofiev¹⁰⁸, F. Prokoshin^{31b}, S. Protopopescu²⁴, J. Proudfoot⁵, X. Prudent⁴³, M. Przybycien³⁷, H. Przysieszniak⁴, S. Psoroulas²⁰, E. Ptacek¹¹⁴, E. Pueschel⁸⁴, J. Purdham⁸⁷, M. Purohit^{24,ac}, P. Puzo¹¹⁵, Y. Pylypchenko⁶², J. Qian⁸⁷, A. Quadt⁵⁴, D.R. Quarrie¹⁴, W.B. Quayle¹⁷³, F. Quinonez^{31a}, M. Raas¹⁰⁴, V. Radescu⁴¹, P. Radloff¹¹⁴, T. Rador^{18a}, F. Ragusa^{89a,89b}, G. Rahal¹⁷⁸, A.M. Rahimi¹⁰⁹, D. Rahm²⁴, S. Rajagopalan²⁴, M. Rammensee⁴⁸, M. Rammes¹⁴¹, A.S. Randle-Conde³⁹, K. Randrianarivony²⁸, F. Rauscher⁹⁸, T.C. Rave⁴⁸, M. Raymond²⁹, A.L. Read¹¹⁷, D.M. Rebuffi^{119a,119b}, A. Redelbach¹⁷⁴, G. Redlinger²⁴, R. Reece¹²⁰, K. Reeves⁴⁰, E. Reinherz-Aronis¹⁵³, A. Reinsch¹¹⁴, I. Reisinger⁴², C. Rembser²⁹, Z.L. Ren¹⁵¹, A. Renaud¹¹⁵, M. Rescigno^{132a}, S. Resconi^{89a}, B. Resende¹³⁶, P. Reznicek⁹⁸, R. Rezvani¹⁵⁸, R. Richter⁹⁹, E. Richter-Was^{4,af}, M. Ridel⁷⁸, M. Rijpstra¹⁰⁵, M. Rijssenbeek¹⁴⁸, A. Rimoldi^{119a,119b}, L. Rinaldi^{19a}, R.R. Rios³⁹, I. Riu¹¹, G. Rivoltella^{89a,89b}, F. Rizatdinova¹¹², E. Rizvi⁷⁵, S.H. Robertson^{85,k}, A. Robichaud-Veronneau¹¹⁸, D. Robinson²⁷, J.E.M. Robinson⁷⁷, A. Robson⁵³, J.G. Rocha de Lima¹⁰⁶, C. Roda^{122a,122b}, D. Roda Dos Santos²⁹, A. Roe⁵⁴, S. Roe²⁹, O. Röhne¹¹⁷, S. Rolli¹⁶¹, A. Romaniouk⁹⁶, M. Romano^{19a,19b}, G. Romeo²⁶, E. Romero Adam¹⁶⁷, L. Roos⁷⁸, E. Ros¹⁶⁷, S. Rosati^{132a}, K. Rosbach⁴⁹, A. Rose¹⁴⁹, M. Rose⁷⁶, G.A. Rosenbaum¹⁵⁸, E.I. Rosenberg⁶³, P.L. Rosendahl¹³, O. Rosenthal¹⁴¹, L. Rosselet⁴⁹, V. Rossetti¹¹, E. Rossi^{132a,132b}, L.P. Rossi^{50a}, M. Rotaru^{25a}, I. Roth¹⁷², J. Rothberg¹³⁸, D. Rousseau¹¹⁵, C.R. Royon¹³⁶, A. Rozanov⁸³, Y. Rozen¹⁵², X. Ruan^{32a,ag}, F. Rubbo¹¹, I. Rubinskiy⁴¹, B. Ruckert⁹⁸, N. Ruckstuhl¹⁰⁵, V.I. Rud⁹⁷, C. Rudolph⁴³, G. Rudolph⁶¹, F. Rühr⁶, F. Ruggieri^{134a,134b}, A. Ruiz-Martinez⁶³, L. Rummyantsev⁶⁴, K. Runge⁴⁸, Z. Rurikova⁴⁸, N.A. Rusakovich⁶⁴, J.P. Rutherford⁶, C. Ruwiedel^{14,*}, P. Ruzicka¹²⁵, Y.F. Ryabov¹²¹, P. Ryan⁸⁸, M. Rybar¹²⁶, G. Rybkin¹¹⁵, N.C. Ryder¹¹⁸, A.F. Saavedra¹⁵⁰, I. Sadeh¹⁵³, H.F.W. Sadrozinski¹³⁷, R. Sadykov⁶⁴, F. Safai Tehrani^{132a}, H. Sakamoto¹⁵⁵, G. Salamanna⁷⁵, A. Salamon^{133a}, M. Saleem¹¹¹, D. Salek²⁹, D. Salihagic⁹⁹, A. Salnikov¹⁴³, J. Salt¹⁶⁷, B.M. Salvachua Ferrando⁵, D. Salvatore^{36a,36b}, F. Salvatore¹⁴⁹, A. Salvucci¹⁰⁴, A. Salzburger²⁹, D. Sampsonidis¹⁵⁴, B.H. Samset¹¹⁷, A. Sanchez^{102a,102b}, V. Sanchez Martinez¹⁶⁷, H. Sandaker¹³, H.G. Sander⁸¹, M.P. Sanders⁹⁸, M. Sandhoff¹⁷⁵, T. Sandoval²⁷, C. Sandoval¹⁶², R. Sandstroem⁹⁹, D.P.C. Sankey¹²⁹, A. Sansoni⁴⁷, C. Santamarina Rios⁸⁵, C. Santoni³³, R. Santonico^{133a,133b}, H. Santos^{124a}, J.G. Saraiva^{124a}, T. Sarangi¹⁷³, E. Sarkisyan-Grinbaum⁷, F. Sarri^{122a,122b}, G. Sartisohn¹⁷⁵, O. Sasaki⁶⁵, N. Sasao⁶⁷, I. Satsounkevitch⁹⁰, G. Sauvage^{4,*}, E. Sauvan⁴, J.B. Sauvan¹¹⁵, P. Savard^{158,d}, V. Savinov¹²³, D.O. Savu²⁹, L. Sawyer^{24,m}, D.H. Saxon⁵³, J. Saxon¹²⁰, C. Sbarra^{19a}, A. Sbrizzi^{19a,19b}, O. Scallan⁹³, D.A. Scannicchio¹⁶³, M. Scarcella¹⁵⁰, J. Schaarschmidt¹¹⁵, P. Schacht⁹⁹, D. Schaefer¹²⁰, U. Schäfer⁸¹, S. Schaepe²⁰, S. Schaetzel^{158b}, A.C. Schaffer¹¹⁵, D. Schaile⁹⁸, R.D. Schamberger¹⁴⁸, A.G. Schamov¹⁰⁷, V. Scharf^{58a}, V.A. Schegelsky¹²¹, D. Scheirich⁸⁷, M. Schernau¹⁶³, M.I. Scherzer³⁴, C. Schiavi^{50a,50b}, J. Schieck⁹⁸, M. Schioppa^{36a,36b}, S. Schlenker²⁹, E. Schmidt⁴⁸, K. Schmieden²⁰, C. Schmitt⁸¹, S. Schmitt^{58b}, M. Schmitz²⁰, B. Schneider¹⁶, U. Schnoor⁴³, A. Schoening^{58b}, M. Schott²⁹, D. Schouten^{159a}, J. Schovancova¹²⁵, M. Schram⁸⁵, C. Schroeder⁸¹, N. Schroer^{58c}, M.J. Schultens²⁰, J. Schultes¹⁷⁵, H.-C. Schultz-Coulon^{58a}, H. Schulz¹⁵, J.W. Schumacher²⁰, M. Schumacher⁴⁸, B.A. Schumm¹³⁷, Ph. Schune¹³⁶, C. Schwanenberger⁸², A. Schwartzman¹⁴³, Ph. Schwemling⁷⁸, R. Schwienhorst⁸⁸, R. Schwierz⁴³, J. Schwindling¹³⁶, T. Schwindt²⁰, M. Schwoerer⁴, G. Sciolla²², W.G. Scott¹²⁹, J. Searcy¹¹⁴, G. Sedov⁴¹, E. Sedykh¹²¹, S.C. Seidel¹⁰³, A. Seiden¹³⁷, F. Seifert⁴³, J.M. Seixas^{23a}, G. Sekhniaidze^{102a}, S.J. Sekula³⁹, K.E. Selbach⁴⁵, D.M. Seliverstov¹²¹, B. Sellden^{146a}, G. Sellers⁷³, M. Seman^{144b}, N. Semprini-Cesari^{19a,19b}, C. Serfon⁹⁸, L. Serin¹¹⁵, L. Serkin⁵⁴, R. Seuster⁹⁹, H. Severini¹¹¹, A. Sfyrila²⁹, E. Shabalina⁵⁴, M. Shamim¹¹⁴, L.Y. Shan^{32a}, J.T. Shank²¹, Q.T. Shao⁸⁶, M. Shapiro¹⁴, P.B. Shatalov⁹⁵, K. Shaw^{164a,164c}, D. Sherman¹⁷⁶, P. Sherwood⁷⁷, A. Shibata¹⁰⁸, H. Shichi¹⁰¹, S. Shimizu²⁹, M. Shimojima¹⁰⁰, T. Shin⁵⁶, M. Shiyakova⁶⁴, A. Shmeleva⁹⁴, M.J. Shochet³⁰, D. Short¹¹⁸, S. Shrestha⁶³, E. Shulga⁹⁶, M.A. Shupe⁶, P. Sicho¹²⁵, A. Sidoti^{132a}, F. Siegert⁴⁸, Dj. Sijacki^{12a}, O. Silbert¹⁷², J. Silva^{124a}, Y. Silver¹⁵³, D. Silverstein¹⁴³, S.B. Silverstein^{146a}, V. Simak¹²⁷, O. Simard¹³⁶, Lj. Simic^{12a}, S. Simion¹¹⁵, B. Simmons⁷⁷, R. Simoniello^{89a,89b}, M. Simonyan³⁵, P. Sinervo¹⁵⁸, N.B. Sinev¹¹⁴, V. Sipica¹⁴¹, G. Siragusa¹⁷⁴, A. Sircar²⁴, A.N. Sisakyan^{64,*}, S.Yu. Sivoklov⁹⁷, J. Sjölin^{146a,146b}, T.B. Sjurson¹³, L.A. Skinnari¹⁴, H.P. Skottowe⁵⁷, K. Skovpen¹⁰⁷, P. Skubic¹¹¹, M. Slater¹⁷, T. Slavicek¹²⁷, K. Sliwa¹⁶¹, V. Smakhtin¹⁷², B.H. Smart⁴⁵, S.Yu. Smirnov⁹⁶, Y. Smirnov⁹⁶, L.N. Smirnova⁹⁷, O. Smirnova⁷⁹, B.C. Smith⁵⁷, D. Smith¹⁴³, K.M. Smith⁵³, M. Smizanska⁷¹, K. Smolek¹²⁷, A.A. Snesarev⁹⁴, S.W. Snow⁸², J. Snow¹¹¹, S. Snyder²⁴, R. Sobie^{169,k}, J. Sodomka¹²⁷, A. Soffer¹⁵³, C.A. Solans¹⁶⁷, M. Solar¹²⁷, J. Solc¹²⁷, E.Yu. Soldatov⁹⁶, U. Soldevila¹⁶⁷, E. Solfaroli Camillocci^{132a,132b}, A.A. Solodkov¹²⁸, O.V. Solovyanov¹²⁸, N. Soni², V. Sopko¹²⁷, B. Sopko¹²⁷, M. Sosebee⁷, R. Soualah^{164a,164c}, A. Soukharev¹⁰⁷, S. Spagnolo^{72a,72b}, F. Spano⁷⁶, R. Spighi^{19a}, G. Spigo²⁹, F. Spila^{132a,132b}, R. Spiwok²⁹, M. Spousta^{126,ah}, T. Spreitzer¹⁵⁸, B. Spurlock⁷, R.D. St. Denis⁵³, J. Stahlman¹²⁰, R. Stamen^{58a}, E. Stanecka³⁸, R.W. Stanek⁵, C. Stanescu^{134a}, M. Stanescu-Bellu⁴¹, S. Stapnes¹¹⁷, E.A. Starchenko¹²⁸, J. Stark⁵⁵, P. Staroba¹²⁵, P. Starovoitov⁴¹, A. Staude⁹⁸,

P. Stavina^{144a,*}, G. Steele⁵³, P. Steinbach⁴³, P. Steinberg²⁴, I. Stekl¹²⁷, B. Stelzer¹⁴², H.J. Stelzer⁸⁸,
 O. Stelzer-Chilton^{159a}, H. Stenzel⁵², S. Stern⁹⁹, G.A. Stewart²⁹, J.A. Stillings²⁰, M.C. Stockton⁸⁵, K. Stoerig⁴⁸,
 G. Stoicea^{25a}, S. Stonjek⁹⁹, P. Strachota¹²⁶, A.R. Stradling⁷, A. Straessner⁴³, J. Strandberg¹⁴⁷,
 S. Strandberg^{146a,146b}, A. Strandlie¹¹⁷, M. Strang¹⁰⁹, E. Strauss¹⁴³, M. Strauss¹¹¹, P. Strizenc^{144b}, R. Ströhmer¹⁷⁴,
 D.M. Strom¹¹⁴, J.A. Strong^{76,*}, R. Stroynowski³⁹, J. Strube¹²⁹, B. Stugu¹³, I. Stumer^{24,*}, J. Stupak¹⁴⁸,
 P. Sturm¹⁷⁵, N.A. Styles⁴¹, D.A. Soh^{151,w}, D. Su¹⁴³, HS. Subramania², A. Succurro¹¹, Y. Sugaya¹¹⁶, C. Suhr¹⁰⁶,
 K. Suita⁶⁶, M. Suk¹²⁶, V.V. Sulim⁹⁴, S. Sultansoy^{3d}, T. Sumida⁶⁷, X. Sun⁵⁵, J.E. Sundermann⁴⁸, K. Suruliz¹³⁹,
 G. Susinno^{36a,36b}, M.R. Sutton¹⁴⁹, Y. Suzuki⁶⁵, Y. Suzuki⁶⁶, M. Svatos¹²⁵, S. Swedish¹⁶⁸, I. Sykora^{144a},
 T. Sykora¹²⁶, J. Sánchez¹⁶⁷, D. Ta¹⁰⁵, K. Tackmann⁴¹, A. Taffard¹⁶³, R. Tafirout^{159a}, N. Taiblum¹⁵³,
 Y. Takahashi¹⁰¹, H. Takai²⁴, R. Takashima⁶⁸, H. Takeda⁶⁶, T. Takeshita¹⁴⁰, Y. Takubo⁶⁵, M. Talby⁸³,
 A. Talyshev^{107,f}, M.C. Tamsett²⁴, J. Tanaka¹⁵⁵, R. Tanaka¹¹⁵, S. Tanaka¹³¹, S. Tanaka⁶⁵, A.J. Tanasijczuk¹⁴²,
 K. Tani⁶⁶, N. Tannoury⁸³, S. Tapprogge⁸¹, D. Tardiif¹⁵⁸, S. Tarem¹⁵², F. Tarrade²⁸, G.F. Tartarelli^{89a}, P. Tas¹²⁶,
 M. Tasevsky¹²⁵, E. Tassi^{36a,36b}, M. Tatarkhanov¹⁴, Y. Tayalati^{135d}, C. Taylor⁷⁷, F.E. Taylor⁹², G.N. Taylor⁸⁶,
 W. Taylor^{159b}, M. Teinturier¹¹⁵, M. Teixeira Dias Castanheira⁷⁵, P. Teixeira-Dias⁷⁶, K.K. Temming⁴⁸,
 H. Ten Kate²⁹, P.K. Teng¹⁵¹, S. Terada⁶⁵, K. Terashi¹⁵⁵, J. Terron⁸⁰, M. Testa⁴⁷, R.J. Teuscher^{158,k}, J. Therhaag²⁰,
 T. Theveneaux-Pelzer⁷⁸, S. Thoma⁴⁸, J.P. Thomas¹⁷, E.N. Thompson³⁴, P.D. Thompson¹⁷, P.D. Thompson¹⁵⁸,
 A.S. Thompson⁵³, L.A. Thomsen³⁵, E. Thomson¹²⁰, M. Thomson²⁷, R.P. Thun⁸⁷, F. Tian³⁴, M.J. Tibbets¹⁴,
 T. Tic¹²⁵, V.O. Tikhomirov⁹⁴, Y.A. Tikhonov^{107,f}, S. Timoshenko⁹⁶, P. Tipton¹⁷⁶, F.J. Tique Aires Viegas²⁹,
 S. Tisserant⁸³, T. Todorov⁴, S. Todorova-Nova¹⁶¹, B. Toggerson¹⁶³, J. Tojo⁶⁹, S. Tokár^{144a}, K. Tokunaga⁶⁶,
 K. Tokushuku⁶⁵, K. Tollefson⁸⁸, M. Tomoto¹⁰¹, L. Tompkins³⁰, K. Toms¹⁰³, A. Tonoyan¹³, C. Topfel¹⁶,
 N.D. Topilin⁶⁴, I. Torchiani²⁹, E. Torrence¹¹⁴, H. Torres⁷⁸, E. Torró Pastor¹⁶⁷, J. Toth^{83,ad}, F. Touchard⁸³,
 D.R. Tovey¹³⁹, T. Trefzger¹⁷⁴, L. Tremblet²⁹, A. Tricoli²⁹, I.M. Trigger^{159a}, S. Trincaz-Duvoid⁷⁸, M.F. Tripiana⁷⁰,
 W. Trischuk¹⁵⁸, B. Trocmé⁵⁵, C. Troncon^{89a}, M. Trottier-McDonald¹⁴², M. Trzebinski³⁸, A. Trzupek³⁸,
 C. Tsarouchas²⁹, J.C.-L. Tseng¹¹⁸, M. Tsiakiris¹⁰⁵, P.V. Tsiarehka⁹⁰, D. Tsionou^{4,ai}, G. Tsipolitis⁹,
 S. Tsiskaridze¹¹, V. Tsiskaridze⁴⁸, E.G. Tskhadadze^{51a}, I.I. Tsukerman⁹⁵, V. Tsulaia¹⁴, J.-W. Tsung²⁰, S. Tsuno⁶⁵,
 D. Tsybychev¹⁴⁸, A. Tua¹³⁹, A. Tudorache^{25a}, V. Tudorache^{25a}, J.M. Tuggle³⁰, M. Turala³⁸, D. Turecek¹²⁷,
 I. Turk Cakir^{3e}, E. Turlay¹⁰⁵, R. Turra^{89a,89b}, P.M. Tuts³⁴, A. Tykhonov⁷⁴, M. Tylmad^{146a,146b}, M. Tyndel¹²⁹,
 G. Tzanakos⁸, K. Uchida²⁰, I. Ueda¹⁵⁵, R. Ueno²⁸, M. Uglund¹³, M. Uhlenbrock²⁰, M. Uhrmacher⁵⁴, F. Ukegawa¹⁶⁰,
 G. Unal²⁹, A. Undrus²⁴, G. Unel¹⁶³, Y. Unno⁶⁵, D. Urbaniec³⁴, G. Usai⁷, M. Uslenghi^{119a,119b}, L. Vacavant⁸³,
 V. Vacek¹²⁷, B. Vachon⁸⁵, S. Vahsen¹⁴, J. Valenta¹²⁵, P. Valente^{132a}, S. Valentinetti^{19a,19b}, S. Valkar¹²⁶,
 E. Valladolid Gallego¹⁶⁷, S. Vallecorsa¹⁵², J.A. Valls Ferrer¹⁶⁷, H. van der Graaf¹⁰⁵, E. van der Kraaij¹⁰⁵,
 R. Van Der Leeuw¹⁰⁵, E. van der Poel¹⁰⁵, D. van der Ster²⁹, N. van Eldik²⁹, P. van Gemmeren⁵, I. van Vulpen¹⁰⁵,
 M. Vanadia⁹⁹, W. Vandelli²⁹, A. Vaniachine⁵, P. Vankov⁴¹, F. Vannucci⁷⁸, R. Vari^{132a}, T. Varol⁸⁴, D. Varouchas¹⁴,
 A. Vartapetian⁷, K.E. Varvell¹⁵⁰, V.I. Vassilakopoulos⁵⁶, F. Vazeille³³, T. Vazquez Schroeder⁵⁴, G. Vegni^{89a,89b},
 J.J. Veillet¹¹⁵, F. Veloso^{124a}, R. Veness²⁹, S. Veneziano^{132a}, A. Ventura^{72a,72b}, D. Ventura⁸⁴, M. Venturi⁴⁸,
 N. Venturi¹⁵⁸, V. Vercesi^{119a}, M. Verducci¹³⁸, W. Verkerke¹⁰⁵, J.C. Vermeulen¹⁰⁵, A. Vest⁴³, M.C. Vetterli^{142,d},
 I. Vichou¹⁶⁵, T. Vickey^{145b,aj}, O.E. Vickey Boeriu^{145b}, G.H.A. Viehhauser¹¹⁸, S. Viel¹⁶⁸, M. Villa^{19a,19b},
 M. Villaplana Perez¹⁶⁷, E. Vilucchi⁴⁷, M.G. Vincker²⁸, E. Vinek²⁹, V.B. Vinogradov⁶⁴, M. Virchaux^{136,*}, J. Virzi¹⁴,
 O. Vitells¹⁷², M. Viti⁴¹, I. Vivarelli⁴⁸, F. Vives Vaque², S. Vlachos⁹, D. Vladouiu⁹⁸, M. Vlasak¹²⁷, A. Vogel²⁰,
 P. Vokac¹²⁷, G. Volpi⁴⁷, M. Volpi⁸⁶, G. Volpini^{89a}, H. von der Schmitt⁹⁹, J. von Loeben⁹⁹, H. von Radziewski⁴⁸,
 E. von Toerne²⁰, V. Vorobel¹²⁶, V. Vorwerk¹¹, M. Vos¹⁶⁷, R. Voss²⁹, T.T. Voss¹⁷⁵, J.H. Vosseveld⁷³, N. Vranjes¹³⁶,
 M. Vranjes Milosavljevic¹⁰⁵, V. Vrba¹²⁵, M. Vreeswijk¹⁰⁵, T. Vu Anh⁴⁸, R. Vuillermet²⁹, I. Vukotic¹¹⁵,
 W. Wagner¹⁷⁵, P. Wagner¹²⁰, H. Wahlen¹⁷⁵, S. Wahrenmund⁴³, J. Wakabayashi¹⁰¹, S. Walch⁸⁷, J. Walder⁷¹,
 R. Walker⁹⁸, W. Walkowiak¹⁴¹, R. Wall¹⁷⁶, P. Waller⁷³, C. Wang⁴⁴, H. Wang¹⁷³, H. Wang^{32b,ak}, J. Wang¹⁵¹,
 J. Wang⁵⁵, R. Wang¹⁰³, S.M. Wang¹⁵¹, T. Wang²⁰, A. Warburton⁸⁵, C.P. Ward²⁷, M. Warsinsky⁴⁸, A. Washbrook⁴⁵,
 C. Wasicki⁴¹, P.M. Watkins¹⁷, A.T. Watson¹⁷, I.J. Watson¹⁵⁰, M.F. Watson¹⁷, G. Watts¹³⁸, S. Watts⁸²,
 A.T. Waugh¹⁵⁰, B.M. Waugh⁷⁷, M. Weber¹²⁹, M.S. Weber¹⁶, P. Weber⁵⁴, A.R. Weidberg¹¹⁸, P. Weigell⁹⁹,
 J. Weingarten⁵⁴, C. Weiser⁴⁸, H. Wellenstein²², P.S. Wells²⁹, T. Wenaus²⁴, D. Wendland¹⁵, Z. Weng^{151,w},
 T. Wengler²⁹, S. Wenig²⁹, N. Wermes²⁰, M. Werner⁴⁸, P. Werner²⁹, M. Werth¹⁶³, M. Wessels^{58a}, J. Wetter¹⁶¹,
 C. Weydert⁵⁵, K. Whalen²⁸, S.J. Wheeler-Ellis¹⁶³, A. White⁷, M.J. White⁸⁶, S. White^{122a,122b}, S.R. Whitehead¹¹⁸,
 D. Whiteson¹⁶³, D. Whittington⁶⁰, F. Wicek¹¹⁵, D. Wicke¹⁷⁵, F.J. Wickens¹²⁹, W. Wiedenmann¹⁷³, M. Wielers¹²⁹,
 P. Wienemann²⁰, C. Wiglesworth⁷⁵, L.A.M. Wiik-Fuchs⁴⁸, P.A. Wijeratne⁷⁷, A. Wildauer¹⁶⁷, M.A. Wildt^{41,s},
 I. Wilhelm¹²⁶, H.G. Wilkens²⁹, J.Z. Will⁹⁸, E. Williams³⁴, H.H. Williams¹²⁰, W. Willis³⁴, S. Willocq⁸⁴,
 J.A. Wilson¹⁷, M.G. Wilson¹⁴³, A. Wilson⁸⁷, I. Wingerter-Seez⁴, S. Winkelmann⁴⁸, F. Winklmeier²⁹, M. Wittgen¹⁴³,
 M.W. Wolter³⁸, H. Wolters^{124a,h}, W.C. Wong⁴⁰, G. Wooden⁸⁷, B.K. Wosiek³⁸, J. Wotschack²⁹, M.J. Woudstra⁸²,
 K.W. Wozniak³⁸, K. Wraight⁵³, C. Wright⁵³, M. Wright⁵³, B. Wrona⁷³, S.L. Wu¹⁷³, X. Wu⁴⁹, Y. Wu^{32b,al},
 E. Wulf³⁴, B.M. Wynne⁴⁵, S. Xella³⁵, M. Xiao¹³⁶, S. Xie⁴⁸, C. Xu^{32b,z}, D. Xu¹³⁹, B. Yabsley¹⁵⁰, S. Yacoub^{145b},
 M. Yamada⁶⁵, H. Yamaguchi¹⁵⁵, A. Yamamoto⁶⁵, K. Yamamoto⁶³, S. Yamamoto¹⁵⁵, T. Yamamura¹⁵⁵,

T. Yamanaka¹⁵⁵, J. Yamaoka⁴⁴, T. Yamazaki¹⁵⁵, Y. Yamazaki⁶⁶, Z. Yan²¹, H. Yang⁸⁷, U.K. Yang⁸², Y. Yang⁶⁰, Z. Yang^{146a,146b}, S. Yanush⁹¹, L. Yao^{32a}, Y. Yao¹⁴, Y. Yasu⁶⁵, G.V. Ybeles Smit¹³⁰, J. Ye³⁹, S. Ye²⁴, M. Yilmaz^{3c}, R. Yoosofmiya¹²³, K. Yorita¹⁷¹, R. Yoshida⁵, C. Young¹⁴³, C.J. Young¹¹⁸, S. Youssef²¹, D. Yu²⁴, J. Yu⁷, J. Yu¹¹², L. Yuan⁶⁶, A. Yurkewicz¹⁰⁶, B. Zabinski³⁸, R. Zaidan⁶², A.M. Zaitsev¹²⁸, Z. Zajacova²⁹, L. Zanello^{132a,132b}, A. Zaytsev¹⁰⁷, C. Zeitnitz¹⁷⁵, M. Zeman¹²⁵, A. Zemla³⁸, C. Zender²⁰, O. Zenin¹²⁸, T. Ženiš^{144a}, Z. Zinonos^{122a,122b}, S. Zenz¹⁴, D. Zerwas¹¹⁵, G. Zevi della Porta⁵⁷, Z. Zhan^{32d}, D. Zhang^{32b,ak}, H. Zhang⁸⁸, J. Zhang⁵, X. Zhang^{32d}, Z. Zhang¹¹⁵, L. Zhao¹⁰⁸, T. Zhao¹³⁸, Z. Zhao^{32b}, A. Zhemchugov⁶⁴, J. Zhong¹¹⁸, B. Zhou⁸⁷, N. Zhou¹⁶³, Y. Zhou¹⁵¹, C.G. Zhu^{32d}, H. Zhu⁴¹, J. Zhu⁸⁷, Y. Zhu^{32b}, X. Zhuang⁹⁸, V. Zhuravlov⁹⁹, D. Zieminska⁶⁰, R. Zimmermann²⁰, S. Zimmermann²⁰, S. Zimmermann⁴⁸, M. Ziolkowski¹⁴¹, R. Zitoun⁴, L. Živković³⁴, V.V. Zmouchko^{128,*}, G. Zobernig¹⁷³, A. Zoccoli^{19a,19b}, M. zur Nedden¹⁵, V. Zutshi¹⁰⁶, L. Zwalinski²⁹.

¹ Physics Department, SUNY Albany, Albany NY, United States of America

² Department of Physics, University of Alberta, Edmonton AB, Canada

³ ^(a)Department of Physics, Ankara University, Ankara; ^(b)Department of Physics, Dumlupinar University, Kutahya;

^(c)Department of Physics, Gazi University, Ankara; ^(d)Division of Physics, TOBB University of Economics and Technology, Ankara; ^(e)Turkish Atomic Energy Authority, Ankara, Turkey

⁴ LAPP, CNRS/IN2P3 and Université de Savoie, Annecy-le-Vieux, France

⁵ High Energy Physics Division, Argonne National Laboratory, Argonne IL, United States of America

⁶ Department of Physics, University of Arizona, Tucson AZ, United States of America

⁷ Department of Physics, The University of Texas at Arlington, Arlington TX, United States of America

⁸ Physics Department, University of Athens, Athens, Greece

⁹ Physics Department, National Technical University of Athens, Zografou, Greece

¹⁰ Institute of Physics, Azerbaijan Academy of Sciences, Baku, Azerbaijan

¹¹ Institut de Física d'Altes Energies and Departament de Física de la Universitat Autònoma de Barcelona and ICREA, Barcelona, Spain

¹² ^(a)Institute of Physics, University of Belgrade, Belgrade; ^(b)Vinca Institute of Nuclear Sciences, University of Belgrade, Belgrade, Serbia

¹³ Department for Physics and Technology, University of Bergen, Bergen, Norway

¹⁴ Physics Division, Lawrence Berkeley National Laboratory and University of California, Berkeley CA, United States of America

¹⁵ Department of Physics, Humboldt University, Berlin, Germany

¹⁶ Albert Einstein Center for Fundamental Physics and Laboratory for High Energy Physics, University of Bern, Bern, Switzerland

¹⁷ School of Physics and Astronomy, University of Birmingham, Birmingham, United Kingdom

¹⁸ ^(a)Department of Physics, Bogazici University, Istanbul; ^(b)Division of Physics, Dogus University, Istanbul;

^(c)Department of Physics Engineering, Gaziantep University, Gaziantep; ^(d)Department of Physics, Istanbul Technical University, Istanbul, Turkey

¹⁹ ^(a)INFN Sezione di Bologna; ^(b)Dipartimento di Fisica, Università di Bologna, Bologna, Italy

²⁰ Physikalisches Institut, University of Bonn, Bonn, Germany

²¹ Department of Physics, Boston University, Boston MA, United States of America

²² Department of Physics, Brandeis University, Waltham MA, United States of America

²³ ^(a)Universidade Federal do Rio De Janeiro COPPE/EE/IF, Rio de Janeiro; ^(b)Federal University of Juiz de Fora (UFJF), Juiz de Fora; ^(c)Federal University of Sao Joao del Rei (UFSJ), Sao Joao del Rei; ^(d)Instituto de Fisica, Universidade de Sao Paulo, Sao Paulo, Brazil

²⁴ Physics Department, Brookhaven National Laboratory, Upton NY, United States of America

²⁵ ^(a)National Institute of Physics and Nuclear Engineering, Bucharest; ^(b)University Politehnica Bucharest, Bucharest; ^(c)West University in Timisoara, Timisoara, Romania

²⁶ Departamento de Física, Universidad de Buenos Aires, Buenos Aires, Argentina

²⁷ Cavendish Laboratory, University of Cambridge, Cambridge, United Kingdom

²⁸ Department of Physics, Carleton University, Ottawa ON, Canada

²⁹ CERN, Geneva, Switzerland

³⁰ Enrico Fermi Institute, University of Chicago, Chicago IL, United States of America

³¹ ^(a)Departamento de Física, Pontificia Universidad Católica de Chile, Santiago; ^(b)Departamento de Física, Universidad Técnica Federico Santa María, Valparaíso, Chile

³² ^(a)Institute of High Energy Physics, Chinese Academy of Sciences, Beijing; ^(b)Department of Modern Physics, University of Science and Technology of China, Anhui; ^(c)Department of Physics, Nanjing University, Jiangsu;

^(d)School of Physics, Shandong University, Shandong, China

³³ Laboratoire de Physique Corpusculaire, Clermont Université and Université Blaise Pascal and CNRS/IN2P3,

Aubiere Cedex, France

³⁴ Nevis Laboratory, Columbia University, Irvington NY, United States of America

³⁵ Niels Bohr Institute, University of Copenhagen, Kobenhavn, Denmark

³⁶ ^(a)INFN Gruppo Collegato di Cosenza; ^(b)Dipartimento di Fisica, Università della Calabria, Arcavata di Rende, Italy

³⁷ AGH University of Science and Technology, Faculty of Physics and Applied Computer Science, Krakow, Poland

³⁸ The Henryk Niewodniczanski Institute of Nuclear Physics, Polish Academy of Sciences, Krakow, Poland

³⁹ Physics Department, Southern Methodist University, Dallas TX, United States of America

⁴⁰ Physics Department, University of Texas at Dallas, Richardson TX, United States of America

⁴¹ DESY, Hamburg and Zeuthen, Germany

⁴² Institut für Experimentelle Physik IV, Technische Universität Dortmund, Dortmund, Germany

⁴³ Institut für Kern- und Teilchenphysik, Technical University Dresden, Dresden, Germany

⁴⁴ Department of Physics, Duke University, Durham NC, United States of America

⁴⁵ SUPA - School of Physics and Astronomy, University of Edinburgh, Edinburgh, United Kingdom

⁴⁶ Fachhochschule Wiener Neustadt, Johannes Gutenbergstrasse 32700 Wiener Neustadt, Austria

⁴⁷ INFN Laboratori Nazionali di Frascati, Frascati, Italy

⁴⁸ Fakultät für Mathematik und Physik, Albert-Ludwigs-Universität, Freiburg i.Br., Germany

⁴⁹ Section de Physique, Université de Genève, Geneva, Switzerland

⁵⁰ ^(a)INFN Sezione di Genova; ^(b)Dipartimento di Fisica, Università di Genova, Genova, Italy

⁵¹ ^(a)E.Andronikashvili Institute of Physics, Tbilisi State University, Tbilisi; ^(b)High Energy Physics Institute, Tbilisi State University, Tbilisi, Georgia

⁵² II Physikalisches Institut, Justus-Liebig-Universität Giessen, Giessen, Germany

⁵³ SUPA - School of Physics and Astronomy, University of Glasgow, Glasgow, United Kingdom

⁵⁴ II Physikalisches Institut, Georg-August-Universität, Göttingen, Germany

⁵⁵ Laboratoire de Physique Subatomique et de Cosmologie, Université Joseph Fourier and CNRS/IN2P3 and Institut National Polytechnique de Grenoble, Grenoble, France

⁵⁶ Department of Physics, Hampton University, Hampton VA, United States of America

⁵⁷ Laboratory for Particle Physics and Cosmology, Harvard University, Cambridge MA, United States of America

⁵⁸ ^(a)Kirchhoff-Institut für Physik, Ruprecht-Karls-Universität Heidelberg, Heidelberg; ^(b)Physikalisches Institut, Ruprecht-Karls-Universität Heidelberg, Heidelberg; ^(c)ZITI Institut für technische Informatik, Ruprecht-Karls-Universität Heidelberg, Mannheim, Germany

⁵⁹ Faculty of Applied Information Science, Hiroshima Institute of Technology, Hiroshima, Japan

⁶⁰ Department of Physics, Indiana University, Bloomington IN, United States of America

⁶¹ Institut für Astro- und Teilchenphysik, Leopold-Franzens-Universität, Innsbruck, Austria

⁶² University of Iowa, Iowa City IA, United States of America

⁶³ Department of Physics and Astronomy, Iowa State University, Ames IA, United States of America

⁶⁴ Joint Institute for Nuclear Research, JINR Dubna, Dubna, Russia

⁶⁵ KEK, High Energy Accelerator Research Organization, Tsukuba, Japan

⁶⁶ Graduate School of Science, Kobe University, Kobe, Japan

⁶⁷ Faculty of Science, Kyoto University, Kyoto, Japan

⁶⁸ Kyoto University of Education, Kyoto, Japan

⁶⁹ Department of Physics, Kyushu University, Fukuoka, Japan

⁷⁰ Instituto de Física La Plata, Universidad Nacional de La Plata and CONICET, La Plata, Argentina

⁷¹ Physics Department, Lancaster University, Lancaster, United Kingdom

⁷² ^(a)INFN Sezione di Lecce; ^(b)Dipartimento di Matematica e Fisica, Università del Salento, Lecce, Italy

⁷³ Oliver Lodge Laboratory, University of Liverpool, Liverpool, United Kingdom

⁷⁴ Department of Physics, Jožef Stefan Institute and University of Ljubljana, Ljubljana, Slovenia

⁷⁵ School of Physics and Astronomy, Queen Mary University of London, London, United Kingdom

⁷⁶ Department of Physics, Royal Holloway University of London, Surrey, United Kingdom

⁷⁷ Department of Physics and Astronomy, University College London, London, United Kingdom

⁷⁸ Laboratoire de Physique Nucléaire et de Hautes Energies, UPMC and Université Paris-Diderot and CNRS/IN2P3, Paris, France

⁷⁹ Fysiska institutionen, Lunds universitet, Lund, Sweden

⁸⁰ Departamento de Física Teórica C-15, Universidad Autónoma de Madrid, Madrid, Spain

⁸¹ Institut für Physik, Universität Mainz, Mainz, Germany

⁸² School of Physics and Astronomy, University of Manchester, Manchester, United Kingdom

⁸³ CPPM, Aix-Marseille Université and CNRS/IN2P3, Marseille, France

⁸⁴ Department of Physics, University of Massachusetts, Amherst MA, United States of America

- 85 Department of Physics, McGill University, Montreal QC, Canada
- 86 School of Physics, University of Melbourne, Victoria, Australia
- 87 Department of Physics, The University of Michigan, Ann Arbor MI, United States of America
- 88 Department of Physics and Astronomy, Michigan State University, East Lansing MI, United States of America
- 89 ^(a)INFN Sezione di Milano; ^(b)Dipartimento di Fisica, Università di Milano, Milano, Italy
- 90 B.I. Stepanov Institute of Physics, National Academy of Sciences of Belarus, Minsk, Republic of Belarus
- 91 National Scientific and Educational Centre for Particle and High Energy Physics, Minsk, Republic of Belarus
- 92 Department of Physics, Massachusetts Institute of Technology, Cambridge MA, United States of America
- 93 Group of Particle Physics, University of Montreal, Montreal QC, Canada
- 94 P.N. Lebedev Institute of Physics, Academy of Sciences, Moscow, Russia
- 95 Institute for Theoretical and Experimental Physics (ITEP), Moscow, Russia
- 96 Moscow Engineering and Physics Institute (MEPhI), Moscow, Russia
- 97 Skobeltsyn Institute of Nuclear Physics, Lomonosov Moscow State University, Moscow, Russia
- 98 Fakultät für Physik, Ludwig-Maximilians-Universität München, München, Germany
- 99 Max-Planck-Institut für Physik (Werner-Heisenberg-Institut), München, Germany
- 100 Nagasaki Institute of Applied Science, Nagasaki, Japan
- 101 Graduate School of Science and Kobayashi-Maskawa Institute, Nagoya University, Nagoya, Japan
- 102 ^(a)INFN Sezione di Napoli; ^(b)Dipartimento di Scienze Fisiche, Università di Napoli, Napoli, Italy
- 103 Department of Physics and Astronomy, University of New Mexico, Albuquerque NM, United States of America
- 104 Institute for Mathematics, Astrophysics and Particle Physics, Radboud University Nijmegen/Nikhef, Nijmegen, Netherlands
- 105 Nikhef National Institute for Subatomic Physics and University of Amsterdam, Amsterdam, Netherlands
- 106 Department of Physics, Northern Illinois University, DeKalb IL, United States of America
- 107 Budker Institute of Nuclear Physics, SB RAS, Novosibirsk, Russia
- 108 Department of Physics, New York University, New York NY, United States of America
- 109 Ohio State University, Columbus OH, United States of America
- 110 Faculty of Science, Okayama University, Okayama, Japan
- 111 Homer L. Dodge Department of Physics and Astronomy, University of Oklahoma, Norman OK, United States of America
- 112 Department of Physics, Oklahoma State University, Stillwater OK, United States of America
- 113 Palacký University, RCPTM, Olomouc, Czech Republic
- 114 Center for High Energy Physics, University of Oregon, Eugene OR, United States of America
- 115 LAL, Université Paris-Sud and CNRS/IN2P3, Orsay, France
- 116 Graduate School of Science, Osaka University, Osaka, Japan
- 117 Department of Physics, University of Oslo, Oslo, Norway
- 118 Department of Physics, Oxford University, Oxford, United Kingdom
- 119 ^(a)INFN Sezione di Pavia; ^(b)Dipartimento di Fisica, Università di Pavia, Pavia, Italy
- 120 Department of Physics, University of Pennsylvania, Philadelphia PA, United States of America
- 121 Petersburg Nuclear Physics Institute, Gatchina, Russia
- 122 ^(a)INFN Sezione di Pisa; ^(b)Dipartimento di Fisica E. Fermi, Università di Pisa, Pisa, Italy
- 123 Department of Physics and Astronomy, University of Pittsburgh, Pittsburgh PA, United States of America
- 124 ^(a)Laboratorio de Instrumentacao e Fisica Experimental de Particulas - LIP, Lisboa, Portugal; ^(b)Departamento de Fisica Teorica y del Cosmos and CAFPE, Universidad de Granada, Granada, Spain
- 125 Institute of Physics, Academy of Sciences of the Czech Republic, Praha, Czech Republic
- 126 Faculty of Mathematics and Physics, Charles University in Prague, Praha, Czech Republic
- 127 Czech Technical University in Prague, Praha, Czech Republic
- 128 State Research Center Institute for High Energy Physics, Protvino, Russia
- 129 Particle Physics Department, Rutherford Appleton Laboratory, Didcot, United Kingdom
- 130 Physics Department, University of Regina, Regina SK, Canada
- 131 Ritsumeikan University, Kusatsu, Shiga, Japan
- 132 ^(a)INFN Sezione di Roma I; ^(b)Dipartimento di Fisica, Università La Sapienza, Roma, Italy
- 133 ^(a)INFN Sezione di Roma Tor Vergata; ^(b)Dipartimento di Fisica, Università di Roma Tor Vergata, Roma, Italy
- 134 ^(a)INFN Sezione di Roma Tre; ^(b)Dipartimento di Fisica, Università Roma Tre, Roma, Italy
- 135 ^(a)Faculté des Sciences Ain Chock, Réseau Universitaire de Physique des Hautes Energies - Université Hassan II, Casablanca; ^(b)Centre National de l'Energie des Sciences Techniques Nucleaires, Rabat; ^(c)Faculté des Sciences Semlalia, Université Cadi Ayyad, LPHEA-Marrakech; ^(d)Faculté des Sciences, Université Mohamed Premier and LPTPM, Oujda; ^(e)Faculté des sciences, Université Mohammed V-Agdal, Rabat, Morocco
- 136 DSM/IRFU (Institut de Recherches sur les Lois Fondamentales de l'Univers), CEA Saclay (Commissariat a

l'Energie Atomique), Gif-sur-Yvette, France

¹³⁷ Santa Cruz Institute for Particle Physics, University of California Santa Cruz, Santa Cruz CA, United States of America

¹³⁸ Department of Physics, University of Washington, Seattle WA, United States of America

¹³⁹ Department of Physics and Astronomy, University of Sheffield, Sheffield, United Kingdom

¹⁴⁰ Department of Physics, Shinshu University, Nagano, Japan

¹⁴¹ Fachbereich Physik, Universität Siegen, Siegen, Germany

¹⁴² Department of Physics, Simon Fraser University, Burnaby BC, Canada

¹⁴³ SLAC National Accelerator Laboratory, Stanford CA, United States of America

¹⁴⁴ ^(a) Faculty of Mathematics, Physics & Informatics, Comenius University, Bratislava; ^(b) Department of Subnuclear Physics, Institute of Experimental Physics of the Slovak Academy of Sciences, Kosice, Slovak Republic

¹⁴⁵ ^(a) Department of Physics, University of Johannesburg, Johannesburg; ^(b) School of Physics, University of the Witwatersrand, Johannesburg, South Africa

¹⁴⁶ ^(a) Department of Physics, Stockholm University; ^(b) The Oskar Klein Centre, Stockholm, Sweden

¹⁴⁷ Physics Department, Royal Institute of Technology, Stockholm, Sweden

¹⁴⁸ Departments of Physics & Astronomy and Chemistry, Stony Brook University, Stony Brook NY, United States of America

¹⁴⁹ Department of Physics and Astronomy, University of Sussex, Brighton, United Kingdom

¹⁵⁰ School of Physics, University of Sydney, Sydney, Australia

¹⁵¹ Institute of Physics, Academia Sinica, Taipei, Taiwan

¹⁵² Department of Physics, Technion: Israel Institute of Technology, Haifa, Israel

¹⁵³ Raymond and Beverly Sackler School of Physics and Astronomy, Tel Aviv University, Tel Aviv, Israel

¹⁵⁴ Department of Physics, Aristotle University of Thessaloniki, Thessaloniki, Greece

¹⁵⁵ International Center for Elementary Particle Physics and Department of Physics, The University of Tokyo, Tokyo, Japan

¹⁵⁶ Graduate School of Science and Technology, Tokyo Metropolitan University, Tokyo, Japan

¹⁵⁷ Department of Physics, Tokyo Institute of Technology, Tokyo, Japan

¹⁵⁸ Department of Physics, University of Toronto, Toronto ON, Canada

¹⁵⁹ ^(a) TRIUMF, Vancouver BC; ^(b) Department of Physics and Astronomy, York University, Toronto ON, Canada

¹⁶⁰ Institute of Pure and Applied Sciences, University of Tsukuba, 1-1-1 Tennodai, Tsukuba, Ibaraki 305-8571, Japan

¹⁶¹ Science and Technology Center, Tufts University, Medford MA, United States of America

¹⁶² Centro de Investigaciones, Universidad Antonio Narino, Bogota, Colombia

¹⁶³ Department of Physics and Astronomy, University of California Irvine, Irvine CA, United States of America

¹⁶⁴ ^(a) INFN Gruppo Collegato di Udine; ^(b) ICTP, Trieste; ^(c) Dipartimento di Chimica, Fisica e Ambiente, Università di Udine, Udine, Italy

¹⁶⁵ Department of Physics, University of Illinois, Urbana IL, United States of America

¹⁶⁶ Department of Physics and Astronomy, University of Uppsala, Uppsala, Sweden

¹⁶⁷ Instituto de Física Corpuscular (IFIC) and Departamento de Física Atómica, Molecular y Nuclear and Departamento de Ingeniería Electrónica and Instituto de Microelectrónica de Barcelona (IMB-CNM), University of Valencia and CSIC, Valencia, Spain

¹⁶⁸ Department of Physics, University of British Columbia, Vancouver BC, Canada

¹⁶⁹ Department of Physics and Astronomy, University of Victoria, Victoria BC, Canada

¹⁷⁰ Department of Physics, University of Warwick, Coventry, United Kingdom

¹⁷¹ Waseda University, Tokyo, Japan

¹⁷² Department of Particle Physics, The Weizmann Institute of Science, Rehovot, Israel

¹⁷³ Department of Physics, University of Wisconsin, Madison WI, United States of America

¹⁷⁴ Fakultät für Physik und Astronomie, Julius-Maximilians-Universität, Würzburg, Germany

¹⁷⁵ Fachbereich C Physik, Bergische Universität Wuppertal, Wuppertal, Germany

¹⁷⁶ Department of Physics, Yale University, New Haven CT, United States of America

¹⁷⁷ Yerevan Physics Institute, Yerevan, Armenia

¹⁷⁸ Domaine scientifique de la Doua, Centre de Calcul CNRS/IN2P3, Villeurbanne Cedex, France

^a Also at Laboratório de Instrumentação e Física Experimental de Partículas - LIP, Lisboa, Portugal

^b Also at Faculdade de Ciências and CFNUL, Universidade de Lisboa, Lisboa, Portugal

^c Also at Particle Physics Department, Rutherford Appleton Laboratory, Didcot, United Kingdom

^d Also at TRIUMF, Vancouver BC, Canada

^e Also at Department of Physics, California State University, Fresno CA, United States of America

^f Also at Novosibirsk State University, Novosibirsk, Russia

^g Also at Fermilab, Batavia IL, United States of America

- h* Also at Department of Physics, University of Coimbra, Coimbra, Portugal
- i* Also at Department of Physics, UASLP, San Luis Potosi, Mexico
- j* Also at Università di Napoli Parthenope, Napoli, Italy
- k* Also at Institute of Particle Physics (IPP), Canada
- l* Also at Department of Physics, Middle East Technical University, Ankara, Turkey
- m* Also at Louisiana Tech University, Ruston LA, United States of America
- n* Also at Dep Física and CEFITEC of Faculdade de Ciências e Tecnologia, Universidade Nova de Lisboa, Caparica, Portugal
- o* Also at Department of Physics and Astronomy, University College London, London, United Kingdom
- p* Also at Group of Particle Physics, University of Montreal, Montreal QC, Canada
- q* Also at Department of Physics, University of Cape Town, Cape Town, South Africa
- r* Also at Institute of Physics, Azerbaijan Academy of Sciences, Baku, Azerbaijan
- s* Also at Institut für Experimentalphysik, Universität Hamburg, Hamburg, Germany
- t* Also at Manhattan College, New York NY, United States of America
- u* Also at School of Physics, Shandong University, Shandong, China
- v* Also at CPPM, Aix-Marseille Université and CNRS/IN2P3, Marseille, France
- w* Also at School of Physics and Engineering, Sun Yat-sen University, Guanzhou, China
- x* Also at Academia Sinica Grid Computing, Institute of Physics, Academia Sinica, Taipei, Taiwan
- y* Also at Dipartimento di Fisica, Università La Sapienza, Roma, Italy
- z* Also at DSM/IRFU (Institut de Recherches sur les Lois Fondamentales de l'Univers), CEA Saclay (Commissariat a l'Energie Atomique), Gif-sur-Yvette, France
- aa* Also at Section de Physique, Université de Genève, Geneva, Switzerland
- ab* Also at Departamento de Física, Universidade de Minho, Braga, Portugal
- ac* Also at Department of Physics and Astronomy, University of South Carolina, Columbia SC, United States of America
- ad* Also at Institute for Particle and Nuclear Physics, Wigner Research Centre for Physics, Budapest, Hungary
- ae* Also at California Institute of Technology, Pasadena CA, United States of America
- af* Also at Institute of Physics, Jagiellonian University, Krakow, Poland
- ag* Also at LAL, Université Paris-Sud and CNRS/IN2P3, Orsay, France
- ah* Also at Nevis Laboratory, Columbia University, Irvington NY, United States of America
- ai* Also at Department of Physics and Astronomy, University of Sheffield, Sheffield, United Kingdom
- aj* Also at Department of Physics, Oxford University, Oxford, United Kingdom
- ak* Also at Institute of Physics, Academia Sinica, Taipei, Taiwan
- al* Also at Department of Physics, The University of Michigan, Ann Arbor MI, United States of America
- * Deceased